SEMI-ANNUAL TECHNICAL REPORT

to the

AIR FORCE OFFICE OF SCIENTIFIC RESEARCH

from

Eugene Herrin

and

Tom Goforth

Dallas Geophysical Laboratory
Southern Methodist University
Dallas, Texas 75275

DARPA Order: 3291
Program Code: TF10
Name of Contractor: Southern Methodist University
Effective Date of Contract: July 15, 1976
Contract Expiration Date: September 30, 1979
Total Amount of Contract Dollars: $407,466
Contract Number: F49620-76-C-0030
Principal Investigator and Phone Number: Eugene Herrin
AC 214 692-2760
Program Manager and Phone Number: Truman Cook, Director of
Research Administration
AC 214 692-2031
Title of Work: Propagation Path Effects for Rayleigh and
Love Waves
University Account Number: 80-88

Sponsored by
Defense Advanced Research Projects Agency
DARPA Order No. 3291

UNCLASSIFIED

SECURITY CLASSIFICATION OF THIS PAGE (When Data Entered)

REPORT DOCUMENTATION PAGE

READ INSTRUCTIONS BEFORE COMPLETING FORM

1. REPORT NUMBER: AFOSR TR-79-1317	2. GOVT ACCESSION NO.
3. RECIPIENT'S CATALOG NUMBER	
4. TITLE (and Subtitle): ENERGY DISSIPATION OF RAYLEIGH WAVES DUE TO ABSORPTION ALONG THE PATH BY THE USE OF FINITE ELEMENT METHOD.	5. TYPE OF REPORT & PERIOD COVERED: Scientific Interim rept.
	6. PERFORMING ORG. REPORT NUMBER
7. AUTHOR(s): Eugene Herrin, Tom Goforth, Ali A. Feizpour	8. CONTRACT OR GRANT NUMBER(s): F49620-76-C-0030, DARPA Order-3291
9. PERFORMING ORGANIZATION NAME AND ADDRESS: Dallas Geophysical Laboratory, Southern Methodist University, Dallas, Texas 75275	10. PROGRAM ELEMENT, PROJECT, TASK AREA & WORK UNIT NUMBERS: 61101E 0D60 A.O.3291-30
11. CONTROLLING OFFICE NAME AND ADDRESS: DARPA/NMR, 1400 Wilson Blvd., Arlington, VA 22209	12. REPORT DATE: 31 July 1979
	13. NUMBER OF PAGES: 163
14. MONITORING AGENCY NAME & ADDRESS (if different from Controlling Office): AFOSR/NP, Bolling AFB, Wash DC 20332	15. SECURITY CLASS. (of this report): unclassified
	15a. DECLASSIFICATION/DOWNGRADING SCHEDULE

16. DISTRIBUTION STATEMENT (of this Report)

Approved for public release; distribution unlimited.

16 3291

17 30

17. DISTRIBUTION STATEMENT (of the abstract entered in Block 20, if different from Report)

18. SUPPLEMENTARY NOTES

19. KEY WORDS (Continue on reverse side if necessary and identify by block number)

407 712 DM

20. ABSTRACT (Continue on reverse side if necessary and identify by block number)

A normally incident Rayleigh wave may be used for the investigation of a general vertical boundary and the attenuation of a viscoelastic medium. Use of energy conservation and proper boundary conditions produce 2 N second order differential equations, N being the number of viscoelastic layers in the medium. The homogeneous part of the differential equations can be transformed into an eigenvalue problem by the use of finite element technique; the eigenvalue and eigenvectors of the eigenvalue problem are the wavenumbers and the displacement amplitudes of the viscoelastic layered medium. The real and imaginary parts

DD FORM 1 JAN 73 1473 EDITION OF 1 NOV 65 IS OBSOLETE

UNCLASSIFIED

of the wavenumber determine the phase velocity and the attenuation of the layered medium, respectively. Dispersion and the attenuation curves can be obtained by using different periods. The above wavenumbers can be used in the inhomogeneous differential equation; this equation contains the effect of the vertical boundary; solution of this equation determines the displacement at the vertical boundary. The displacements at the left and right sides of the boundary may be used in the energy equation to determine the reflected and the transmitted energy, respectively. The difference between the incident and transmitted energy determines the difference between the wavenumbers at the left and right hand sides of the vertical boundary. Addition of these differences to the wavenumbers of the left hand boundary would result in the formation of the dispersion curve at the right hand boundary.

ENERGY DISSIPATION OF RAYLEIGH WAVES DUE TO ABSORPTION ALONG THE PATH BY THE USE OF FINITE ELEMENT METHOD

by

Ali A. Feizpour

Geophysical Laboratory
Southern Methodist University
Dallas, Texas 75275
31 July 1979

ABSTRACT

A normally incident Rayleigh wave may be used for the investigation of a general vertical boundary and the attenuation of a viscoelastic medium. Use of energy conservation and proper boundary conditions produce 2 N second order differential equations, N being the number of viscoelastic layers in the medium. The homogeneous part of the differential equations can be transformed into an eigenvalue problem by the use of finite element technique; the eigenvalue and eigenvectors of the eigenvalue problem are the wavenumbers and the displacement amplitudes of the viscoelastic layered medium. The real and imaginary parts of the wavenumber determine the phase velocity and the attenuation of the layered medium, respectively. Dispersion and the attenuation curves can be obtained by using different periods. The above wavenumbers can be used in the inhomogeneous differential equation; this equation contains the effect of the vertical boundary; solution of this equation determines the displacement at the vertical boundary. The displacements at the left and right sides of the boundary may be used in the energy equation to determine the reflected and the transmitted energy, respectively. The difference between

the incident and transmitted energy determines the difference between the wavenumbers at the left and right hand sides of the vertical boundary. Addition of these differences to the wavenumbers of the left hand boundary would result in the formation of the dispersion curve at the right hand boundary.

TABLE OF CONTENTS

Table of Contents - Continued

PREFACE

The attenuation of a surface wave along its path is of interest in many branches of physical science; among the noted are solid mechanics, acoustics, and seismology. The aim of this dissertation is to present a method of Rayleigh wave propagation in a viscoelastic solid constrained by one or two vertical boundaries. The material is arranged to present a summary of viscoelastic behavior of solid, an introduction to the method of finite element for the derivation and solution of governing equations, a discussion on energy conservation in elastic and viscoelastic solids, and presentation of a perturbation theory for the calculation of the phase velocity due to a vertical boundary, followed by a chapter on application of data to the method.

I hope that this dissertation will be a stimulant for interested investigators, to be critical of the material herein, and to be encouraged enough to further test the validity of the theory by using other distinct models. As a reference, the text is supplemented by a relatively vast number of references, which provide a great deal of information for understanding the subject.

I would like to thank Professor E. Herrin for his advice through the course of my research and for his critical opinion of this dissertation. I would also like to thank Doctors B. Mohraz, D. Blackwell, T. Goforth, H. Mack, and W. Peeples, for their criticisms and encouragements.

I also wish to express my appreciation to Dr. L. Drake; his computer program and his personal assistance greatly contributed to my research. Finally, I am grateful to my wife, Jeneva, for her patience and encouraging attitude during this study.

Support for this study was provided by the Defense Advanced Research Projects Agency under Contract AFOSR F49620-76-C-0030 monitored by the U.S. Air Force Office of Scientific Research; by National Science Foundation Grant EAR-77-13714; and by Institute for the Study of Earth and Man Grant 20-91-235.

LIST OF SYMBOLS

CHAPTER II

σ	Stress in one dimension
σ_{ij}	Stress tensor
σ_{ν}	Two dimensional stress vector normal to a line whose direction cosine is ν
ϵ	Strain in one dimension
ϵ_{ij}	Strain tensor
η_{v}	Coefficient of viscosity
μ	Shear rigidity
τ_{σ}	Stress relaxation under constant strain
τ_{ε}	Strain relaxation under constant stress
ψ	Energy density
λ	Young modulus
K	Bulk modulus
K_e	Effective bulk modulus
μ_e	Effective rigidity
$\underline{D}$	Matrix moduli 3 x 3
$\hat{\epsilon}$	Strain vector
$\sigma_{ij,j}$	Space derivative of the stress tensor
F_i	Force vector per unit volume
ρ	Density

CHAPTER III

F	Total force
$\underline{K}$	Stiffness matrix
$\hat{U}$	Vector displacements
$\underline{M}$	Mass matrix
$\underline{B}$	Space operating matrix
$\underline{D'}$	Matrix moduli 2 x 3
DZ	Operating matrix in Z direction
$\underline{N}$	Matrix of shape function
$\hat{v}$	Displacement vector
η	Local coordinate of tne layer
α	A multiplier
$\underline{V}$	Matrix with columns v
$\hat{P}$	Force at the boundary
$\underline{L}$	Boundary matrix
$\underline{K_e}$	Element stiffness matrix

CHAPTER IV

E	Incident energy
K	Wavenumber
β	Absorption in the x direction
γ	Absorption in the z direction
$\underline{D_v}$	Matrix moduli 2 x 3
E_r	Reflected energy
E_t	Transmitted energy

Q^{-1}	Attenuation
$\Delta \underline{D}$	Change in matrix moduli
$\Delta \rho$	Change in densities

CHAPTER V

V_p	P wave velocity
V_s	S wave velocity
Q_β	Shear quality factor
Q_α	Compressional quality factor

CHAPTER I

INTRODUCTION

Rayleigh wave amplitude decays as it propagates through the earth. The amount of the decay observed is invariably more than what the theory predicts. This anomaly is due to the loss mechanisms or the energy dissipation in the medium; thus the observed Rayleigh wave amplitude is a function of energy dissipation or attenuation.

Attenuation of Rayleigh wave is due to anelasticity and geometrical discontinuities of the earth. Anelasticity of the earth may be thought of as the imperfection in crystal structure such as point defects, dislocation across which the atoms are not aligned in accordance with the normal lattice structure, and interatomic bonds at grain boundaries. Geometrical discontinuities, among others (23, 24), cause the distortion of the plane of propagation of Rayleigh waves from the great circle and therefore there is a loss of energy or attenuation.

In a dissipating medium the deformation of a solid is a function of time, temperature and space. Creep phenomenon is a deformation process in which there is a time dependent strain under a constant applied stress and relaxation phenomenon is a time dependent stress under a constant strain. A solid manifesting creep and relaxation phenomena is called viscoelastic. If a deformation is due to discontinuities in the medium or the amplitude decay is only a function of position, the dissipation

of the wave energy is of the hysteretic type (Figure 1), and the amount of this loss must be determined by the average energy dissipation in a hysteresis loop over one cycle of harmonic motion and is a function of displacement amplitude.

To narrow the gap between the observed and predicted Rayleigh wave amplitude the effect of viscoelasticity and geometrical discontinuities must be taken into account. A few workers have studies the viscoelastic behavior of Rayleigh waves for an isotropic homogeneous layered half-space. Press and Healy (94) derived an expression for the absorption coefficient and a dispersion relation assuming complex velocities for shear, longitudinal and Rayleigh waves respectively. King and Sheard (56) used a dissipation function for a general anisotropic medium and derived a dispersion relation for an isotropic layered half-space equivalent to that of Press and Healy (94). Borcherdt (15) also formulated a similar theoretical expression for a layered half-space. Auld (8) determined the attenuation of Rayleigh waves due to viscous damping in the medium by using King and Shread's dissipation function (56). He concluded that the Rayleigh wave attenuation is mostly due to shear viscosity of the medium. For observational studies of the dissipation of Rayleigh waves the reader is referred to Anderson, et al (5) and Tryggvason (115).

The effect of geometrical discontinuities on the propagation of Rayleigh waves have been a problem of seismologists for many years. Several studies have been devoted to the description of the field around wedges and corners using approximate analytical techniques: e.g., Lapwood (66), Mal and Knopoff (82), McGarr (85) and Alsop et al (2). Several theoretical studies have also been done in more recent years

with, in most part, the assumption of weak horizontal inhomogeneity on assumption of a small change in elastic parameters. Among the more important are, Babish et al. (9), Kennett (55) and Mukitina et al. (88).

The observed distorted Rayleigh wave through the continental margins or the oceanic ridges has been studied by Capon (19, 20) and by Evernden (31, 32, 33) and the amount of distortion has been approximated analytically by Gjevik (39) who has used ray tracing theory and perturbation theory. The distortion of Rayleigh waves from the great circle has also been studied by Crampin (23, 24) who has stated that the distortion is due to a layer of anisotropic olivine in the upper mantle.

The finite element method has been used, in recent years, in wave propagation problems of seismology. Lysmer (78) and Lysmer and Waas (79) developed a lumped mass method to study the propagation of Rayleigh and shear waves in a homogeneous layered medium. Lysmer and Drake (80) introduced the method of consistent mass matrix of the finite element method to seismology. Drake (28, 29) studied the propagation of Love and Rayleigh waves in a nonhorizontally layered medium. Drake (26) also studied the motion of Rayleigh waves at a continental boundary. Waas (117) improved the method of finite element to a general two dimensional problem and Kausel et al. (54) extended the method to a three dimensional problem in which Rayleigh wave corresponds to a vertical cross section and Love wave corresponds to a horizontal cross section of the medium. Smith (107) applied the method

of finite element to body wave propagation. Finally Segol et al. (105) studied the propagation of a Rayleigh wave being obstructed by trenches.

In this dissertation the finite element method is used to study the attenuation of Rayleigh waves due to viscoelasticity i.e., viscosity, temperature, partial melting, etc., and determine a dissipative factor due to a vertical boundary. The model consists of a heterogeneous medium bounded by two vertical boundaries (Figure 4). These two boundaries are the common boundaries between the heterogeneous medium and two semiinfinite horizontal layered media extending to left and right. For the two viscoelastic layered media a second order differential equation similar to that of a damping oscillator is obtained in which the damping factor is a matrix whose entries are the viscoelastic parameters of the medium. The solution of this equation determines the wavenumbers and the amount of attenuation of Rayleigh waves in the horizontal direction. Use of the boundary conditions at the vertical boundaries results in the equation of motion of the heterogeneous medium whose solution yields the horizontal and vertical displacement of the heterogeneous medium. These displacements and the wavenumbers of the layered regions are used in the energy conservation theorem along with a perturbation theory to determine the amount of absorption due to viscoelasticity of the region and the change in the wavenumbers due to vertical boundaries. The adjusted wavenumbers of the right hand boundary may be used to determine the dispersion curve and the amount of attenuation at the right hand boundary.

CHAPTER II

VISCOELASTICITY

A. Summary

The phenomenon of viscoelasticity is a broad subject in the study of materials in the gaseous, liquid, and solid states. Interested readers are referred to the selected texts on the subject by Bland (13), Christensen (22), Gross (44), Kolsky (60, 61), Litvitz and Davis (72), Mathson (84) and Zener (122) for theoretical studies, and Anderson (3, 4), Anderson et al. (5, 6), Gordon (41, 42, 43), Hart et al. (45), Jackson and Anderson (50), Liu et al. (74), Magnitsky and Zharkov (81) and Orowan (90) for seismological interest. A brief review for the problem at hand will be presented here.

B. Uniaxial Deformation

Viscoelastic materials combine elastic and viscous effects; therefore, it is possible to model the material of the viscoelastic earth by networks made of simple elastic and viscous elements. The simpliest model is a spring and a dashpot in series or parallel and is called a Maxwell or Voigt element, respectively. Mathematically the stress-strain relation for the model is

$$\frac{\sigma}{\eta_v} + \frac{\dot{\sigma}}{\mu} = \dot{\varepsilon} \tag{2.1}$$

for the Maxwell element, and

$$\mu\varepsilon + \eta_v\dot{\varepsilon} = \sigma \tag{2.2}$$

for the Voigt element, where σ is the stress, ε is the strain, $\dot{\varepsilon}$ the rate of the strain, μ is the elastic modulus of the spring and η is the coefficient of viscosity of the dashpot (Figure 2). A combination of a spring with elastic modulus μ_1 either in series with a Voigt element or in parallel with a Maxwell element will produce a relation

$$\dot{\sigma}\tau_\sigma + \sigma = M_r(\varepsilon + \tau_\varepsilon\dot{\varepsilon}) \tag{2.3}$$

called the standard linear solid, where

$$\tau_\sigma = \frac{\eta_v}{\mu + \mu_1}, \quad \tau_\varepsilon = \frac{\eta_v}{\mu}, \quad M_r = \frac{\mu_1\mu}{\mu_1 + \mu} \tag{2.4}$$

are the stress relaxation time under constant strain, the strain relaxation under constant stress, and the deformation or relaxed elastic modulus, respectively.

The solution of Equation 2.1 for a constant strain results in a decaying exponential function of the form

$$\sigma(t) = \sigma_0 \text{ EXP } (-\mu/\eta_v t) \tag{2.5}$$

which is called the relaxation function. Similarly the solution of Equation 2.2 for a constant stress results in an increasing exponential function of the form

$$\varepsilon(t) = \frac{\sigma_0}{\mu}(1 - e^{-\mu/\eta_v t}) \tag{2.6}$$

which is called a creep function (Figure 3). The solution of Equation 2.3

yields the relaxation and creep functions of the form

$$\sigma(t) = M_r\varepsilon(t) + M_r \frac{\tau_\varepsilon}{\tau_\sigma} \text{EXP}\ (-\ t/\tau_\sigma) \int_{-\infty}^{t} \text{EXP}\ (\tau/\tau_\sigma)\dot{\varepsilon}(\tau)d\tau$$

and (2.7)

$$\varepsilon(t) = \frac{1}{M_r}\sigma(t) + \frac{1}{M_r}\frac{\tau_\sigma}{\tau_\varepsilon} \text{EXP}\ (-\ t/\tau_\varepsilon) \int_{-\infty}^{t} \text{EXP}(\tau/\tau_\varepsilon)\dot{\sigma}(\tau)d\tau$$

Equations 2.7 represent the Boltzmann after-effect. The verbal statement of these equations by Boltzmann is that for all real solids the relation between stress or strain components at any time depends not only on their instantaneous values at that time, but on the whole history of deformation from the time at which the material was formed. It is now possible to represent the viscoelastic behavior of the real material by either a large number of Maxwell elements and springs joined in parallel or a large number of Voigt elements and springs joined in series. The arrangement of the springs represent the molecular position of material and the dashpots represent the perturbation factor for the distortion of molecular positions. Thus the generalized relaxation and creep function for uniaxial deformation is given by

$$\sigma(t) = M_r\varepsilon(t) + M_r \sum_{i=1}^{N} \frac{\tau_{\varepsilon_i}}{\tau_{\sigma_i}} \text{EXP}\ (-\ t/\tau_{\sigma_i}) \int_{-\infty}^{t} \text{EXP}(\tau/\tau_{\sigma_i})\dot{\varepsilon}(\tau)d\tau$$

and (2.8)

$$\varepsilon(t) = \frac{1}{M_r}\sigma(t) + \frac{1}{M_r} \sum_{i=1}^{N} \frac{\tau_{\sigma_i}}{\tau_{\varepsilon_i}} \text{EXP}\ (-\ t/\tau_{\varepsilon_i}) \int_{\infty}^{t} \text{EXP}\ (\tau/\tau_{\varepsilon_i})\dot{\sigma}(\tau)d\tau$$

Equations 2.8 represent the Boltzmann superposition principle.

C. Three Dimensional Deformation

For a general linear viscoelastic model consider the energy density (67),

$$\psi = 1/2\ C_{ijKL}\ \epsilon_{ij}\ \epsilon_{KL} \tag{2.9}$$

where ϵ's are strains and C_{ijKL}, generally complex, are the moduli of the medium. For an anisotropic medium C_{ijKL} contain 21 independent complex coefficients. For an isotropic medium these coefficients reduce to two elastic constants in an elastic medium, whereas, in the viscoelastic medium the two coefficients are not constant and may be a function of time, temperature, position or other thermodynamic parameters. Therefore, in an isotropic viscoelastic medium Equation 2.9 can be written as

$$\psi = 1/2\ \lambda\ \delta_{ij}\ \epsilon_{ii}^{\,2} + \mu\epsilon_{ij}^{\,2} + 1/2\ \lambda'(t, T, \bar{x}, \gamma)\delta_{ij}\ \epsilon_{ii}^{\,2} + \mu'(t, T, \bar{x}, \gamma)\epsilon_{ij}^{\,2} \tag{2.10}$$

where λ and μ are Lame' constants, λ' and μ' the coefficients which depend on the viscoelastic behavior of the medium. Since Equation 2.10 is a scalar function, the stress field can be obtained by a directional derivative with respect to the strain tensor as

$$\sigma_{ij} = \lambda\delta_{ij}\ \epsilon_{ii} + 2\ \mu\epsilon_{ij} + \lambda'(t, T, \bar{x}, \gamma)\delta_{ij}\ \epsilon_{ii} + 2\ \mu'(t,T,\bar{x},\gamma)\epsilon_{ij} \tag{2.11}$$

The first two terms in Equation 2.11 represent the familiar form of the stress-strain relation in an isotropic homogeneous medium and the last two terms are due to the viscoelasticity of the medium.

D. Effective Moduli for a Relaxing Medium

For functionals λ' and μ', the effective moduli of the stressed medium can be obtained by either substitution of Equation 2.11 into Equation 2.7 and integrating it through the limits of integration, or by formation of a relation similar to Equation 2.3, using Equation 2.11; the latter is a more convenient way to choose. For this purpose we may write Equation 2.11 in terms of shear and dilatational components. Using the strain tensor

$$\varepsilon_{ij} = (\varepsilon_{ij} - 1/3\ \delta_{ij}\varepsilon_{ii}) + 1/3\ \delta_{ij}\varepsilon_{ii}\ , \tag{2.12}$$

Equation 2.11 becomes

$$\sigma_{ij} = 2\mu(\varepsilon_{ij} - 1/3\ \delta_{ij}\varepsilon_{ii}) + K\varepsilon_{ii}\delta_{ij} + 2\mu'(\dot{\varepsilon}_{ij} - 1/3\ \delta_{ij}\dot{\varepsilon}_{ii}) + K'\dot{\varepsilon}_{ii}\delta_{ij} \tag{2.13}$$

where $K = \lambda + 2/3\mu$ is called dilational or bulk modulus. Separating the stress tensor of Equation 2.13 into the compressional and sheer component, the result, in the form of Equation 2.3, can be written as

$$\begin{aligned} \sigma_{ii} + \tau_\nu\ \dot{\sigma}_{ii} &= -\ K\ \varepsilon_{ii} - \tau_\nu\ K_\infty\ \dot{\varepsilon}_{ii} \\ \sigma_{ij} + \tau_s\ \dot{\sigma}_{ij} &= \mu\varepsilon_{ij} + \tau_s\ \mu_\infty\ \varepsilon_{ij} \end{aligned} \tag{2.14}$$

where τ_ν and τ_s are relaxation times, $K_\infty = K\ ^\tau s/\tau_\nu$ and $\mu_\infty = \mu^\tau\nu/\tau_s$. The assumption of a harmonic stress in Equations 2.14 will produce a relation of the form

$$\sigma_{ii}(\omega) = - K_e(\omega)\, \varepsilon_{ii}(\omega) \tag{2.15}$$

$$\sigma_{ij}(\omega) = \mu_e(\omega)\, \varepsilon_{ij}(\omega) \tag{2.16}$$

where

$$K_e(\omega) = K[1 - (1 - \tau_s/\tau_v)\omega^2\tau_v^2/(1 + \omega^2\tau_v^2) - i\omega\,(1 - \tau_s/\tau_v)\,\tau_v/(1 + \omega^2\tau_v^2)]$$

$$\mu_e(\omega) = \mu\,[1 - (1 - \frac{\tau_v}{\tau_s})\omega^2\tau_s^2/(1 + \omega^2\tau_s^2) - i\omega\,(1 - \tau_v/\tau_s)\tau_s/(1 + \omega^2\tau_s^2)] \tag{2.17}$$

Equation 2.17 is identical to Equation 2.16 of Liu et al. (74) which was derived independently. It is clear now that the effective moduli of a viscoelastic wave and therefore the velocity of the wave is a function of frequency which has been claimed by many investigators for body waves and recently by a few for surface waves. Futterman (38) and Lomintz (77) theorized the concept of frequency dependence of the phase velocity of body waves. Kogan (59), Lamb (65), Liu et al. (74), Magnitsky and Zharkov (81), Mason (83) and Strick (109) have studied the frequency dependent velocity of body waves and concluded the validity of Futterman's theory. Most recently a few studies have been devoted to frequency dependent phase velocity of surface wave and the free oscillation of the earth by Liu and Archambeau (73, 75), Park and Rockwell (92), Randall (95) and Kanamori and Anderson (53).

E. Two Dimensional Deformation

The six independent components of the stress tensor in a three dimensional, isotropic medium reduce to three independent components in two dimensions. Therefore, an x - z plane propagation would result in a zero stress in y direction such that

$$\sigma_{xy} = \sigma_{yy} = \sigma_{zy} = 0 \tag{2.18}$$

Starting with the first two terms of Equation 2.11 (for derivation of the equations of motion, the inelastic part of the stress tensor need not be included for the moment),

$$\sigma_{ij} = \lambda \delta_{ij} \varepsilon_{ii} + 2\mu \varepsilon_{ij} \qquad \begin{matrix} i = 1,3 \\ j = 1,3 \end{matrix} \tag{2.19}$$

and the constraint relation, Equation 2.18, the nonzero three independent component of the stress in two dimensional systems are

$$\sigma_{11} = \sigma_{xx} = \lambda\varepsilon_{xx} + 2\mu \varepsilon_{xx} + \lambda\varepsilon_{zz}$$

$$\sigma_{13} = \sigma_{xz} = 2\mu \varepsilon_{xz}$$

$$\sigma_{33} = \sigma_{zz} = \lambda\varepsilon_{xx} + 2\mu \varepsilon_{zz} + \lambda\varepsilon_{zz} \tag{2.20}$$

where the components of the strain tensor are obtained from the relation

$$\varepsilon_{ij} = 1/2 \left(\frac{\partial U_i}{\partial x_j} + \frac{\partial U_j}{\partial x_i}\right) \qquad \begin{matrix} i = 1,3 \\ j = 1,3 \end{matrix} \tag{2.21}$$

as

$$\varepsilon_{11} = \varepsilon_{xx} = 1/2\left(\frac{\partial U_x}{\partial x} + \frac{\partial U_x}{\partial x}\right) = \frac{\partial U_x}{\partial x}$$

$$\varepsilon_{13} = \varepsilon_{xz} = 1/2\left(\frac{\partial U_x}{\partial z} + \frac{\partial U_z}{\partial x}\right) \qquad (2.22)$$

$$\varepsilon_{33} = \varepsilon_{zz} = 1/2\left(\frac{\partial U_z}{\partial z} + \frac{\partial U_z}{\partial z}\right) = \frac{\partial U_z}{\partial z}$$

where

U_x and U_z are horizontal and vertical displacements of the propagating plane wave respectively. Substituting Equations 2.22 into Equations 2.20 and expressing the stress components in a vector form, the result is

$$\hat{\sigma} = (\sigma_{xx}, \sigma_{zz}, \sigma_{xz}) = \underline{D}\,\hat{\varepsilon} \qquad (2.23)$$

where

$$\underline{D} = \begin{bmatrix} \lambda+2\mu & \lambda & 0 \\ \lambda & \lambda+2\mu & 0 \\ 0 & 0 & \mu \end{bmatrix}, \quad \hat{\varepsilon} = \left(\frac{\partial U_x}{\partial x}, \frac{\partial U_z}{\partial z}, \frac{\partial U_z}{\partial x} + \frac{\partial U_x}{\partial z}\right) \qquad (2.24)$$

Equation 2.23 is derived for an elastic medium; for an inelastic medium the Lame' constants in Equation 2.23 must be replaced by the effective moduli of Equation 2.17.

F. Wave Equation in Cartesian Coordinates

Using the stress tensor of Equation 2.19 the wave equation is obtained by

$$\sigma_{ij,j} = \frac{\partial}{\partial x_j}(\sigma_{ij}) = F_i \qquad (2.25)$$

If the force F_i is assumed to be the inertia force then

$$\frac{\partial}{\partial x_j}(\sigma_{ij}) = \rho \ddot{U}_i \tag{2.26}$$

where ρ is the density and double dot denotes the acceleration. Assumption of a hormonic plane wave allows a displacement of the form

$$U_i = U_i(x,z)e^{i\omega t} \tag{2.27}$$

where

$$U_i = (U_x, U_z)$$

Substitution of Equations 2.20, 2.22 and 2.27 into Equation 2.26 leads to a two dimensional equation of motion

$$\begin{aligned} -\rho\omega^2 U_x &= (\lambda + \mu)\left(\frac{\partial^2 U_x}{\partial x^2} + \frac{\partial^2 U_z}{\partial x \partial z}\right) + \mu\left(\frac{\partial^2 U_x}{\partial x^2} + \frac{\partial^2 U_x}{\partial z^2}\right) \\ -\rho\omega^2 U_z &= (\lambda + \mu)\left(\frac{\partial^2 U_x}{\partial x \partial z} + \frac{\partial^2 U_z}{\partial z^2}\right) + \mu\left(\frac{\partial^2 U_z}{\partial x^2} + \frac{\partial^2 U_z}{\partial z^2}\right) \end{aligned} \tag{2.28}$$

Since the displacement U_i is a function of x and z, an independent product of the function of x and z may be replaced by $U_i(x,z)$

$$\begin{aligned} U_x(x,z) &= U_x(z)W(x) \\ U_z(x,z) &= U_z(z)W(x) \end{aligned} \tag{2.29}$$

Substitution of Equations 2.29 into Equations 2.28 yields the coupled ordinary second order differential equations

$$\mu \frac{d^2U_x}{dz^2} - iK(\lambda + \mu)\frac{dU_z}{dz} - K^2(\lambda + 2\mu)U_x + \rho\omega^2 U_x = 0$$

$$(\lambda + 2\mu)\frac{d^2U_z}{dz^2} - iK(\lambda + \mu)\frac{dU_x}{dz} - K^2\mu U_z + \rho\omega^2 U_z = 0 \qquad (2.30)$$

and

$$\frac{d^2W}{dx^2} + K^2W = 0 \qquad (2.31)$$

Equation 2.31 has a solution of the form

$$W(x) = e^{-iKx} \qquad (2.32)$$

and Equation 2.27 may be expressed by

$$U_x = U_x(z)e^{i(\omega t - Kx)}$$

$$U_z = U_z(z)e^{i(\omega t - Kx)} \qquad (2.33)$$

the amplitudes $U_x(z)$ and $U_z(z)$ are obtained by the solution of the differential Equations 2.30.

So far there has not been any restriction on the condition of Equation 2.30 and the amplitudes $U_x(z)$ and $U_z(z)$ Equation 2.30 may be solved for a general plane wave. Our interest is in a solution with proper constraints to produce a Rayleigh wave, a plane wave that propagates in one direction and dissipates in the direction normal to the direction of propagation. In general, these two directions need not be perpendicular; when the medium of propagation is viscoelastic the

direction of propagation and dissipation of Rayleigh wave are not perpendicular. In this case the wave is called a generalized Rayleigh wave and is discussed in more detail in Chapter IV.

To acquire a Rayleigh wave solution, in an N layered medium, from Equation 2.33, we analyze Equation 2.30. For an N layered medium Equation 2.30 constitutes 2N second order differential equations. The boundary conditions required for the solution of these equations are continuity of the stresses and displacements at each interfaces, zero stress at free surface, and zero displacement amplitude at a distance far from the surface. The stresses considered are the stress normal to the plane interface and the shear stress on the plane interface; they are given by

$$\sigma_{zz} = \lambda \frac{\partial U_x}{\partial x} + (\lambda + 2\mu) \frac{\partial U_z}{\partial z}$$

$$\sigma_{xz} = \mu\left(\frac{\partial U_x}{\partial z} + \frac{\partial U_z}{\partial x}\right) \tag{2.34}$$

There must be continuity at the interfaces where the Lame' constants just above and below the interfaces may be different. Thus, the conditions for the stresses are

$$\lambda_1 \frac{\partial U_x}{\partial x} + (\lambda_1 + 2\mu) \frac{\partial U}{\partial z} = 0, \quad \mu_1\left(\frac{\partial U_x}{\partial z} + \frac{\partial U_z}{\partial x}\right) = 0 \tag{2.35}$$

on the surface and

$$\lambda_{j-1} \frac{\partial U_x}{\partial x} + (\lambda_{j-1} + 2\mu_{j-1}) \frac{\partial U_z}{\partial z} = \lambda'_{j-1} \frac{\partial U_x}{\partial x} + (\lambda'_{j-1} + 2\mu_{j-1}) \frac{\partial U_z}{\partial z}$$

$$\mu_{j-1}\left(\frac{\partial U_x}{\partial z} + \frac{\partial U_z}{\partial x}\right) = \mu'_{j-1}\left(\frac{\partial U_x}{\partial z} + \frac{\partial U_z}{\partial x}\right) \tag{2.36}$$

$j = 2,\ldots N$, at the interfaces. Also the conditions for continuity of displacements are

$$U_{x_j} = U'_{x_j} \quad \text{and} \quad U_{z_j} = U'_{z_j} \quad j = 2,\ldots N \tag{2.37}$$

and for Z_{N+1} far enough below the surface

$$U_{x_{N+1}} = 0 \quad \text{and} \quad U_{z_{N+1}} = 0 \; . \tag{2.38}$$

With these boundary conditions the solution of Equation 2.30 will lead to an eigenvalue problem whose solutions are extremely difficult. For this reason we leave further discussion of Equation 2.30 for the next chapter in which we discuss the finite element method.

CHAPTER III

THEORETTICAL BACKGROUND OF THE FINITE ELEMENT METHOD

A. Summary

For a detailed review of the method of finite element the reader is referred to the texts by Bathe and Wilson (11), Desai and Abel (25), Norrie and de Vries (89), Richards (97), Segerlind (103) and Zienkiewicz (124) for mathematical and engineering application, and by Lysmer (78), Lysmer and Waas (79), Lysmer and Drake (80), Segol et al. (105) and Waas (117) for seismological applications. A summary of the derivation of the essential equations will be discussed in this chapter.

The finite element technique has been brought to seismology in recent years. It seems to be more successful than the method of finite difference. The basic difference between the two techniques is that in the finite difference method the continuous medium is used to derive a set of differential equations which are replaced by finite difference equations. In the finite element technique the continuous medium is first approximated and the governing differential equations are solved numerically. Therefore, in the finite element technique the basic assumption is to divide the continuous layered medium into a discrete system consisting of, for example, rectangular elements each having four nodal points. The displacement of the structure is equivalent to

the displacement of the nodal points and all the forces between the elements and the external forces are transmitted through the nodal points.

The forces that produce displacements within an element are represented by

$$\hat{F} = \underline{K}\hat{U} \tag{3.1}$$

where $\underline{K}$ is called the stiffness matrix depending on the orientation and properties of the elements. If the inertia force is present Equation 3.1 is written as

$$\hat{F} = (\underline{K} - \omega^2 \underline{M})\, \hat{U} \tag{3.2}$$

where $\underline{M}$ is the mass matrix of the element and ω is the frequency of the vibration. Since the number of elements have to be finite the structure must be bounded. For this reason the structure with irregular geometry, I, is joined, along the vertical planes, to the regions, L and R, which extend infinitely to the left and to the right, respectively (Figure 4). Regions L and R consist of horizontal layers which are welded together at their interfaces and may differ in their material properties and thickness. For this configuration the finite element method is used to analyze the motion in the irregular zone I and a discrete theory, which is essentially a one dimensional finite element, is used to analyze the motion of the layered zones. The natural layers of the L and R zones must be subdivided into a larger number of layers so that the nodal points of the elements in the irregular zone at the vertical boundaries coincide with the layer interfaces. The thickness of the

element is determined by the wave length of the S wave in the layered zones (104).

B. Setup of the Method

The irregular region of zone I consists of an assemblage of quadrilateral elements interconnected at their nodal points. A typical element e is defined by its nodes i, j, K and L. The displacements at the element nodes are taken as unknown and the solution within each element is approximated by a shape function $\underline{N}$ that varies linearly along the boundaries, i.e.,

$$\hat{U} = \underline{N}\hat{V} = [N_i, N_j, N_K, N_L]\,(V_i, V_j, V_K, V_L) \tag{3.3}$$

in which, for a plane wave propagation,

$$\hat{V}_i = (V_1, V_2)i \quad \text{etc.} \tag{3.4}$$

are the horizontal and vertical displacements at the element's node i, etc., and the martix $\underline{N}^T$ is the shape function in terms of (ξ, η), the local coordinates of the element. The component N_i, etc. of the matrix $\underline{N}^T$ is unity at the node i, etc. and is equal to zero at other nodes. The above displacement is related to the strain by

$$\hat{\epsilon} = \underline{B}\hat{U} \tag{3.5}$$

where

$$\underline{B} = \begin{bmatrix} \frac{\partial}{\partial x} & 0 \\ 0 & \frac{\partial}{\partial z} \\ \frac{\partial}{\partial x} & \frac{\partial}{\partial z} \end{bmatrix}, \quad \hat{U} = (U_x, U_z) \quad . \tag{3.6}$$

If the strain energy, or the energy density , defined in Chapter IIB, exists, then as in Chapter IIB, its derivative with respect to the strain tensor is the stress field and is given by

$$\frac{\partial \psi}{\partial \epsilon_{ij}} = \sigma_{ij} \tag{3.7}$$

The elastic part of the stress in Equation 3.7 in terms of the strain is given by

$$\sigma_{ij} = \lambda \epsilon_{ij} \delta_{ij} + 2\mu \epsilon_{ij} \tag{3.8}$$

Equation 3.7 can be written equivalently as

$$\delta\psi = \sigma_{ij} \delta \epsilon_{ij} \tag{3.9}$$

which is the virtual work done by the force F_i per unit of volume and the surface force T_i per unit of area (37). For static equilibrium the expression

$$\int_V \sigma_{ij} \delta \epsilon_{ij} dv = \int_V F_i \delta U_i dv + \int_S T_i \delta U_i ds \tag{3.10}$$

is called the principle of virtual work produced by the virtual displacement δU_i. Equation 3.10 will be used to derive the equation of motion of an element in the irregular region I. If the body force F_i is the inertia force per unit of volume, a set of inhomogeneous differential equations can be derived by rewriting Equation 3.10 as

$$\int_V (\sigma_{ij} \delta \epsilon_{ij} - F_i \delta U_i) dv = \int_S T_i \delta U_i ds \tag{3.11}$$

This equation, with T_i equal to zero can also be used to derive a homogeneous second order differential equation for the layered medium, L and

R of Figure 4, as

$$\int_v (\sigma_{ij}\ \delta\ \varepsilon_{ij} - F_i\ \ U_i)dv = 0\ . \tag{3.12}$$

The first term of this equation can be written as

$$\int_v \sigma_{ij}\ \delta\ \varepsilon_{ij}dv = \int_v \sigma_{ij}(\delta U_{ij} + \delta U_{ji})dv$$

$$= -\int_v \delta_{ij,j}\ \delta U_i dv + \int \sigma_{ij}\ \hat{\nu}\ \delta U_i ds, \tag{3.13}$$

using the familiar expression

$$\varepsilon_{ij} = 1/2\left(\frac{\partial U_i}{\partial x_j} + \frac{\partial U_j}{\partial x_i}\right) \tag{3.14}$$

and the Gauss's theorem. Substitution of Equation 3.13 into Equation 2.12 gives

$$\int_v (\sigma_{ij,j} + F_i)\ \delta U_i dv - \int_s \sigma_{ij}\ \hat{\nu}\ \delta U_i ds = 0 \tag{3.15}$$

which for an arbitrary δU_i satisfies the equation of motion

$$\sigma_{ij,j} + F_i = 0 \tag{3.16}$$

and either

$$\delta U_i = 0 \tag{3.17}$$

on the rigid boundary or

$$\sigma_{ij}\ \hat{\nu} = 0, \tag{3.18}$$

the surface boundary condition.

Equation 3.15 determines the motion of the wave in the horizontal layers L and R. The first integrand of this equation is the general equation of motion and the second integrand is the horizontal boundary condition, i.e., in a plane wave case, the normal stress in the z direction and the shear stress on the plane interfaces. For convenience we write Equation 3.15 in a vector form as

$$\int_V \delta\hat{U}^T \cdot \hat{W}\, dv - \int_S \delta\hat{U}^T \cdot \sigma\, \hat{\nu}\, ds = 0 \tag{3.19}$$

where W is the equation of motion, and T represents complex conjugate transpose.

C. Rayleigh Wave Motion

The displacement of the medium in the horizontal and vertical directions produced by the propagation of a Rayleigh wave can be represented by (1)

$$\begin{aligned} U_x &= U_x(x,z)\, e^{i\omega t} \\ U_z &= U_z(x,z)\, e^{i\omega t} \end{aligned} \tag{3.20}$$

Substitution of this equation into the equations of motion, with no force present, and the separation of variables in the usual way would result in

$$\begin{aligned} U_x(x,z) &= U_x(z)\, e^{-iKx} \\ U_z(x,z) &= U_z(z)\, e^{-iKx} \end{aligned} \tag{3.21}$$

Substitution of Equation 3.21 into Equation 3.20 will produce the vector displacement of Equation 3.19 as

$$\hat{U} = (U_x(z),\ U_z(z))e^{i(\omega t - Kx)} \tag{3.22}$$

The six component stress tensor in three dimensions will reduce to a three component stress vector in two dimensions and is given by

$$\hat{\sigma} = (\sigma_{xx},\ \sigma_{zz},\ \sigma_{xz}) \tag{3.23}$$

where, from Equation 3.8

$$\begin{aligned} \sigma_{xx} &= (\lambda + 2\mu)\frac{\partial U_x}{\partial x} + \lambda\frac{\partial U_z}{\partial z} \\ \sigma_{zz} &= \lambda\frac{\partial U_x}{\partial x} + (\lambda + 2\mu)\frac{\partial U_z}{\partial z} \\ \sigma_{xz} &= \mu\left(\frac{\partial U_x}{\partial z} + \frac{\partial U_z}{\partial x}\right) . \end{aligned} \tag{3.24}$$

Therefore,

$$\hat{\sigma} = \underline{D}\,\hat{\varepsilon} \tag{3.25}$$

where

$$\underline{D} = \begin{bmatrix} \lambda+2\mu & \lambda & 0 \\ \lambda & \lambda+2\mu & 0 \\ 0 & 0 & \mu \end{bmatrix} \tag{3.25a}$$

$$\hat{\varepsilon} = \left(\frac{\partial U_x}{\partial x},\ \frac{\partial U_z}{\partial z},\ \frac{\partial U_z}{\partial x} + \frac{\partial U_x}{\partial z}\right) \tag{3.26}$$

At the interfaces the stress component in the x direction is zero and the surface stress $\hat{\sigma v}$ in Equation 3.19, and the matrix $\underline{D}$ in this case are

$$\hat{\sigma v} = (\sigma_{zz}, \sigma_{xz}) , \tag{3.27}$$

$$\underline{D}' = \begin{bmatrix} \lambda & \lambda+2\mu & 0 \\ 0 & 0 & \mu \end{bmatrix} , \tag{3.28}$$

then

$$\hat{\sigma v} = \underline{D}'\hat{\epsilon} \tag{3.29}$$

respectively. Substituting Equations 3.22, 3.24-3.26 and 3.27- 3.29 into Equation 3.19 and assuming that F_i is the inertia force per unit of volume we have

$$\int_V (\delta\hat{\epsilon}^T \cdot \underline{D}\,\hat{\epsilon} - \rho\omega^2\, \delta\hat{U}^T \cdot \hat{U})dxdz - \int_S \delta\hat{U}^T \cdot \underline{D}'\,\hat{\epsilon}\, dx \tag{3.30}$$

where the elemental volume dv and surface ds in three dimension reduce to dxdz and dx in two dimensions, respectively. Using Gauss's theorem on the last term of Equation 3.30 we get

$$\int_S \delta\hat{U}^T \cdot \underline{D}'\,\hat{\epsilon}\, dx = \int_V DZ^T\, (\delta\hat{U}^T \cdot \underline{D}'\,\hat{\epsilon}\,)dxdz \tag{3.31}$$

where $DZ^T = \frac{\partial}{\partial z}\begin{bmatrix} 1 & 0 \\ 0 & 1 \end{bmatrix}^T$ and T represents transpose. Since $\frac{\partial}{\partial z}$ operates on a product vectors $\delta\hat{U}$ and $\hat{\epsilon}$ the right hand side of Equation 3.31 expands to

$$\int_V \frac{\partial}{\partial z} I^T(\delta\hat{U}^T \cdot \underline{D}'\hat{\epsilon}\,)dxdz = \int_V DZ^T\, \delta\hat{U}^T \cdot (\underline{D}'\hat{\epsilon}\,)dxdz$$

$$+ \int_V \delta\hat{U}^T \cdot \underline{D}'\, DZ^T\, \hat{\epsilon}^T\, dxdz \tag{3.32}$$

If we rewrite Equation 3.6

$$\hat{\varepsilon} = \left(\frac{\partial U_x}{\partial x} , \frac{\partial U_z}{\partial z} , \frac{\partial U_z}{\partial x} + \frac{\partial U_x}{\partial z} \right) = \begin{bmatrix} \frac{\partial}{\partial x} & 0 \\ 0 & \frac{\partial}{\partial z} \\ \frac{\partial}{\partial z} & \frac{\partial}{\partial x} \end{bmatrix} (U_x, U_z) \qquad (3.33)$$

$$\hat{\varepsilon}^T = \left(\begin{bmatrix} \frac{\partial}{\partial x} & 0 \\ 0 & \frac{\partial}{\partial z} \\ \frac{\partial}{\partial z} & \frac{\partial}{\partial x} \end{bmatrix} (U_x, U_z) \right)^T \qquad (3.34)$$

and substitute Equations 3.32 - 3.34 into Equation 3.30 we have

$$\int (\delta U^T \cdot \underline{H}\, \hat{U} - DZ^T\, \hat{U}^T \cdot \underline{H}'\, \hat{U})\, dxdz = 0 \qquad (3.35)$$

where

$$\underline{H} = \begin{bmatrix} K^2(\lambda + 2\mu) - \rho\omega^2 & iK\lambda \frac{\partial}{\partial z} \\ iK\mu \frac{\partial}{\partial z} & K^2\mu - \rho\omega^2 \end{bmatrix} \qquad (3.36)$$

and

$$\underline{H}' = \begin{bmatrix} - iK\lambda & (\lambda + 2\mu) \frac{\partial}{\partial z} \\ \mu \frac{\partial}{\partial z} & - iK\mu \end{bmatrix} \qquad (3.37)$$

Equations 3.35 involves partial derivatives with respect to z of the displacement U in Equation 3.22 which is an implicit function of z. The differential equations obtained in this way will possess the unknowns

in the argument of the exponential functions and thus their solution are nearly impossible. For this reason we use the technique of the finite element to derive equations that may be solved conveniently.

For the layered region we use a one dimensional element, i.e., an element with two nodal points for the two horizontal plane interfaces sharing the j^{th} layer as shown in Figure 5. Let the displacement vector U be approximated by,

$$\hat{U} = \underline{N}\,\hat{V} \tag{3.38}$$

so that

$$\hat{U}^T = \hat{V}^T\,\underline{N}^T \tag{3.39}$$

The partial derivative of this with respect to z is

$$\frac{\partial}{\partial z}\hat{U}^T = \hat{V}^T\,\frac{\partial}{\partial z}\underline{N}^T \tag{3.40}$$

where, from Equation 3.3, for a linear expansion

$$\underline{N} = [N_i,\ N_j] = 1/2\begin{bmatrix} 1-\eta & 0 & 1+\eta & 0 \\ 0 & 1-\eta & 0 & 1+\eta \end{bmatrix} \tag{3.41}$$

If the origin is at the midpoint of the layer then

$$\eta = \frac{z}{h/2} \tag{3.42}$$

$z = -h/2$, $\eta = -1$ at the top of the layer and $z = h/2$, $\eta = 1$ at the bottom of the layer (124) as shown in Figure 5.

Substitution of Equations 3.38-3.40 into Equation 3.35 results in

$$\sum_{\text{Layers}} \int_x \delta\hat{V}^T \left(\int_z K^2 \underline{N}^T \underline{a}\, \underline{N} + iK\underline{N}^T \underline{c}\, \frac{\partial}{\partial z}\underline{N} - \rho\omega^2 \underline{N}^T\underline{N} + \frac{\partial}{\partial z}\underline{N}^T\, \underline{g}\, \frac{\partial}{\partial z}\underline{N} \right.$$

$$\left. + iK\, \frac{\partial}{\partial z}\underline{N}^T \underline{c}^T \underline{N} \right) \hat{V}\, dxdz = 0 \qquad (3.43)$$

where

$$\underline{a} = \begin{bmatrix} \lambda + 2\mu & 0 \\ 0 & \mu \end{bmatrix}, \quad \underline{c} = \begin{bmatrix} 0 & \lambda \\ \mu & 0 \end{bmatrix}, \text{ and } \underline{g} = \begin{bmatrix} \mu & 0 \\ 0 & \lambda + 2\mu \end{bmatrix} \qquad (3.44)$$

Evaluation of the integral for each layer gives

$$\int_0^h \frac{\partial}{\partial z}\underline{N}^T\, \underline{g}\, \frac{\partial}{\partial z}\underline{N}\, dz = \underline{G}_j$$

$$\int_0^h \underline{N}^T\, \underline{a}\, \underline{N}\, dz = \underline{A}_j \qquad (3.45)$$

$$\int_0^h \frac{\partial}{\partial z}\underline{N}^T\, \underline{c}\, \underline{N}\, dz = \underline{C}_j$$

$$\int_0^h \underline{N}^T\, \underline{N}\, dz = \underline{M}_j$$

And from Equation 3.42

$$\frac{\partial}{\partial z} = \frac{1}{h/2}\frac{\partial}{\partial \eta} \qquad (3.46)$$

so that

$$\frac{\partial}{\partial z}\underline{N} = \frac{1}{h/2}\frac{\partial}{\partial \eta}\left(1/2 \begin{bmatrix} 1-\eta & 0 & 1+\eta & 0 \\ 0 & 1-\eta & 0 & 1+\eta \end{bmatrix} \right) = \frac{1}{h}\begin{bmatrix} -1 & 0 & 1 & 0 \\ 0 & -1 & 0 & 1 \end{bmatrix} \qquad (3.47)$$

Substitution of Equations 3.41, 3.42 and 3.46 into the first of Equations 3.45 leads to

$$\int_0^h \frac{\partial}{\partial z}\underline{N}^T \underline{g} \frac{\partial}{\partial z}\underline{N}\, dz = h/2 \int_{-1}^{1} \frac{1}{h^2} \begin{bmatrix} -1 & 0 \\ 0 & -1 \\ 1 & 0 \\ 0 & 1 \end{bmatrix} \begin{bmatrix} \mu & 0 \\ 0 & \lambda+2\mu \end{bmatrix} \begin{bmatrix} -1 & 0 & 1 & 0 \\ 0 & -1 & 0 & 1 \end{bmatrix} dn$$

or

$$\underline{G}_j = \frac{1}{h_j} \begin{bmatrix} \mu & 0 & -\mu & 0 \\ 0 & \lambda+2\mu & 0 & -(\lambda+2\mu) \\ -\mu & 0 & \mu & 0 \\ 0 & -(\lambda+2\mu) & 0 & \lambda+2\mu \end{bmatrix} \tag{3.48}$$

Similarly,

$$\underline{A}_j = \frac{h_j}{6} \begin{bmatrix} 2(\lambda+2\mu) & 0 & \lambda+2\mu & 0 \\ 0 & 2\mu & 0 & \mu \\ \lambda+2\mu & 0 & 2(\lambda+2\mu) & 0 \\ 0 & \mu & 0 & 2\mu \end{bmatrix}, \quad \underline{C}_j = 1/2 \begin{bmatrix} 0 & \lambda & 0 & -\lambda \\ \mu & 0 & -\mu & 0 \\ 0 & \lambda & 0 & -\lambda \\ \mu & 0 & -\mu & 0 \end{bmatrix} \tag{3.49}$$

$$\underline{M}_j = \rho_j\, h_j/6 \begin{bmatrix} 2 & 0 & 1 & 0 \\ 0 & 2 & 0 & 1 \\ 1 & 0 & 2 & 0 \\ 0 & 1 & 0 & 2 \end{bmatrix} \tag{3.50}$$

The j^{th} layer matrice $\underline{A}_j$, $\underline{B}_j$, $\underline{C}_j$ and $\underline{M}_j$ are the same matrices introduced by Lysmer and Drake (80) which were derived originally by Lysmer and Waas (79) by a different method. Addition of these submatrices over the

layers by the method of Lysmer and Drake (80), as shown in Figure 6 for a typical matrix $\underline{A}_j$, will result in

$$\int_x \delta V^T (K^2 \underline{A} - iK\underline{C} + iK\underline{C}^T + \underline{G} - \omega^2 \underline{M})\ \hat{V}\ dx = 0 \qquad (3.51)$$

For an arbitrary virtual displacement vector δV^T (37) we may write, since the expression in parentheses is independent of x,

$$(K^2 \underline{A} - iK\underline{C} + iK\underline{C}^T + \underline{G} - \omega^2 \underline{M})\ \hat{V} = 0 \qquad (3.52)$$

Equation 3.52 represents a nonlinear eigenvalue problem with eigenvalue K^2 and eigenvector $\underline{V}$ whose solution is usually obtained by the vector iteration method. The analysis of the derivation of the solution of Equation 3.52 will not be presented here but the reader is recommended to refer to the excellent texts by Bathe and Wilson (11), Waas (117), and Zienkiewicz (124) for engineering applications and by Ruhe (100), Papaconstantinov (91), and Wilkinson (120) for theoretical discussions. At a particular frequency, the generalized eigenvalue problem (Equation 3.52) has 4N eigenvalues $\sum_i^{2N} K_i^2$ and corresponding eigenvectors $\sum^{2N} \hat{V}_i$, N being the number of layers. The eigenvalues may be, real, imaginary or complex.

In the derivation of our eigenvalue problem we assumed that the matrix moduli $\underline{D}$ be real. For a viscoelastic model we may substitute the effective moduli of Equation 2.17 of Chapter II into matrix D, which is

$$\underline{D} = \begin{bmatrix} \lambda_e+2\mu_e & \lambda_e & 0 \\ \lambda_e & \lambda_e+2\mu_e & 0 \\ 0 & 0 & \mu_e \end{bmatrix} \qquad (3.53)$$

where

$$\lambda_e = K_e - 2/3\ \mu_e \tag{3.54}$$

and subscript e stands for effective or complex moduli. If matrix $\underline{D}$ is real, the motion of the Rayleigh wave in the layers is determined by the number of real wave numbers obtained from the solution of the eigenvalue problem. If matrix $\underline{D}$ is complex the eigenvalue problem has complex eigenvalues. The real part of the eigenvalue determines the phase velocity of the wave in the layers and the imaginary part determines the attenuation of the wave in the horizontal direction. Thus,

$$\text{phase velocity} = \frac{\text{omega}}{\text{REAL (wavenumber)}} \tag{3.55}$$

$$\text{attenuation} = 2\ \frac{\text{IMAG (wavenumber)}}{\text{REAL (wavenumber)}} \tag{3.55a}$$

According to the theory of linear differential equation, if each eigenvalue and the corresponding independent eigenvectors determine a solution then a linear combination of these solutions is also a solution. Therefore, if K_i for $i = 1, 2N$ are the eigenvalues and $\hat{V}_i$ for $i = 1, 2N$ are the corresponding eigenvectors the complete motion of the layered region may be obtained by superposition of these solutions as

$$\hat{U} = \sum_{i}^{2N} \alpha_i\ \hat{V}_i\ e^{i(\omega t - K_i x)} \tag{3.56}$$

in which each multiplier α is an amplitude factor specifying the contribution of the mode i to the total motion. At the boundary with no phase change the motion is

$$\hat{U} = \underline{V}\ \hat{\alpha} \tag{3.57}$$

where $\underline{V}$ is the matrix whose columns are the eigenvectors $\hat{V}_i$. If the displacement $\hat{U}$ in Equation 3.57 is known, the multiplier vector α can be solved for as

$$\hat{\alpha} = \underline{V}^{-1} \hat{U} \tag{3.58}$$

D. Vertical Boundary

Let us rewrite Equation 3.11

$$\int_V (\sigma_{ij}\ \delta\epsilon_{ij} - F_i\ \delta U_i)dv = \int_S T_i\ \delta U_i ds \tag{3.59}$$

and substitute Equation 3.13 into it; the result is

$$\int_V (\sigma_{ij,j} + F_i)\ \delta U_i dv + \int_S (T_i - \sigma_{ij}\nu)\ \delta U_i ds = 0 \tag{3.60}$$

This equation can be satisfied, for an arbitrary δU_i, if

$$\sigma_{ij,j} + F_i = 0\ , \tag{3.61}$$

the equation of motion, and either

$$\delta U_i = 0 \tag{3.62}$$

on the rigid boundary or

$$\int_S (T_i - \sigma_{ij}\nu)\ \delta U_i\ ds = 0\ , \tag{3.63}$$

the surface boundary condition on the vertical plane. The elemental surface ds in this case is dz, therefore,

$$\int_S T_i\ \delta U_i dz = \int_S \sigma_{ij}\nu\ \delta U_i dz \tag{3.64}$$

On the vertical plane the stress component in the z direction is zero and the surface stress $\sigma_{ij}\nu$ in Equation 3.64, in vector form, is

$$\hat{\sigma\nu} = (\sigma_{xx}, \sigma_{xz}) \tag{3.65}$$

and the matrix moduli corresponding to Equation 3.28, in this case is

$$\underline{D_v} = \begin{bmatrix} \lambda+2 & \lambda & 0 \\ 0 & 0 & \mu \end{bmatrix} \tag{3.66}$$

Now the right hand side of Equation 3.63 becomes

$$\int_S \hat{\sigma\nu} \cdot \delta\hat{U}\, dz = \int_S \delta\hat{U}^T \cdot \underline{D_v}\, \hat{\epsilon}\, dz \tag{3.67}$$

Substituting Equations 3.33, 3.38-3.42, and 3.57 into Equation 3.67, we have

$$\sum_{\text{Layers}} \int_S \hat{\sigma\nu} \cdot \delta\hat{U}\, dz = (i\, \underline{A}\, \underline{V}\, \underline{K} - \underline{C}\, \underline{V})\, \hat{\alpha}\, \delta\hat{V} \tag{3.68}$$

The derivation of this equation takes the same steps that lead to the derivation of Equation 3.52. In Equation 3.68 all matrices and the vector $\hat{\alpha}$ have been defined except for the matrix $\underline{K}$. Matrix $\underline{K}$ is a diagonal matrix whose diagonal elements are the eigenvalues obtained from the solution of the eigenvalue problem. Equation 3.68 represents the force applied at the boundary with the assumption that the finite element region is removed. The reaction forces acting on the finite element region follow then from the equilibrium consideration, i.e., a force equal and opposite to that of Equation 3.68

$$\hat{P} = (i\, \underline{A}\, \underline{V}\, \underline{K} - \underline{C}\, \underline{V})\, \hat{\alpha} \tag{3.69}$$

Substitution of $\hat{\alpha}$ from Equation 3.58 into Equation 3.69 yields

$$\hat{P} = \underline{L}\,\hat{U} \tag{3.70}$$

where

$$\underline{L} = i\,\underline{A}\,\underline{V}\,\underline{K}\,\underline{V}^{-1} - C \tag{3.71}$$

is called the stiffness matrix of the vertical boundary.

E. Motion in the Finite Element Region

Rewriting Equation 3.10 with the assumption that the inertia force be F_i, we have, in vector form,

$$\int_V \hat{\sigma} \cdot \hat{\delta\varepsilon}\, dv - \rho\omega^2\ \hat{U}^T \cdot \hat{U})\, dxdz = \int_S \delta\hat{U}^T \cdot T\hat{v}\, dz \tag{3.72}$$

The left hand side of Equation 3.72 can be written as

$$\int_V (\delta\varepsilon^T \cdot \underline{D}\hat{\varepsilon} - \rho\omega\ \ \delta\hat{U}^T \cdot \hat{U})\, dxdz = \int_V (\delta\hat{U}^T\underline{B}^T \cdot \underline{D}\,\underline{B}\,\hat{U} - \rho\omega^2\,\delta\hat{U}^T \cdot \hat{U})\, dxdz \tag{3.73}$$

where matrix $\underline{B}$ is given by Equation 3.6. Substituting Equations 3.38-3.42 into the expression 3.73, Equation 3.72 becomes

$$\int_V (\delta\hat{V}^T\underline{N}\,\underline{B}^T \cdot \underline{D}\,\underline{B}\,\underline{N}^T\hat{V} - \rho\omega^2\,\delta\hat{V}^T\underline{N} \cdot \underline{N}^T\hat{V})\, dxdz = \pm \int_S \delta\hat{V}^T\underline{N} \cdot T\hat{v}\ \ dz \tag{3.74}$$

where, from Equation 3.73, for a two dimensional expansion

$$\underline{N} = [N_i, N_j, N_K, N_L] = \begin{bmatrix} \tfrac{1}{2}\eta(\eta-1) & 0 & 1-\eta^2 & 0 & \tfrac{1}{2}\eta(\eta+1) & 0 \\ 0 & \tfrac{1}{2}\eta(\eta-1) & 0 & 1-\eta^2 & 0 & \tfrac{1}{2}\eta(\eta+1) \end{bmatrix} \tag{3.75}$$

The integration limits on the right hand side of Equation 3.74 is through the two vertical boundaries on the left and right hand sides of the irregular region and the $\pm$ signs represent the forces that are acting to or away from the finite element region. All in all, there are a maximum of four different forces acting at the vertical boundaries thatare determined from the right hand side of Equation 3.74. One of these forces was determined by Equation 3.69. If the incident energy is from the left then there are three forces acting at the vertical boundaries. A force P_L determined by Equation 3.69 due to the incident energy at the left hand boundary, a force P_R due to reflection of energy at the left boundary, and a force P_T due to transmission of energy at the right boundary. Thus, the right hand side of Equation 3.74 is integrated to produce the above three forces, for an arbitrary $\delta\hat{V}^T$. Substitution of Equations 3.6, 3.25a, and 3.75 into Equation 3.74, the first term on the left hand side is integrated, for an arbitrary $\delta\hat{V}^T$, to give

$$\int_V \underline{N}\,\underline{B}^T \cdot \underline{D}\,\underline{B}\,\underline{N}^T \, dv = \underline{K_e} \tag{3.76}$$

Matrix $\underline{K_e}$ is an 8 by 8 stiffness matrix originating from four nodal points of the element, each node having a horizontal and a vertical force. To obtain the stiffness matrix for all elements Equation 3.76 must be summed over the elements. Thus,

$$\sum_{\text{Elements}} \underline{K_e} = \underline{K} \tag{3.77}$$

Substitution of the contribution from Equations 3.45, 3.69, and 3.77 into Equation 3.74 will get

$$(\underline{K} - \omega^2 \underline{M})\,\hat{V} = P_T - P_L - P_R \tag{3.78}$$

or

$$(\underline{K} - \omega^2 \underline{M})\,\hat{V} = \underline{T}\hat{V}_T - \underline{L}\hat{V}_L - \underline{R}\hat{V}_R = \underline{T}\hat{V}_T - \underline{L}\hat{V}_L - \underline{R}(\hat{V}_L + \hat{V}_R) + \underline{R}\hat{V}_L \tag{3.79}$$

The vector $\hat{V}$ represents the horizontal and vertical displacements of the nodal points of the irregular region. Vector $\hat{V}_L$ is the known displacements at the left hand boundary, obtained from the solution of the eigenvalue problem. The unknown vectors $\hat{V}_R$, the reflected displacements, and vector $\hat{V}_T$, the right hand boundary displacement can be incorporated into vector $\hat{V}$ as follows. The first 2N elements of vector $\hat{V}$ are equal to vector $\hat{V}_L$ and if the vectors $\hat{V}_L + \hat{V}_R$ are substituted for the 2N elements of vector $\hat{V}$, then the unknown vector V_R can be solved for by

$$\hat{V}_R = \hat{V}_{2N} - \hat{V}_L \,. \tag{3.80}$$

The last 2N elements of vector $\hat{V}$ are equal to vector $\hat{V}_T$. Therefore, Equation 3.79 can be written as

$$(\underline{K} - \omega^2\underline{M} + \underline{R} - \underline{T})\,\hat{V} = (\underline{R} - \underline{L})\,\hat{V}_L \,. \tag{3.81}$$

The unknown vector $\hat{V}$ in this equation can be solved for by the standard method (28, 29).

CHAPTER IV

ENERGY OF A PROPAGATING WAVE

A. Summary

Elasticity theory assumes the medium of propagation to be conservative, a condition in which no energy is lost or changed into other forms. In reality this process if thermodynamically reversible only if it occurs with infinitisimal speed, so that the thermodynamic equilibrium is established in the body at every instant. Stressed body however, is in motion and has finite velocity. The body is not in equilibrium at every instant and, therefore, processes such as stress-induced ordering or thermal displacement of the point defect, change in dislocation through the crystal lattice, and viscous sliding at grain boundaries will take place in it and cause it to return to equilibrium. The existence of these processes has the result that the motion is irreversible, since they require the overcoming of a barrier to initiation. At the end of each cycle of stress it is impossible to reproduce exactly the state of the start; hence, there will be hysteresis effects and energy dissipation or attenuation (Figure 1). Because of these effects the amplitude of the propagating Rayleigh wave falls off somewhat more rapidly than elastic theory predicts. Although attenuation is extremely important in practice, it must still be, in some sense, small, since otherwise waves would not propagate to any appreciable

distance. For large attenuation the propagation process becomes one of the diffusion rather than propagation. Since waves propagate, the assumption of small attenuation keeps the theory of elasticity valid.

The dissipation of energy arises from such a variety of mechanisms that is impossible to discuss them all here. The most effective of all mechanisms fall into the class of viscoelasticity in which the energy of the wave field is taken up by processes such as defect in mobility, diffusion rate, phase change, etc., and is restored partially or completely to the field with a delay. As a result of this delay, the restored energy finds itself partially out of phase with the original wave and destructive interference takes place (114).

B. Energy Flux Vector

The energy flux vector $E_i(t)$ at time t is defined as the rate at which energy leaves the material across an element of area normal to the x_i - axis, measured per unit area. It is given by

$$E_i(t) = - \sigma_{ij}(t) \dot{U}_j(t) \qquad (4.1)$$

where $\dot{U}_j$ is the velocity vector created by the application of the stress tensor σ_{ij}, the minus sign is the indication that the energy is leaving the material. For an isotropic, elastic medium, the direction of the energy flow is normal to the wavefront. Equation 4.1 fluctuates with time and a mean energy flux vector is defined as the average of $E_i(t)$ over a cycle. Thus,

$$\bar{E}_i = \frac{\omega}{2\pi} \int_0^{\frac{2\pi}{\omega}} E_i(t)\, dt \qquad (4.2)$$

The energy flux vector, E_i, contains three components. Corresponding to the directions of propagation, i.e., in vector form,

$$E_i = \hat{E} = \underline{\sigma} \cdot \frac{\partial}{\partial t} \hat{U} \qquad (4.3)$$

where matrix $\underline{\sigma}$ and vector $\frac{\partial}{\partial t} \hat{U}$ are given by

$$\underline{\sigma} = \begin{bmatrix} \sigma_{xx} & \sigma_{xy} & \sigma_{xz} \\ \sigma_{yx} & \sigma_{yy} & \sigma_{yz} \\ \sigma_{zx} & \sigma_{zy} & \sigma_{zz} \end{bmatrix} ,$$

$$\frac{\partial}{\partial t} \hat{U} = \frac{\partial}{\partial t} \begin{bmatrix} U_x \\ U_y \\ U_z \end{bmatrix} \text{ EXP } (i(\omega t - K_x x - K_y y - K_z z)) \qquad (4.4)$$

For a plane wave propagation in the x direction, vector $\hat{E}$ reduces to a one dimensional energy flux, E, and is given by, setting i = 1, and j = 1,3 in Equation 4.1, we have

$$E = \left(\frac{\partial}{\partial t} \hat{U} \right)^T \cdot \hat{\sigma} \qquad (4.5)$$

where vectors $\hat{\sigma}$ and $\frac{\partial}{\partial t} \hat{U}$ are given by

$$\hat{\sigma} = (\sigma_{xx}, \sigma_{xz}) , \quad \frac{\partial}{\partial t} \hat{U} = \frac{\partial}{\partial t} (U_x, U_z) \text{ EXP } (i(\omega t - Kx)) \qquad (4.6)$$

the stress vector represents normal and shear stresses on the surface area normal to the direction of propagation. The energy in Equation 4.5

in an elastic medium is normal to the wavefront, i.e., the energy is propagating in the x direction normal to the z axis, only if the propagation constant K is real. Let us analyze the state of vector $\hat{K}$ in general. From Equation 4.4, vector $\hat{K}$ in a plane propagation is

$$\hat{K} = K_x\hat{x} + K_z\hat{z} \tag{4.7}$$

where $\hat{x}$ and $\hat{z}$ represent direction cosines in the x and z directions, respectively. If the matrix moduli $\underline{D}$ in Chapter III contains the effective moduli K_e and μ_e, discussed in Chapter II, Section C, then vector $\hat{K}$ is complex and is given by

$$\hat{K} = \hat{K}_R - i\hat{K}_I \ . \tag{4.7a}$$

Rewriting the vector $\hat{U}$ of Equation 4.4 in two dimensions

$$\hat{U} = \begin{pmatrix} U_x(z) \\ U_z(z) \end{pmatrix} \text{ EXP } (i(\omega t - \hat{K} \cdot \hat{X})), \tag{4.8}$$

where

$$\hat{X} = x\hat{x} + z\hat{z}, \tag{4.9}$$

and substituting Equation 4.7 we have

$$\hat{U} = \hat{U}(z)e^{-\hat{K_I}\cdot\hat{X}} \ e^{i(\omega t - \hat{K}_R\cdot\hat{X})} \tag{4.10}$$

where K_I is called the attenuation vector. To include attenuation from the vector U(z) it is better to write Equation 4.10 as

$$\hat{U} = |\hat{U}(z)| \ e^{-\hat{K_I}\cdot\hat{X}} \ e^{i(\omega t - \hat{K}_R\cdot\hat{X})} \tag{4.11}$$

The dot product $\hat{K}_I \cdot \hat{X}$ can be expanded as

$$\hat{K}_I \cdot \hat{X} = \beta X + \gamma z + \text{ARG}(\hat{U}(z)) \tag{4.12}$$

where β and γ represent the components of $\hat{K}_I$ in x and z directions, respectively, and $\text{ARG}(\hat{U}(z))$ is the attenuation factor due to the vector $\hat{U}(z)$. The existence of a surface wave depends on whether vector $\hat{K}_I$ is zero or not.

The attenuation vector $\hat{K}_I$, given by Equation 4.7a, is not, in general, perpendicular to the propagation vector $\hat{K}_R$; the angle θ between the directions of the two vectors is between zero and $\pi/2$, i.e.,

$$0 < \theta \leq \pi/2. \tag{4.13}$$

when $\theta = 0$, $\hat{K}_I = \hat{0}$, and therefore there exists an undamped wave. When $\theta = \pi/2$, the direction of attenuation vector $\hat{K}_I$ is perpendicular to the direction of propagation vector $\hat{K}_R$ and the wave propagates in the direction normal to the surface of constant phase and attenuates in the direction normal to the surface of constant amplitude. This occurs when $\beta = \gamma = 0$ in Equation 4.12 and the attenuation is due to the vector $\hat{U}(z)$; that is, the amplitude will dampout in the z direction. This is the classical Rayleigh wave.

The surface of constant phase may be used to determine the phase velocity of the wave by setting the progressive part of Equation 4.11 equal to a constant, say, $\pi/2$,

$$e^{i(\omega t - \hat{K}\cdot\hat{X})} = e^{\pi/2} \tag{4.14}$$

or

$$\omega t - \hat{K} \cdot \hat{X} = - i\pi/2 \tag{4.15}$$

Performing the dot product in Equation 4.15 we get,

$$\omega t - K_x X - K_z Z = - i\pi/2 \ . \tag{4.16}$$

Taking the partial derivative of x and z with respect to t in Equation 4.16, we have,

$$\omega - K_x \frac{\partial x}{\partial t} = 0, \qquad \omega - K_z \frac{\partial z}{\partial t} = 0 \tag{4.17}$$

Solving for $\frac{\partial x}{\partial t}$ and $\frac{\partial z}{\partial t}$, the phase velocities in the horizontal and vertical directions are given by

$$V_x = \frac{\omega}{K_x} , \quad V_z = \frac{\omega}{K_z} \tag{4.18}$$

If the vector $\hat{K}$ is complex then

$$K_x = K_x + i\beta , \quad K_z = K_z + i\gamma , \tag{4.19}$$

and

$$V_x = \frac{\omega}{K_x+i\beta} = \frac{\omega(K_x-i\beta)}{K_x^2 + \beta^2} = \frac{\omega K_x}{K_x^2+\beta^2} - i \frac{\beta\omega}{K_x^2+\beta^2} , \tag{4.20}$$

or approximately

$$V_x = V_x - i\beta V_x = V_x(1 - i\beta), \tag{4.21}$$

for small β such that $\beta^2 \to 0$. Similarly,

$$V_z = V_z(1 - i\gamma), \tag{4.22}$$

for small γ such that $\gamma^2 \to 0$. The size of β and γ are ordinarily between .01 and .001 of the K_x and of the K_z, respectively so that the above assumption is valid.

C. Energy Flux in Terms of the Wave-Number and the Amplitude

Let us rewrite Equation 4.5 and integrate it through a period as in Equation 4.2; the result is

$$\bar{E} = \frac{\omega}{2\pi} \int_0^{\frac{2\pi}{\omega}} E \, dt = \frac{\omega}{2\pi} \int_0^{\frac{2\pi}{\omega}} \left(\frac{\partial}{\partial t} \hat{U}\right)^T \cdot \hat{\sigma} \, dt \tag{4.23}$$

Since most of this study is concerned with the energy and its balance, the analysis of the derivation of the energy relationship seems essential. Thus, we study Equation 4.23 in detail. Consider the dot product $\hat{U}^T \cdot \hat{\sigma}$ which is the energy density normal to the z plane; the energy through that plane is

$$\int_0^h \hat{U}^T \cdot \hat{\sigma} \, dz = \int_0^h \hat{U}^T \cdot \underline{D_v} \, \hat{\varepsilon} \, dz \tag{4.24}$$

where

$$\underline{D_v} = \begin{bmatrix} \lambda+2\mu & \lambda & 0 \\ 0 & 0 & \mu \end{bmatrix} \tag{4.25}$$

and

$$\hat{\varepsilon} = \begin{bmatrix} \frac{\partial}{\partial x} & 0 \\ 0 & \frac{\partial}{\partial z} \\ \frac{\partial}{\partial z} & \frac{\partial}{\partial x} \end{bmatrix} (U_x, U_z) \tag{4.25a}$$

Decomposing the matrix in Equation 4.25 as

$$\begin{bmatrix} \frac{\partial}{\partial x} & 0 \\ 0 & \frac{\partial}{\partial z} \\ \frac{\partial}{\partial z} & \frac{\partial}{\partial x} \end{bmatrix} = \begin{bmatrix} \frac{\partial}{\partial x} & 0 \\ 0 & 0 \\ 0 & \frac{\partial}{\partial x} \end{bmatrix} + \begin{bmatrix} 0 & 0 \\ 0 & \frac{\partial}{\partial z} \\ \frac{\partial}{\partial z} & 0 \end{bmatrix} \tag{4.26}$$

and substituting this and Equation 4.25 into Equation 4.24 gives

$$\int_0^h \hat{U}^T \cdot \underline{D_v} \hat{\varepsilon} dz = \int_0^h \hat{U}^T \cdot \left(\begin{bmatrix} \lambda+2\mu & \lambda & 0 \\ 0 & 0 & \mu \end{bmatrix} \begin{bmatrix} 0 & 0 \\ 0 & \frac{\partial}{\partial z} \\ \frac{\partial}{\partial z} & 0 \end{bmatrix} + \begin{bmatrix} \lambda+2\mu & \lambda & 0 \\ 0 & 0 & \mu \end{bmatrix} \begin{bmatrix} \frac{\partial}{\partial x} & 0 \\ 0 & 0 \\ 0 & \frac{\partial}{\partial x} \end{bmatrix} \right) \hat{U} dz$$

$$= \int_0^h \hat{U}^T \left(\begin{bmatrix} 0 & \lambda \frac{\partial}{\partial z} \\ \mu \frac{\partial}{\partial z} & 0 \end{bmatrix} + \begin{bmatrix} (\lambda+2\mu)(-iK) & 0 \\ 0 & -iK\mu \end{bmatrix} \right) \hat{U} \, dz$$

or

$$\int_0^h \hat{U}^T \cdot \underline{D_v} \hat{\varepsilon} dz = \int_0^h \hat{U}^T \left(\begin{bmatrix} 0 & \lambda \\ \mu & 0 \end{bmatrix} \frac{\partial}{\partial z} - iK \begin{bmatrix} \lambda+2\mu & 0 \\ 0 & \mu \end{bmatrix} \right) \hat{U} \, dz. \tag{4.27}$$

Substituting Equations 3.38, 3.40 and 3.42 into Equation 4.27 we have

$$\int_0^h \hat{U}^T \cdot \underline{D}_v \hat{\epsilon} dz = \int_0^h \hat{V}^T \cdot \underline{N}^T \underline{C} \frac{\partial}{\partial z} \underline{N} \hat{V} \, dz - iK \int_0^h \hat{V}^T \cdot \underline{N}^T \underline{a} \underline{N} \hat{V} \, dz \tag{4.28}$$

where

$$\underline{C} = \begin{bmatrix} 0 & \lambda \\ \mu & 0 \end{bmatrix}, \quad \underline{a} = \begin{bmatrix} \lambda+2\mu & 0 \\ 0 & \mu \end{bmatrix} \tag{4.29}$$

From Equation 3.42, if we substitute

$$\frac{\partial}{\partial z} = \frac{1}{h/2} \frac{\partial}{\partial \mu} \tag{4.30}$$

and

$$\frac{\partial}{\partial z} \underline{N} = \frac{1}{h} \begin{bmatrix} -1 & 0 & 1 & 0 \\ 0 & -1 & 0 & 1 \end{bmatrix} \tag{4.31}$$

into Equation 4.28 and changing the variable of integration we have

$$\int_0^h \hat{U}^T \cdot \underline{D}_v \hat{\epsilon} dz = \int_{-1}^1 \hat{V}^T 1/2 \begin{bmatrix} 1-\eta & 0 \\ 0 & 1-\eta \\ 1+\eta & 0 \\ 0 & 1+\eta \end{bmatrix} \underline{C} \frac{1}{h} \begin{bmatrix} -1 & 0 & 1 & 0 \\ 0 & -1 & 0 & 1 \end{bmatrix} \hat{V} \frac{h}{2} d\eta$$

$$- iK \int_{-1}^1 \hat{V}^T 1/2 \begin{bmatrix} 1-\eta & 0 \\ 0 & 1-\eta \\ 1+\eta & 0 \\ 0 & 1+\eta \end{bmatrix} \underline{a} \frac{1}{2} \begin{bmatrix} 1-\eta & 0 & 1+\eta & 0 \\ 0 & 1-\eta & 0 & 1+\eta \end{bmatrix} \hat{V} \frac{h}{2} d\eta \tag{4.32}$$

or

$$\int_0^h \hat{U}^T \cdot \underline{D_v} \hat{\epsilon} dz = \int_{-1}^{1} \hat{V}^T \cdot \frac{1}{4} \underline{R} \hat{V} \, d\eta - iK \int_{-1}^{1} \hat{V}^T \frac{1}{8} h \underline{S} \hat{V} \, d\eta \qquad (4.33)$$

where

$$\underline{R} = \begin{bmatrix} 0 & -\lambda(1-\eta) & 0 & \lambda(1-\eta) \\ -\mu(1-\eta) & 0 & \mu(1-\eta) & 0 \\ 0 & -\lambda(1+\eta) & 0 & \lambda(1+\eta) \\ -\mu(1+\eta) & 0 & \mu(1+\eta) & 0 \end{bmatrix} \qquad (4.34)$$

and

$$\underline{S} = \begin{bmatrix} (1-\eta)^2(\lambda+2\mu) & 0 & (1-\eta^2)(\lambda+2\mu) & 0 \\ 0 & (1-\eta)^2\mu & 0 & (1-\eta^2)\mu \\ (1-\eta)^2(\lambda+2\mu) & 0 & (1+\eta)^2(\lambda+2\mu) & 0 \\ 0 & (1-\eta^2)\mu & 0 & (1+\eta)^2\mu \end{bmatrix} \qquad (4.35)$$

Integration of Equation 4.33 yields

$$\int_0^h \hat{U}^T \cdot \underline{D_v} \hat{\epsilon} dz = \hat{V}^T \cdot \underline{C_j} \hat{V} + iK \hat{V}^T \cdot \underline{A_j} \hat{V} = \hat{V}^T \cdot (\underline{C_j} + iK\underline{A_j}) \hat{V} \qquad (4.36)$$

for the j^{th} layer. Where

$$\underline{C_j} = \frac{1}{2} \begin{bmatrix} 0 & \lambda & 0 & -\lambda \\ \mu & 0 & -\mu & 0 \\ 0 & \lambda & 0 & -\lambda \\ \mu & 0 & -\mu & 0 \end{bmatrix}, \text{ and } \underline{A_j} = \frac{h_j}{6} \begin{bmatrix} 2(\lambda+2\mu) & 0 & \lambda+2\mu & 0 \\ 0 & 2\mu & 0 & \mu \\ \lambda+2\mu & 0 & 2(\lambda+2\mu) & 0 \\ 0 & \mu & 0 & 2\mu \end{bmatrix} \qquad (4.37)$$

Summing up Equation 4.36 over all layers results in

$$\sum_{\text{Layers}} \int_0^h \hat{U}^T \cdot \underline{D_v} \hat{\epsilon} dz = \sum_{j=1}^{2N} \hat{V}^T \cdot (\underline{C_j} + iK\underline{A_j}) \hat{V} = \hat{V}^T \cdot (\underline{C} + iK\underline{A}) \hat{V} \qquad (4.38)$$

Recall that

$$\hat{U} = \hat{U}(z)e^{i(\omega t - Kx)} \quad , \quad \text{and} \quad \hat{U} = \underline{N}\,\hat{V} \tag{4.39}$$

therefore,

$$\hat{V} = \hat{V}e^{i(\omega t - Kx)} \quad \text{and} \quad \frac{\partial}{\partial t}\hat{V} = i\omega\hat{V} \; . \tag{4.40}$$

Substituting Equations 4.38 and 4.40 into Equation 4.23, with a realistic definition, the average energy which is carried across the vertical boundary, by the mode K, is given by

$$\hat{E} = \frac{\omega}{2\pi}\int_0^{\frac{2\pi}{\omega}} R(i\omega\hat{V})^T \cdot (\underline{C} + iK\underline{A})\, R(\hat{V})dt \tag{4.41}$$

when matrices $\underline{A}$ and $\underline{C}$ are real, and by

$$E = \frac{\omega}{2\pi}\int_0^{\frac{2\pi}{\omega}} R(i\omega\hat{V})^T \cdot (R(\underline{C}) + iKR(\underline{A}))R(\hat{V})dt \tag{4.42}$$

when matrices $\underline{A}$ and $\underline{C}$ are complex, where R represents the real part. Now let

$$\hat{V} = (\hat{V}_1 + i\hat{V}_2)e^{i\omega t} = (\hat{V}_1 + i\hat{V}_2)(\cos\,\omega t + i\,\sin\,\omega t) \tag{4.43}$$

Then substituting

$$R(\hat{V}) = \hat{V}_1\,\cos\,\omega t - \hat{V}_2\,\sin\,\omega t,$$

$$R(i\omega\hat{V}) = -\,\omega(\hat{V}_1\,\sin\,\omega t + \hat{V}_2\,\cos\,\omega t) \tag{4.44}$$

$$R(i\omega V)^T \cdot R(\hat{V}) = -\,\omega V_1^T \cdot \hat{V}_1\,\sin\,\omega t\,\cos\,\omega t - V_1^T \cdot \hat{V}_2\,\cos^2\,\omega t +$$

$$\omega V_1^T \cdot \hat{V}_2\,\sin^2\,\omega t + V_2^T \cdot \hat{V}_2\,\sin\,\omega t\,\cos\,\omega t \tag{4.45}$$

and

$$\frac{\omega}{2\pi}\int_0^{\frac{2\pi}{\omega}} \sin\omega t\cos\omega t\,dt = 0,\quad \frac{\omega}{2\pi}\int_0^{\frac{2\pi}{\omega}} \sin^2\omega t dt = \frac{\omega}{2\pi}\int_0^{\frac{2\pi}{\omega}} \cos^2\omega t dt = 1/2 \tag{4.46}$$

into Equation 4.41 yields,

$$\hat{E} = \frac{\omega}{2}(\hat{V}_1^T\cdot(\underline{C}+i\kappa\underline{A})\hat{V}_2 - \hat{V}_2^T\cdot(\underline{C}+i\kappa\underline{A})\hat{V}_1), \tag{4.47}$$

where $\hat{V}_1$ and $\hat{V}_2$ are the real and imaginary of the vector $\hat{V}$.

Equation 4.47 expresses the energy carried by the mode K. If the incident energy of the Rayleigh wave across the vertical boundary is in the fundamental mode K, given by Equation 4.47, then the reflected and transmitted energies must be calculated through the modes which are produced by the incident energy. Therefore, if L is the number of different modes produced by the incident energy then the reflected and transmitted energies are given by

$$E_R = \sum_{s=1}^{L}\frac{\omega}{2}(\hat{V}_{1s}^T\cdot(\underline{C}-iK_s\underline{A})\hat{V}_{2s} - \hat{V}_{2s}^T\cdot(\underline{C}-iK_s\underline{A})\hat{V}_{1s} \tag{4.48}$$

and

$$E_T = \sum_{s=1}^{L}\frac{\omega}{2}(\hat{V}_{1s}^T\cdot(\underline{C}+iK_s\underline{A})\hat{V}_{2s} - \hat{V}_{2s}^T\cdot(\underline{C}+iK_s\underline{A})\hat{V}_{1s}\ , \tag{4.49}$$

respectively.

D. Attenuation

If we substitute the effective moduli of Equation 2.17 into the energy relation Equation 4.47 it produces an additional term called the power loss or dissipated power in the system. This power loss is due to the viscoelastic part of Equation 2.17, and is given by

$$P_D = \frac{\omega}{2} (\hat{V}_1^T \cdot (IM(\underline{C}) + iKIM(\underline{A}))\hat{V}_2 - \hat{V}_2 \cdot (IM(\underline{C}) + iKIM(\underline{A}))\hat{V}_2), \quad (4.48)$$

where IM represents the imaginary part or the viscoelastic part of the matrices $\underline{C}$ and $\underline{A}$. The ratio of the average power loss, Equation 4.48, to the average rate of energy transport, Equation 4.47, is called the attenuation and is denoted by a dimensionless parameter $2\pi Q^{-1}$; thus,

$$2\pi Q^{-1} = \frac{\text{average dissipated power}}{\text{rate of energy transport}} = \frac{P_D}{E} . \quad (4.49)$$

If the complex wavenumber

$$K = K_R + iK_I \quad (4.50)$$

is given, or for a given period, is found from the solution of the eigenvalue problem for the layered region, then the attenuation is given by

$$Q^{-1} = \frac{2K_I}{K_R} . \quad (4.51)$$

Equation 4.49 is general; it can be used for spatial attenuation, i.e., attenuation arising from discontinuities along the path of the wave, or for temporal attenuation, i.e., attenuation arising from time, temperature or other viscoelastic behavior of the medium.

E. Change of Wavenumber at the Vertical Boundary

The existence of reflected energy at the vertical boundary suggests that the phase velocity at the left and the right hand sides of the boundary are different. Since the wave is harmonic then the change in velocity is due to the change in wavenumber. This change must be calculated by means other than from Equation 3.81 whose solution gives the displacements at the vertical boundary.

Auld (7, 8) has used a perturbation theory and has derived a relation to calculate the change in the wavenumber due to various mechanisms. Auld's relation may be revised to be used in seismic waves; the form suitable here may be expressed as

$$\delta K = \omega \frac{\int_z \hat{\varepsilon}^T \cdot \Delta \underline{D}\, \hat{\varepsilon} - \Delta\rho\omega^2 \hat{U}^T \cdot \hat{U})\, dz}{4E} \tag{4.52}$$

where

$$D = \begin{bmatrix} \lambda+2\mu & \lambda & 0 \\ \lambda & \lambda+2\mu & 0 \\ 0 & 0 & \mu \end{bmatrix} , \tag{4.53}$$

$$\hat{\varepsilon} = \left(\frac{\partial U_x}{\partial x} , \frac{\partial U_z}{\partial z} , \frac{\partial U_z}{\partial x} + \frac{\partial U_x}{\partial z} \right) , \tag{4.54}$$

$$\hat{U} = \hat{U}(z) e^{i(\omega t - KX)} , \tag{4.55}$$

E is given by Equation 4.49 and Δ denotes the contrast between the two different media. Use of Equations 3.33 and 3.34 reduces the numerator of Equation 4.52 to

$$L = \int_z \left(\begin{bmatrix} \frac{\partial}{\partial x} & 0 \\ 0 & \frac{\partial}{\partial z} \\ \frac{\partial}{\partial z} & \frac{\partial}{\partial x} \end{bmatrix} \hat{U} \right)^T \cdot \Delta \underline{D} \begin{bmatrix} \frac{\partial}{\partial x} & 0 \\ 0 & \frac{\partial}{\partial z} \\ \frac{\partial}{\partial z} & \frac{\partial}{\partial x} \end{bmatrix} \hat{U} - \Delta\rho\omega^2 \hat{U}^T \cdot \hat{U} \Big) dz . \tag{4.56}$$

Decomposition of the operating martix into two matrices, depending on x or z only, gives

$$\begin{bmatrix} \frac{\partial}{\partial x} & 0 \\ 0 & \frac{\partial}{\partial z} \\ \frac{\partial}{\partial z} & \frac{\partial}{\partial x} \end{bmatrix} = \begin{bmatrix} \frac{\partial}{\partial x} & 0 \\ 0 & 0 \\ 0 & \frac{\partial}{\partial x} \end{bmatrix} + \begin{bmatrix} 0 & 0 \\ 0 & \frac{\partial}{\partial z} \\ \frac{\partial}{\partial z} & 0 \end{bmatrix} \tag{4.57}$$

and operating on the matrix with the partial derivative with respect to x on the corresponding vectors results in

$$L = \int_z ((\nabla z - iKI)\hat{U})^T \cdot \Delta\underline{D}\ (\underline{\nabla z} - iKI)\hat{U} - \rho\omega^2 \hat{U}^T \cdot \hat{U})dz, \tag{4.58}$$

where matrix $\underline{\nabla z}$ is given by the second term of Equation 4.57, and

$$I = \begin{bmatrix} 1 & 0 \\ 0 & 0 \\ 0 & 1 \end{bmatrix}.$$

Again, by using

$$\hat{U} = \underline{N}\ \hat{V} \tag{4.59}$$

$$\underline{N} = \frac{1}{2} \begin{bmatrix} 1-\eta & 0 & 1+\eta & 0 \\ 0 & 1-\eta & 0 & 1+\eta \end{bmatrix}, \quad -1 \leq \eta \leq 1 \tag{4.60}$$

$$\eta = \frac{z}{h/2}, \quad \frac{\partial}{\partial z} = \frac{1}{h/2} \frac{\partial}{\partial \eta} \quad 0 \leq z \leq h \tag{4.61}$$

$$\frac{\partial}{\partial z} \underline{N} = \frac{1}{h} \begin{bmatrix} -1 & 0 & 1 & 0 \\ 0 & -1 & 0 & 1 \end{bmatrix}, \tag{4.62}$$

Equation 4.58 becomes (for the moment we set $\Delta D = D$, $\Delta\rho = \rho$)

$$L = \int_{-1}^{1} (\hat{V}^T \cdot \left(\frac{1}{h} \begin{bmatrix} 0 & 0 & 0 & 0 \\ 0 & -1 & 0 & 1 \\ -1 & 0 & 1 & 0 \end{bmatrix} - iK/2 \begin{bmatrix} 1-\eta & 0 & 1+\eta & 0 \\ 0 & 0 & 0 & 0 \\ 0 & 1-\eta & 0 & 1+\eta \end{bmatrix} \right)^T \underline{D}$$

$$\left(\frac{1}{h} \begin{bmatrix} 0 & 0 & 0 & 0 \\ 0 & -1 & 0 & 1 \\ -1 & 0 & 1 & 0 \end{bmatrix} - iK/2 \begin{bmatrix} 1-\eta & 0 & 1+\eta & 0 \\ 0 & 0 & 0 & 0 \\ 0 & 1-\eta & 0 & 1+\eta \end{bmatrix} \right) \hat{V}$$

$$- \rho \frac{\omega^2}{4} \hat{V}^T \cdot \begin{bmatrix} (1-\eta)^2 & 0 & 1-\eta^2 & 0 \\ 0 & (1-\eta)^2 & 0 & 1-\eta^2 \\ 1-\eta^2 & 0 & (1+\eta)^2 & 0 \\ 0 & 1-\eta^2 & 0 & (1+\eta)^2 \end{bmatrix} \Bigg) \hat{V} h/2 d\eta. \qquad (4.63)$$

After performing the transpose and corresponding multiplications, Equation 4.63 becomes

$$L = \int_{-1}^{1} (\hat{V}^T \cdot \left(\frac{1}{h^2} \begin{bmatrix} \mu & 0 & -\mu & 0 \\ 0 & \lambda+2\mu & 0 & -(\lambda+2\mu) \\ -\mu & 0 & \mu & 0 \\ 0 & -(\lambda+2\mu) & 0 & \lambda+2\mu \end{bmatrix} \right.$$

$$\left. - i \frac{K}{2h} \begin{bmatrix} 0 & -\mu(1-\eta) & 0 & -\mu(1+\eta) \\ -\lambda(1-\eta) & 0 & -\lambda(1+\eta) & 0 \\ 0 & \mu(1-\eta) & 0 & \mu(1+\eta) \\ \lambda(1-\eta) & 0 & \lambda(1+\eta) & 0 \end{bmatrix} \right)$$

$$+ i \frac{K}{2h} \begin{bmatrix} 0 & -\lambda(1-\eta) & 0 & \lambda(1-\eta) \\ -\mu(1-\eta) & 0 & \mu(1-\eta) & 0 \\ 0 & -\lambda(1+\eta) & 0 & \lambda(1+\eta) \\ -\mu(1+\eta) & 0 & \mu(1+\eta) & 0 \end{bmatrix}$$

$$+ \frac{K^2}{4} \begin{bmatrix} (\lambda+2\mu)(1-\eta)^2 & 0 & (\lambda+2\mu)(1-\eta^2) & 0 \\ 0 & \mu(1-\eta)^2 & 0 & \mu(1-\eta^2) \\ (\lambda+2\mu)(1-\eta^2) & 0 & (\lambda+2\mu)(1+\eta)^2 & 0 \\ 0 & \mu(1-\eta^2) & 0 & \mu(1+\eta)^2 \end{bmatrix} \Big) \hat{V}$$

$$- \rho \frac{\omega^2}{4} \hat{V}^T \cdot \begin{bmatrix} (1-\eta)^2 & 0 & 1-\eta^2 & 0 \\ 0 & (1-\eta)^2 & 0 & 1-\eta^2 \\ 1-\eta^2 & 0 & (1+\eta)^2 & 0 \\ 0 & 1-\eta^2 & 0 & (1+\eta)^2 \end{bmatrix} \hat{V} h/2 d\eta \qquad (4.64)$$

Now, the integrations of

$$\int_{-1}^{1} (1-\eta) d\eta = \int_{-1}^{1} (1+\eta) d\eta = 2, \int_{-1}^{1} (1-\eta)^2 d\eta = \int_{-1}^{1} (1+\eta)^2 d\eta = \frac{8}{3}, \qquad (4.65)$$

and

$$\int_{-1}^{1} (1-\eta^2) d\eta = \frac{4}{3},$$

reduces Equation 4.64 into

$$L = \hat{V}^T \cdot (1/2\, \underline{G}_j + iK\underline{F}_j + K^2 \underline{A}_j - \omega^2 \underline{M}_j)\, \hat{V} \qquad (4.66)$$

where matrices $\underline{G}_j$, $\underline{A}_j$, and $\underline{M}_j$ are given by Equations 3.48 - 3.50 and

$$\underline{F}_j = \frac{1}{2}\begin{bmatrix} 0 & -(\lambda-\mu) & 0 & (\lambda+\mu) \\ \lambda-\mu & 0 & \lambda+\mu & 0 \\ 0 & -(\lambda+\mu) & 0 & \lambda-\mu \\ -(\lambda+\mu) & 0 & -(\lambda-\mu) & 0 \end{bmatrix} . \tag{4.67}$$

Since j represents a typical layer, the sum of Equation 4.66 over all layers, when substituted into Equation 4.52 gives, considering now ΔD and ΔP,

$$\delta K = \omega \frac{\hat{V}^T \cdot (1/2\ \Delta\underline{G} + iK\Delta\ \underline{F} + K^2\Delta\ \underline{A} - \omega^2\Delta\ \underline{M})\hat{V}}{4E} \tag{4.68}$$

When calculated, this δK may be added to the wave number of the left hand side of the boundary; the phase velocity of the right hand side of the boundary can be calculated by the expression,

$$V_x = \frac{\omega}{K+\delta K} . \tag{4.69}$$

For different periods the dispersion curve of the desired medium can be computed.

Equation 4.68 may also be used for the determination of attenuation. For this purpose if

$$\delta K = \delta_{K_R} + i\delta K_I \tag{4.70}$$

then

$$\delta K_I = \omega \frac{\hat{V}^T\ (1/2\ \Delta\underline{G}_I + iK\ \Delta\ F_I + K^2\ \Delta\ \underline{A}_I)\hat{V}}{4E} \tag{4.71}$$

and the attenuation is given by

$$Q^{-1} = \frac{2\delta K_I}{\delta K} \tag{4.72}$$

where I stands for the imaginary part. Since attenuations due to various mechanisms are additive, Equation 4.72 may be added to the attenuation obtained due to viscoelastic behavior.

CHAPTER V

APPLICATION OF THE METHOD

A. A Model

To apply a model to the theories discussed in the last chapters, we chose Herrin's models (49) of the Canadian Shield and Basin and Range provinces for the elastic part of the medium. The Basin and Range province is used in the left layered region and the Canadian Shield is used in the right layered region; the order is reversible. For the irregular region we chose different combinations of the Basin and Range province and the Canadian Shield. The data given in Herrin's model are thicknesses, densities, compressional velocities, and shear velocities of the two layered media. To account for the anelasticity in the model a complex part for the compressional velocities and shear velocities may be assumed. Since the elastic moduli are obtained by using the expressions

$$\lambda = \rho(V_p^2 - 2V_s^2) \tag{5.1}$$

$$\mu = \rho V_s^2 , \tag{5.2}$$

where, λ and μ are the elastic moduli of the medium, and V_p and V_s are the real parts of compressional and shear velocities, respectively, then the effective moduli, or complex moduli, as given in Equation 2.17, may be obtained by

$$\lambda_e = \rho(V_p^2 - 2V_s^2) \tag{5.3}$$

$$\mu_e = \rho V_s^2 \tag{5.4}$$

for complex velocities. For this reason, in our model, any viscoelastic behavior of the medium may be incorporated in the imaginary parts of the compressional and shear velocities. Thus, for the viscoelastic part of the medium in this paper, three different sets of data are used: A small enough (.1 percent of the real part) imaginary parts for compressional and shear velocities; a starting constant shear quality factor, Q_β, for the Basin and Range province and a starting constant Q_β for the Canadian Shield; and finally the starting Q_β model of Lee and Solomon (69a), whose Q_β of Western U. S. and East-Central U. S. are used in Basin and Range provinces and Canadian Shield, respectively.

When Q_β is given, the imaginary parts of V_p and V_s are determined by the following expressions. From

$$Q_\beta = \frac{\text{REAL } (V_s)}{2 \text{ IMAG } (V_s)} \tag{5.5}$$

$$V_p = \text{REAL } (V_p) + i \text{ IMAG } (V_p), \tag{5.6}$$

$$V_s = \text{REAL } (V_s) + i \text{ IMAG } (V_s), \tag{5.7}$$

$$\text{IMAG } (V_s) = \frac{\text{REAL } (V_s)}{2Q_\beta} . \tag{5.8}$$

And from (69a),

$$Q_\alpha = \frac{3}{4}\left(\frac{V_p}{V_s}\right)^2 Q_\beta \ , \tag{5.9}$$

we have

$$\text{IMAG}(V_p) = \frac{\text{REAL}\ (V_p)}{2Q_\alpha} \ . \tag{5.10}$$

Both regions of the model are assumed each to contain 15 layers with a total depth of 250 kilometers; this depth includes the crust and upper mantle so that any partial melting zone in the upper mantle may be studied. The irregular region I is divided into 15 by 15 network of elements whose total number of elements and total number of nodal points of the elements are N^2 and $N(N + 1)$, respectively, where N is the number of layers. The slightly adjusted Herrin model for the above geometry is given in Tables 1 and 2. The integer N in Table 2 represents the number of elements, in the finite element region, that have the same property. The numbers assigned to the integer N in Tables 2 and 2A are completely arbitrary.

B. Real Data

A set of periods from 9 to 60 seconds along with the data of Table 1, may be used as an input for the solution of the eigenvalue problem, Equation 3.52, in the layered regions. The fundamental solution of the eigenvalue problem corresponding to each period is the largest eigenvalue or the largest wavenumber selected from the 2N eigenvalues. The phase velocity corresponding to each period is given by

$$\text{PHASE VELOCITY} = \frac{\text{OMEGA}}{\text{WAVENUMBER}} \ , \tag{5.11}$$

for the given period and corresponding frequency.

The computer program RALEE used to calculate the unknown of the medium is the revised form of the program RALEEM written by Drake (29) in 1972. To test the program RALEE we used Lysmer and Drake's (80) data of the Sierra Nevada and calculated the phase velocities of Rayleigh waves for a range of periods of 6 to 10 seconds and the horizontal and vertical amplitudes for a period of 6 seconds. The agreement is excellent for the phase velocities and good for the amplitudes; but the small difference in the amplitudes may be due to scale arbitrariness. The phase velocities are given in Table 16 and the amplitudes are shown in Figure 16.

The wavenumbers and the phase velocities calculated for the two layered systems of the Basin and Range province and the Canadian shields with the data of Table 1 and the periods of 9 to 60 seconds are also given in Tables 3 and 4, and the corresponding dispersion curves are shown in Figures 7 and 8.

To test the effect of layering we reduced the number of layers from 15 to 3 and assumed two layers for the crust and a deep layer for the upper mantle. The computed Rayleigh wave phase velocities are somewhat higher than those of the 15 layered case. The difference may be due somewhat to the averaging data of 15 layers into 3 layers but it is mostly due to the large dimensions of the elements as compared to the wavelength of the shear wave (104).

To test the computer program RALEE for the irregular zone I in the real case, we first assumed the three zones L, I and R of Figure 5 to have the same properties as the Basin and Range provinces and calculated the reflected and transmitted energies. For the period range of

10 to 80 seconds the sum of the reflected and transmitted energies is very close to incident energy. These data are shown in Table 5. Second, we set the boundary between the Basin and Range province and the Canadian Shield at the right hand side of the zone L, i.e., we let the zone L be the Basin and Range province and zones I and R be the Canadian Shield. Third, we set the boundary at the left hand side of the zone R, i.e., we let the zones L and I be the Basin and Range province and zone R be the Canadian Shield. Fourth, we set the boundary at the middle of zone I, i.e., we let the zone L and one-half of the zone I be the Basin and Range province and one-half of the zone I and zone R be the Canadian shield. Finally, we let the zones L and R be the Basin and Range province and the Canadian shield, respectively, but gradually changed the parameters of the zone I from the parameters of the Basin and Range province into the parameters of the Canadian shield. The sum of the reflected and transmitted energies determined for each of the above models in the real case, was found to be almost equal to the incident energy. The transmitted energy in all of the above models, in the real case, is more than 99% except for a few period of 18 to 25, in the second case, in which for each period the reflected energy is the highest, i.e., from .05% to 2.2%. On the other hand, in the third case, the reflected energy is the smallest, i.e., from .007% to .06%. Therefore, the decrease in reflected energy is from left to right with respect to the position of the vertical boundary; nevertheless, the process is reversible. The values for the above cases are given in Tables 6, 6A, 6B, and 6C, respectively.

For the determination of the phase velocity in the irregular region, in the real case, the boundary displacements, determined by Equation 3.81, are used in Equation 4.68; the left boundary displacements are replaced by the vector $\hat{V}^T$ and the right boundary displacements are replaced by the vector $\hat{V}$ in Equation 4.68. Substitution of the resulting δK into Equation 4.69 determines the fundamental mode phase velocity. Repetition of the use of Equations 4.68 and 4.69, corresponding to the number of distinct periods gives the phase velocities of the irregular region for each case mentioned in the previous paragraph. The dispersion curves for each case are shown in Figures 9, 9A, 9B, 9C, and 9D, respectively.

C. Complex Data

The geometry of the model remains the same in the viscoelastic case. Therefore, the real parts of the complex V_p and V_s velocities do not change in the complex case. Since thicknesses, densities, and periods are assumed to be real in the elastic and viscoelastic medium, they will not be repeated again in this section. Thus, for the complex case of the model we assigned three different sets of data to the imaginary parts of the complex V_p and V_s velocities. First, the imaginary parts of the V_p and V_x were assumed to be .1 percent of their corresponding real parts. Second, a constant shear quality factor for each zone of L and R was assumed and the corresponding compressional quality factor Q_α and the imaginary parts of V_p and V_s were calculated. Third, we used the Q_β model of Lee and Solomon (69a) and calculated the corresponding compressional quality factor Q_α and the imaginary

parts of V_p and V_s. The imaginary parts of V_p and V_s for the three cases are shown in Tables 7, 8, and 9.

For the same number of periods that was used in the real case, the values, given in Tables 7, 8, and 9 are used as the input for the solution of complex eigenvalue problem, Equation 3.52, in the layered regions. The fundamental solution of the complex eigenvalue problem corresponding to each period is the largest eigenvalue with a negative imaginary part, selected from 2N eigenvalues. The phase velocity and the attenuation corresponding to each period are given by

$$\text{PHASE VELOCITY} = \frac{\text{OMEGA}}{\text{REAL (WAVENUMBER)}} \tag{5.11a}$$

and

$$\text{ATTENUATION} = \frac{2 \times \text{IMAG (WAVENUMBER)}}{\text{REAL (WAVENUMBER)}} , \tag{5.12a}$$

respectively. The real and imaginary parts of wavenumbers, the phase velocities and the attenuations, corresponding to Tables 7, 8, and 9 are given in Tables 10 - 15 and the corresponding attenuation curves and the dispersion curves are shown in Figures 10 - 15.

For the complex part of the irregular region I we used the imaginary parts for V_p and V_s velocities, obtained from the Q_β of Lee and Solomon (69a), in all cases described for the real case in section B. In each case the sum of the reflected and transmitted energies is considerably less than the incident energy; but the difference is remarkably in accordance with the given Q_β value with respect to the depth where the energy is computed. The attenuated percentage of reflected and transmitted energies are given in Tables 5, 6, 6A, 6B, and 6C.

For consistency of the result, we asked H. Mack (80a) to input our complex data in his computer program VERES. He calculated the transmitted Rayleigh wave energy for the case where the medium is considered to have the parameters of Basin and Range province. His result agrees well with higher periods, fluctuates somewhat with the intermediate periods, and agrees with periods of 13 - 15 seconds as shown in Table 5. For periods lower than 13 seconds his program is not applicable.

The determination of the phase velocity of the irregular region, in the complex case, follows the same procedure of the last subsection; however, since the change in the phase velocities between the real and the complex cases are very small the dispersion curves would look the same as the ones in the real case. Thus, the repetition is not necessary.

Finally, for a check on the result we used the data of Lee and Solomon (69a, pages 77 and 83) in our 15 layered systems and computed the phase velocities and the attenuations for East-Central and Western North America. The result is compared well with their result which is obtained by inversion. The phase velocities and the attenuations are given in Tables 17 and 18 and the corresponding dispersion and attenuation curves are shown in Figures 17, 18, 19, and 20.

CHAPTER VI

SUMMARY AND CONCLUSION

The anomalous decay of surface wave amplitude may be due to viscoelasticity and geometrical discontinuities of the medium. In this paper the path of a Rayleigh wave was assumed to be through the Basin and Range provinces and the Canadian Shield. The two regions were treated as elastic and inelastic; and the surface of intersection between them was considered to be an approximation to a plane vertical boundary.

With the plane vertical boundary removed, the two regions, as a layered system, were studies as separate elastic and viscoelastic media. The Rayleigh wave phase velocities, amplitudes, and the attenuations of the two regions, with the technique of finite element, were computed for a range of periods. The change in phase velocities, in each region due to viscoelasticity in three different cases of data, were from .01 percent to 0.5 percent of elastic phase velocities, an almost negligible amount. Consequently, the dispersion curves, with the range of periods of 9 - 60 seconds, are almost similar in elastic and viscoelastic cases in all three zones. On the other hand, the amplitudes and attenuations, in three cases of different viscoelastic parameters in the layered system, are in accordance with the input data and agree well with the very limited published data. Though small, the difference in amplitude and attenuation due to viscoelasticity appear to be significant and is

in accordance with the amount of imaginary parts of V_p and V_s velocities with respect to the depth of the layers. The result of the use of the model of Lee and Solomon (69a) also confirms the above result, in addition to being in excellent agreement with their result.

The reflected and transmitted energies through the vertical boundary are functions of position of the vertical boundary with respect to the two media of L and R, in the real case. They are in addition to the above condition, functions of attenuation or the Q_β as well, in the viscoelastic case. The reflection of energy, although small in all cases, decreases as the vertical boundary, in our model, moves from left to right; but the process is completely reversible. The highest reflection of energy (.04% to 2.2%) occurs where the vertical boundary is at the right hand side of the zone L so that the zones I and R both have the parameters of the Canadian shield and the zone L has the Basin and Range parameters. The one position of the vertical boundary where the reflected energy has the intermediate value (.04% to .5%) is in the middle of the zone I; the reflected energy in the real and complex cases are almost equal; the sum of the reflected and transmitted energies, in the real case are almost exactly equal to the incident energy and the transmitted energy, in the complex case is the highest.

Due to the fact that the reflected energy, in all of the models tested, is very small, it may be concluded that for a normal incidence of Rayleigh wave at a vertical boundary between the Continental provinces the mode conversion is too small to measure in the real crust. Due to the computer core limitation the number of sublayers and the size of the elements may be somewhat large compared to the wavelength of the shear wave.

TABLE 1

HERRIN'S MODEL OF BASIN AND RANGE PROVINCES AND CANADIAN SHIELD, SLIGHTLY ADJUSTED TO FIT THE FIFTEEN LAYERED MODEL

Basin and Range				Canadian Shield			
Depth (KM)	Density (G/CM^3)	V_p (KM/SEC)	V_s (KM/SEC)	Depth (KM)	Density (G/CM^3)	V_p (KM/SEC)	V_s (KM/SEC)
0-14	2.640	6.000	3.540	0-14	2.610	5.800	3.470
14-19	2.640	6.000	3.560	14-19	2.620	6.700	3.740
19-20	2.640	6.700	3.600	19-20	2.620	6.700	3.740
20-28	2.640	6.695	3.595	20-28	2.620	6.700	3.740
28-30	2.640	6.650	3.550	28-30	2.620	6.700	3.740
30-34	2.900	7.900	4.430	30-34	2.620	7.000	3.820
34-50	2.900	7.900	4.425	34-50	2.900	8.050	4.620
50-60	3.420	7.899	4.420	50-60	2.900	8.050	4.620
60-80	3.400	7.880	4.390	60-80	2.900	8.050	4.620
80-90	3.400	7.860	4.355	80-90	2.920	8.100	4.540
90-100	3.392	7.820	4.320	90-100	3.400	8.400	4.660
100-120	3.382	7.678	4.182	100-120	3.500	8.500	4.500
120-140	3.380	7.730	4.220	120-140	3.500	8.500	4.500
140-150	3.400	7.800	4.270	140-150	3.500	8.500	4.500
150-200	3.400	7.890	4.430	150-200	3.500	8.500	4.500

APPENDIX A

TABLE 2

DATA OF TABLE 1 FOR THE FINITE ELEMENT REGION;
N REPRESENTS THE NUMBER OF ELEMENTS HAVING
THE SAME PROPERTY (REAL CASE)

Depth (KM)	N	Density (KM/CM^3)	N	V_p (KM/SEC)	N	V_s (KM/SEC)	N
		2.64	15	6.00	15	3.54	15
0	14	2.61	1	5.80	1	3.47	1
		2.64	14	6.00	14	3.56	14
14	14	2.62	2	6.70	2	3.74	2
		2.64	13	6.70	13	3.60	13
19	14	2.62	4	6.70	4	3.74	2
		2.64	11	6.69	11	3.59	13
20	14	2.62	6	6.70	6	3.74	4
		2.64	9	6.66	9	3.55	11
38	14	2.62	8	6.70	8	3.74	6
		2.90	7	7.90	7	4.43	9
30	14	2.62	10	7.00	10	3.82	8
		2.90	5	7.90	5	4.42	7
34	14	2.90	12	8.05	12	4.62	10
		3.42	3	7.90	3	4.42	5
50	14	2.90	14	8.05	14	4.62	12
		3.40	1	7.88	1	4.39	3
120	14	2.90	11	8.05	11	4.62	14
		3.40	4	7.86	4	4.36	1
140	14	3.40	13	8.10	13	4.62	11
		2.92	2	7.82	2	4.32	4
150	14	3.50	13	8.40	13	4.62	13
		3.38	2	7.68	2	4.18	2
250	14	3.50	13	8.50	13	4.62	13
		3.38	2	7.73	2	4.22	2
		3.50	13	8.50	13	4.54	13
		3.40	2	7.80	2	4.27	2
		3.50	13	8.13	13	4.66	13
		3.40	2	7.85	2	4.43	2

TABLE 2a

DATA FROM TABLE 2, WITH LEE AND SOLOMON'S DATA, FOR THE FINITE ELEMENT REGION IN COMPLEX CASE

V_p (KM/SEC)			V_s (KM/SEC)		
REAL (V_p)	IMAG (V_p) ($\times 10^{-2}$)	N	REAL (V_s)	IMAG (V_s) ($\times 10^{-2}$)	N
6.00	0.40	15	3.54	6.00	15
5.80	0.14	1	3.47	0.17	1
6.00	0.40	14	3.56	6.00	14
6.70	0.14	2	3.74	0.18	2
6.70	0.40	13	3.60	6.00	13
6.70	0.14	4	3.74	0.18	2
6.69	0.20	11	3.59	0.23	13
6.70	0.14	6	3.74	0.18	4
6.66	0.20	9	3.55	0.23	11
6.70	0.14	8	3.74	0.18	6
7.90	0.20	7	4.43	0.28	9
7.00	0.14	10	3.82	0.18	8
7.90	0.20	5	4.42	0.28	7
8.05	0.17	12	4.62	0.23	10
7.90	0.20	3	4.42	0.28	15
8.05	0.17	14	4.62	0.23	12
7.88	0.20	1	4.39	0.28	3
8.05	0.17	11	4.62	0.28	14
7.86	9.00	4	4.36	13.00	1
8.10	0.17	13	4.62	0.23	11
7.82	9.00	2	4.32	13.00	4
8.40	0.16	13	4.62	0.23	13
7.68	9.00	2	4.18	12.00	2
8.50	0.16	13	4.62	0.23	13
7.73	9.00	2	4.22	12.00	2
8.50	3.60	13	4.54	0.23	13
7.80	9.00	2	4.27	13.00	2
8.13	3.60	13	4.66	5.40	13
7.85	5.00	2	4.30	7.00	2

TABLE 3

FUNDAMENTAL, AND FIRST AND SECOND HIGHER MODE EIGENVALUES AND CORRESPONDING PHASE VELOCITIES OF THE LEFT LAYERS (REAL CASE)

Wavenumbers (KM^{-1})			Phase Velocity (KM/SEC)		
Fundamental Mode	1st Higher Mode	2nd Higher Mode	Fundamental Mode	1st Higher Mode	2nd Higher Mode
0.2009	0.1618	0.1589	3.475	4.315	4.394
0.1806	0.1453	0.1420	3.478	4.323	4.423
0.1497	0.1207	0.1168	3.496	4.337	4.481
0.1179	0.0960	--	3.551	4.363	--
0.0962	0.0792	--	3.627	4.402	--
0.0853	--	--	3.681	--	--
0.0765	--	--	3.732	--	--
0.0662	--	--	3.796	--	--
0.0541	--	--	3.865	--	--
0.0460	--	--	3.902	--	--
0.0400	--	--	3.924	--	--
0.0354	--	--	3.940	--	--
0.0318	--	--	3.955	--	--
0.0262	--	--	3.997	--	--
0.0221	--	--	4.066	--	--

TABLE 4

FUNDAMENTAL, AND FIRST AND SECOND HIGHER MODE EIGENVALUES AND CORRESPONDING PHASE VELOCITIES OF THE RIGHT LAYERS (REAL CASE)

Wavenumbers (KM^{-1})			Phase Velocity (KM/SEC)		
Fundamental Mode	1st Higher Mode	2nd Higher Mode	Fundamental Mode	1st Higher Mode	2nd Higher Mode
0.2002	0.1545	0.1533	3.487	4.522	4.553
0.1799	0.1368	0.1321	3.493	4.537	4.590
0.1490	0.1150	--	3.514	4.552	--
0.1174	0.0915	--	3.569	4.577	--
0.0958	0.0757	--	3.645	4.614	--
0.0849	--	--	3.700	--	--
0.0761	--	--	3.755	--	--
0.0656	--	--	3.830	--	--
0.0533	--	--	3.928	--	--
0.0449	--	--	3.996	--	--
0.0388	--	--	4.045	--	--
0.0342	--	--	4.084	--	--
0.0305	--	--	4.120	--	--
0.0250	--	--	4.198	--	--
0.0208	--	--	4.308	--	--

TABLE 5

DISTINCT PERIODS AND PERCENTAGE OF REFLECTED AND TRANSMITTED ENERGIES PASSING THROUGH THE VERTICAL BOUNDARY (THE CASE WHERE ALL THREE ZONES HAVE THE BASIN AND RANGE PROPERTIES) THE LAST TWO COLUMNS ARE THE RESULT OF H. MACK

	Real		Complex		H. Mack (Complex)	
Period Sec	Reflected Energy	Transmitted Energy	Reflected Energy	Transmitted Energy	Period Sec	Transmitted Energy
10	.0011	99.9954	.0073	84.2120		
12	.0054	99.9945	.0112	88.2821	13.8	87.5
15	.0007	99.9994	.0017	92.5926	14.2	94.0
18	.0010	99.9989	.0024	95.3736	15.1	99.4
20	.0005	99.9988	.0018	96.4662	20.5	99.8
22	.0004	100.0000	.0011	97.0742	22.3	96.6
25	.0001	99.9996	.0002	97.2620	25.6	93.6
30	.0001	99.9996	.0055	96.6856	28.4	93.4
35	.0001	99.9996	.0165	96.1306	32.0	94.0
40	.0001	99.9997	.0186	95.8209	39.4	92.0
45	.0001	99.9997	.0155	95.7497	42.7	94.7
50	.0001	100.0000	.0135	95.7523	46.5	96.0
60	.0001	99.9998	.0122	95.8963	51.2	95.3
70	.0001	99.9996	.0223	96.0832		
80	.0001	100.0000	.0001	96.1831		

TABLE 6

DISTINCT PERIODS AND PERCENTAGE OF REFLECTED AND TRANSMITTED ENERGIES PASSING THROUGH THE VERTICAL BOUNDARY (THE CASE WHERE THE VERTICAL BOUNDARY IS AT THE RIGHT HAND SIDE OF THE ZONE L

Period Sec	Complex		Real	
	Reflected Energy	Transmitted Energy	Reflected Energy	Transmitted Energy
10	.1795	99.1060	.2581	99.7302
12	.0733	99.3311	.0551	99.9465
15	.1209	99.3781	.1396	99.8880
18	2.2780	97.1127	1.9161	98.9499
20	.3447	99.2575	.3268	99.6688
22	1.0353	98.5935	1.0766	98.9225
25	.9698	98.6958	1.0128	98.9857
30	.3175	99.3742	.3549	99.6445
35	.4085	99.2819	.4607	99.5385
40	.1525	99.5212	.1645	99.8983
45	.1209	99.4230	.1318	99.8678
50	.0832	99.4036	.0892	99.9100
60	.0555	99.3044	.0586	99.9413
70	.1309	99.1301	.1081	99.8914
80	.0454	99.0328	.0439	99.9560

TABLE 6A

DISTINCT PERIODS AND PERCENTAGE OF REFLECTED AND TRANSMITTED ENERGIES PASSING THROUGH THE VERTICAL BOUNDARY (THE CASE WHERE THE VERTICAL BOUNDARY IS AT THE LEFT HAND SIDE OF THE ZONE R)

	Real		Complex	
Period Sec	Reflected Energy	Transmitted Energy	Reflected Energy	Transmitted Energy
10	.0127	99.9840	.0259	84.2332
12	.0071	99.9923	.0123	88.2958
15	.0048	99.9943	.0061	92.5954
18	.0344	99.9659	.0342	95.3359
20	.0145	99.9848	.0137	96.4257
22	.0438	99.9541	.0406	97.0042
25	.0497	99.9490	.0468	97.1677
30	.0344	99.9655	.0417	96.6803
35	.0653	99.9338	.0690	96.1376
40	.0125	99.9872	.0240	95.8200
45	.0109	99.9888	.0206	95.6108
50	.0106	99.9895	.0162	95.6320
60	.0118	99.9879	.0149	95.8032
70	.1074	99.8923	.0241	95.9536
80	.0283	99.9718	.0235	96.1427

TABLE 6B

DISTINCT PERIODS AND PERCENTAGE OF REFLECTED AND TRANSMITTED ENERGIES PASSING THROUGH THE VERTICAL BOUNDARY (THE CASE WHERE THE VERTICAL BOUNDARY IS AT THE MIDDLE OF THE ZONE I)

Period Sec	Real		Complex	
	Reflected Energy	Transmitted Energy	Reflected Energy	Transmitted Energy
10	.1410	99.8621	.1414	91.7903
12	.0710	99.9305	.0583	93.9755
15	.0537	99.9441	.0373	96.2030
18	.9384	99.0587	.8457	96.3639
20	.1468	99.8515	.1430	98.0320
22	.5724	99.4253	.5377	97.9097
25	.2310	99.7686	.2317	98.3317
30	.1871	99.7836	.1913	98.1774
35	.2673	99.7323	.2732	97.8066
40	.3002	99.7002	.3195	97.5468
45	.2449	99.7547	.2573	97.4167
50	.2027	99.7973	.2126	97.4084
60	.1677	99.8321	.1750	97.6243
70	.4799	99.5201	.4220	97.1232
80	.6412	99.9581	.0414	97.5714

TABLE 6C

DISTINCT PERIODS AND PERCENTAGE OF REFLECTED AND TRANSMITTED ENERGIES PASSING THROUGH THE VERTICAL BOUNDARY (THE CASE WHERE THE POSITION OF THE VERTICAL BOUNDARY GRADUALLY CHANGES)

Period Sec	Real		Complex	
	Reflected Energy	Transmitted Energy	Reflected Energy	Transmitted Energy
10	.0177	99.9815	.0383	87.122
12	.0119	99.9876	.0165	90.5295
15	.0092	99.9906	.0142	94.0460
18	.0207	99.9767	.0266	96.2619
20	.0073	99.9912	.0080	97.1105
22	.0134	99.9845	.0084	97.5348
25	.0271	99.9707	.0226	97.5493
30	.0278	99.9713	.0114	96.9659
35	.0577	99.9379	.0218	96.3299
40	.0266	99.9728	.0081	95.9103
45	.0140	99.9856	.0065	95.7905
50	.0111	99.9886	.0077	95.7517
60	.0113	99.9879	.0107	95.8399
70	.1399	99.9598	.0582	95.8825
80	.0209	99.9790	.0193	96.0392

TABLE 7

STARTING COMPLEX V_P AND V_S VELOCITIES OF THE LAYERED SYSTEMS, THE IMAGINARY PART BEING .1% OF THE REAL PART

Left Layers				Right Layers			
V_P		V_S		V_P		V_S	
REAL	IMAG ($\times 10^{-2}$)	REAL	IMAG ($\times 10^{-2}$)	REAL	IMAG ($\times 10^{-2}$)	REAL	IMAG ($\times 10^{-2}$)
6.000	0.600	3.540	0.354	5.800	0.580	3.470	0.347
6.000	0.600	3.560	0.356	6.700	0.670	3.740	0.374
6.700	0.670	3.600	0.360	6.700	0.670	3.740	0.374
6.695	0.670	3.595	0.360	6.700	0.670	3.740	0.374
6.650	0.665	3.550	0.355	6.700	0.670	3.740	0.374
7.900	0.790	4.430	0.443	7.000	0.700	3.820	0.382
7.900	0.790	4.425	0.443	8.050	0.805	4.620	0.462
7.899	0.790	4.420	0.442	8.050	0.805	4.620	0.462
7.880	0.788	4.390	0.439	8.050	0.805	4.620	0.462
7.860	0.786	4.355	0.435	8.100	0.810	4.540	0.454
7.820	0.782	4.320	0.432	8.400	0.840	4.660	0.466
7.678	0.768	4.182	0.418	8.500	0.850	4.500	0.450
7.730	0.773	4.220	0.422	8.500	0.850	4.500	0.450
7.800	0.780	4.278	0.428	8.500	0.850	4.500	0.450
7.890	0.789	4.430	0.443	8.500	0.850	4.500	0.450

TABLE 8

THE CONSTANT Q_β, AND CORRESPONDING Q_α, AND THE CORRESPONDING IMAGINARY PARTS OF V_p AND V_s OF THE LAYERED REGIONS

Left Layers (Q_β = 400)			Right Layers (Q_β = 800)		
Q_α	IMAG (V_p) ($\times 10^{-2}$)	IMAG (V_s) ($\times 10^{-2}$)	Q_α	IMAG (V_p) ($\times 10^{-2}$)	IMAG (V_s) ($\times 10^{-2}$)
881	0.34	0.40	1676	0.15	0.19
875	0.34	0.40	1925	0.15	0.23
1039	0.32	0.40	1925	0.15	0.23
1040	0.32	0.40	1925	0.15	0.23
1050	0.40	0.40	1925	0.17	0.24
954	0.40	0.40	2014	0.22	0.29
960	0.40	0.40	1820	0.22	0.29
955	0.40	0.40	1820	0.22	0.29
916	0.40	0.40	1820	0.22	0.28
977	0.40	0.40	1909	0.21	0.29
980	0.40	0.40	1950	0.21	0.28
1011	0.40	0.40	2140	0.21	0.28
1006	0.40	0.40	2140	0.21	0.28
997	0.40	0.40	2140	0.21	0.28
951	0.40	0.40	2140	0.21	0.28

TABLE 9

THE Q_β MODEL OF LEE AND SOLOMON AND CORRESPONDING Q_α, AND CORRESPONDING IMAGINARY PARTS OF V_p AND V_s OF THE LAYERED REGIONS

Left Layers				Right Layers			
Q_β	Q_α	IMAG (V_p) ($\times 10^{-2}$)	IMAG (V_s) ($\times 10^{-2}$)	Q_β	Q_α	IMAG (V_p) ($\times 10^{-2}$)	IMAG (V_s) ($\times 10^{-2}$)
312	672	0.40	6.00	1000	2095	0.14	0.17
312	664	0.40	6.00	1000	2400	0.14	0.18
312	810	0.40	6.00	1000	2400	0.14	0.18
770	2000	0.20	0.23	1000	2400	0.14	0.18
770	2026	0.20	0.23	1000	2400	0.14	0.18
770	1836	0.20	0.23	1000	2518	0.14	0.19
770	1836	0.24	0.28	1000	2277	0.17	0.23
770	1836	0.24	0.28	1000	2277	0.17	0.23
770	1825	0.24	0.28	1000	2277	0.17	0.25
17	40	9.00	13.00	1000	2436	0.17	0.23
17	40	9.00	13.00	1000	2675	0.16	0.23
17	42	9.00	12.00	1000	2675	0.16	0.23
17	43	9.00	12.00	1000	2675	0.16	0.23
17	43	9.00	13.00	44	117	3.60	5.00
34	80	5.00	7.00	44	117	3.60	5.00

TABLE 10

FUNDAMENTAL, AND FIRST AND SECOND HIGHER MODE EIGENVALUES, AND CORRESPONDING PHASE VELOCITIES AND ATTENUATIONS OF THE LEFT LAYERS (THE CASE WHERE THE IMAGINARY PART OF THE INPUT VELOCITY IS .1% OF ITS REAL PART)

Wavenumber (KM^{-1})			Phase Velocity (KM/SEC)			Attenuation ($x10^{-2}$)
Fundamental Mode	1st Higher Mode	2nd Higher Mode	Fundamental Mode	1st Higher Mode	2nd Higher Mode	Fundamental Mode
0.2009	0.1618	0.1589	3.475	4.315	4.394	0.199
0.1806	0.1453	0.1421	3.478	4.323	4.423	0.202
0.1497	0.1207	0.1207	3.497	4.337	4.481	0.208
0.1180	0.0960	--	3.551	4.363	--	0.218
0.0962	--	--	3.627	--	--	0.226
0.0853	--	--	3.681	--	--	0.228
0.0765	--	--	3.732	--	--	0.227
0.0662	--	--	3.796	--	--	0.224
0.0542	--	--	3.866	--	--	0.215
0.0460	--	--	3.902	--	--	0.209
0.0400	--	--	3.924	--	--	0.207
0.0355	--	--	3.940	--	--	0.206
0.0318	--	--	3.955	--	--	0.208
0.0262	--	--	3.997	--	--	0.216
0.0221	--	--	4.066	--	--	0.230

TABLE 11

FUNDAMENTAL, AND FIRST AND SECOND HIGHER MODE EIGENVALUES, AND CORRESPONDING PHASE VELOCITIES AND ATTENUATIONS OF THE RIGHT LAYERS (THE CASE WHERE THE IMAGINARY PART OF THE INPUT VELOCITY IS .1% OF ITS REAL PART)

Wavenumber (KM^{-1})			Phase Velocity			Attenuation ($x10^{-2}$)
Fundamental Mode	1st Higher Mode	2nd Higher Mode	Fundamental Mode	1st Higher Mode	2nd Higher Mode	Fundamental Mode
0.2002	0.1544	0.1532	3.487	4.522	4.553	0.202
0.1799	0.1385	0.1369	3.493	4.537	4.590	0.204
0.1490	0.1150	--	3.514	4.552	--	0.209
0.1174	0.0915	--	3.569	4.578	--	0.218
0.0958	0.0757	--	3.644	4.613	--	0.226
0.0849	--	--	3.700	--	--	0.229
0.0761	--	--	3.755	--	--	0.230
0.0656	--	--	3.830	--	--	0.229
0.0533	--	--	3.928	--	--	0.224
0.0449	--	--	3.996	--	--	0.219
0.0388	--	--	4.045	--	--	0.216
0.0342	--	--	4.084	--	--	0.215
0.0305	--	--	4.120	--	--	0.217
0.0249	--	--	4.198	--	--	0.225
0.0208	--	--	4.308	--	--	0.243

TABLE 12

FUNDAMENTAL, AND FIRST AND SECOND HIGHER MODE EIGENVALUES, AND CORRESPONDING PHASE VELOCITIES AND ATTENUATIONS OF THE LEFT LAYERS (THE CASE WHERE Q_β IS CONSTANT)

Wavenumber (KM^{-1})			Phase Velocity			Attenuation ($\times 10^{-2}$)
Fundamental Mode	1st Higher Mode	2nd Higher Mode	Fundamental Mode	1st Higher Mode	2nd Higher Mode	Fundamental Mode
0.2009	0.1618	0.1589	3.475	4.316	4.394	0.2053
0.1806	0.1453	0.1420	3.478	4.323	4.423	0.2053
0.1497	0.1207	--	3.497	4.337	--	0.2065
0.1179	0.0960	--	3.551	4.363	--	0.2092
0.0962	--	--	3.627	--	--	0.2092
0.0853	--	--	3.681	--	--	0.2068
0.0765	--	--	3.732	--	--	0.2026
0.0662	--	--	3.797	--	--	0.1951
0.0542	--	--	3.866	--	--	0.1848
0.0460	--	--	3.903	--	--	0.1794
0.0400	--	--	3.924	--	--	0.1772
0.0354	--	--	3.939	--	--	0.1768
0.0318	--	--	3.955	--	--	0.1781
0.0262	--	--	3.997	--	--	0.1836
0.0221	--	--	4.067	--	--	0.1940

TABLE 13

FUNDAMENTAL, AND FIRST AND SECOND HIGHER MODE EIGENVALUES, AND CORRESPONDING PHASE VELOCITIES AND ATTENUATIONS OF THE RIGHT LAYERS (THE CASE WHERE Q_β IS CONSTANT)

Wavenumber (KM^{-1})			Phase Velocity			Attenuation ($\times 10^{-2}$)
Fundamental Mode	1st Higher Mode	2nd Higher Mode	Fundamental Mode	1st Higher Mode	2nd Higher Mode	Fundamental Mode
0.2002	0.1544	0.1533	3.487	4.522	4.553	0.1071
0.1799	0.1385	0.1369	3.493	4.537	4.590	0.1081
0.1490	0.1150	--	3.514	4.552	--	0.1108
0.1174	0.0915	--	3.569	4.578	--	0.1160
0.0958	0.0757	--	3.645	4.614	--	0.1205
0.0849	--	--	3.700	--	--	0.1221
0.0761	--	--	3.755	--	--	0.1226
0.0656	--	--	3.830	--	--	0.1216
0.0533	--	--	3.928	--	--	0.1185
0.0449	--	--	3.996	--	--	0.1159
0.0388	--	--	4.045	--	--	0.1146
0.0342	--	--	4.084	--	--	0.1142
0.0305	--	--	4.120	--	--	0.1148
0.0249	--	--	4.198	--	--	0.1187
0.0208	--	--	4.308	--	--	0.1270

TABLE 14

FUNDAMENTAL, AND FIRST AND SECOND HIGHER MODE EIGENVALUES, AND CORRESPONDING PHASE VELOCITIES AND ATTENUATIONS OF THE LEFT LAYERS (THE CASE OF LEE AND SOLOMON'S MODEL)

Wavenumber (KM^{-1})			Phase Velocity			Attenuation ($x10^{-2}$)
Fundamental Mode	1st Higher Mode	2nd Higher Mode	Fundamental Mode	1st Higher Mode	2nd Higher Mode	Fundamental Mode
0.2008	0.1613	0.1591	3.476	4.329	4.389	2.1463
0.1806	0.1449	0.1421	3.479	4.335	4.419	2.0031
0.1497	0.1205	--	3.498	4.345	--	1.7263
0.1179	0.0959	--	3.552	4.368	--	1.3356
0.0962	--	--	3.628	--	--	1.0034
0.0853	--	--	3.682	--	--	0.8519
0.0765	--	--	3.733	--	--	0.7852
0.0662	--	--	3.797	--	--	0.8549
0.0541	--	--	3.867	--	--	1.2567
0.0460	--	--	3.903	--	--	1.7255
0.0400	--	--	3.925	--	--	2.1302
0.0354	--	--	3.941	--	--	2.4612
0.0318	--	--	3.956	--	--	2.7363
0.0262	--	--	3.999	--	--	3.1892
0.0221	--	--	4.068	--	--	3.6047

TABLE 15

FUNDAMENTAL, AND FIRST AND SECOND HIGHER MODE EIGENVALUES AND CORRESPONDING PHASE VELOCITIES AND ATTENUATIONS OF THE RIGHT LAYERS (THE CASE OF LEE AND SOLOMON'S MODEL)

Wavenumber (KM^{-1})			Phase Velocity			Attenuation ($x10^{-2}$)
Fundamental Mode	1st Higher Mode	2nd Higher Mode	Fundamental Mode	1st Higher Mode	2nd Higher Mode	Fundamental Mode
0.2002	0.1543	0.1534	3.487	4.524	4.552	0.0890
0.1799	0.1383	0.1370	3.493	4.541	4.586	0.0891
0.1490	0.1149	--	3.514	4.554	--	0.0901
0.1173	0.0915	--	3.569	4.579	--	0.0928
0.0958	0.0756	--	3.645	4.615	--	0.0958
0.0849	--	--	3.700	--	--	0.0973
0.0761	--	--	3.755	--	--	0.0986
0.0656	--	--	3.830	--	--	0.1012
0.0533	--	--	3.928	--	--	0.1176
0.0449	--	--	3.997	--	--	0.1623
0.0388	--	--	4.045	--	--	0.2346
0.0342	--	--	4.084	--	--	0.3248
0.0305	--	--	4.120	--	--	0.4256
0.0249	--	--	4.198	--	--	0.6517
0.0208	--	--	4.308	--	--	0.9238

TABLE 16

THE SIERRA NEVADA MODEL OF LYSMER AND DRAKE
AND CALCULATED PHASE VELOCITIES USING
LAYERED SYSTEMS

Thickness	Compressional Velocity	Shear Velocity	Density	Period	Phase Velocity	
					Lysmer & Drake	This Study
6.0	5.60	3.10	2.67	6	3.065	3.064
4.5	6.00	3.40	2.70	7	3.105	3.104
5.0	6.10	3.40	2.80	8	3.148	3.147
15.0	6.90	3.90	2.80	9	3.191	3.191
20.0	7.90	4.39	3.30	10	3.236	3.237

TABLE 17

LEE AND SOLOMON'S PHASE VELOCITY

Period	Eastern United States			Western United States		
	Funda-mental Mode	1st Higher Mode	2nd Higher Mode	Funda-mental Mode	1st Higher Mode	2nd Higher Mode
10	3.532	4.468	4.521	3.379	4.454	4.657
12	3.559	4.474	4.543	3.420	4.511	4.758
15	3.620	4.483	4.577	3.489	4.578	4.980
18	3.697	4.494	4.618	3.562	4.658	5.150
20	3.752	4.502	4.652	3.611	4.723	5.232
22	3.805	4.512	4.691	3.657	4.799	--
25	3.874	4.528	4.763	3.720	4.918	--
30	3.958	4.566	4.926	3.802	5.090	--
35	4.006	4.616	--	3.860	5.209	--
45	4.047	--	--	3.941	--	--
50	4.054	--	--	3.975	--	--
60	4.061	--	--	4.044	--	--
70	4.064	--	--	4.116	--	--
80	4.070	--	--	4.190	--	--

TABLE 18

LEE AND SOLOMON'S ATTENUATION ($\times 10^{-2}$)

Period	Eastern United States			Western United States		
	Funda-mental Mode	1st Higher Mode	2nd Higher Mode	Funda-mental Mode	1st Higher Mode	2nd Higher Mode
10	.0903	2.1459	1.7652	.2516	.9800	4.6070
12	.0933	2.1146	1.6871	.2348	.1986	4.1221
15	.0958	2.0682	1.6130	.2125	2.9181	3.9127
18	.0977	2.0344	1.6255	.2017	3.4195	3.7966
20	.0982	2.0239	1.6693	.2122	3.6140	3.6374
22	.0981	2.0230	1.7286	.2482	3.7146	--
25	.0983	2.0344	1.8300	.3657	3.7300	--
30	.1089	2.0665	2.0030	.7190	3.6524	--
35	.1446	2.0970	--	1.1676	3.6649	--
45	.2848	2.1568	--	2.0141	--	--
50	.3737	2.2036	--	2.3602	--	--
60	.5602	2.3752	--	2.8826	--	--
70	.7409	--	--	3.1902	--	--
80	.9083	--	--	3.3239	--	--

APPENDIX B

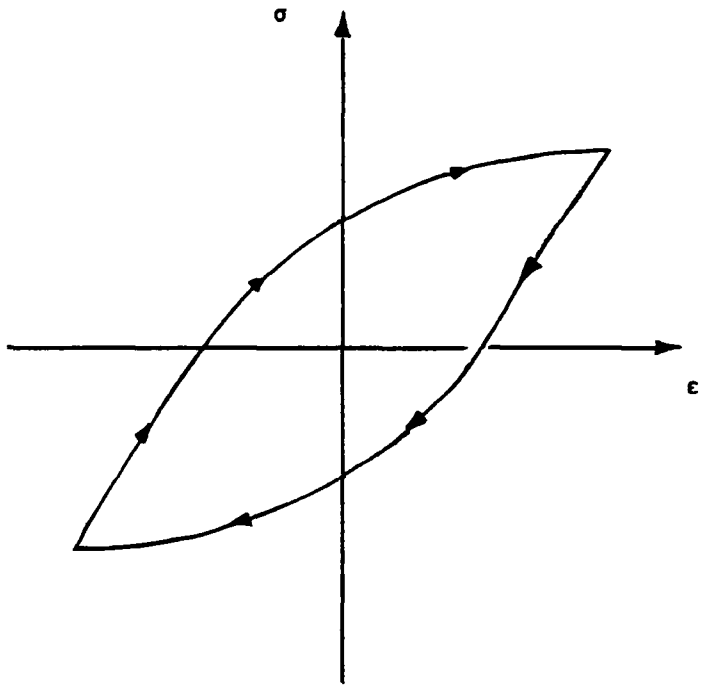

Figure 1. HYSTERETIC EFFECT OF THE VISCOELASTIC SOLID

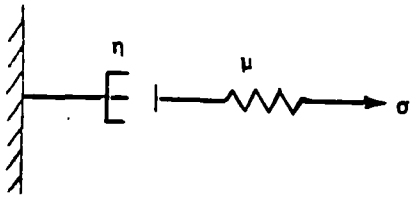

MAXWELL ELEMENT

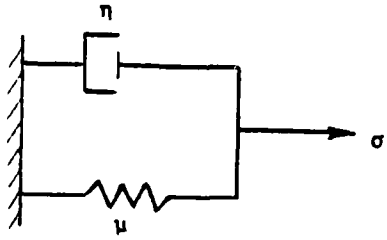

VOIGT ELEMENT

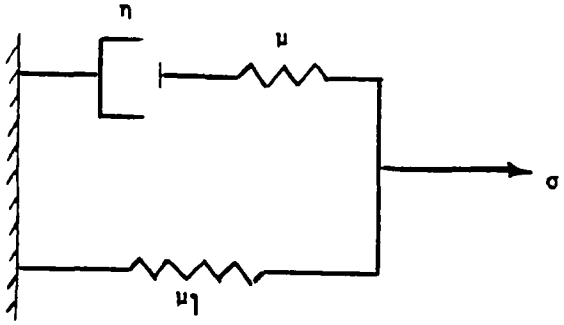

STANDARD LINEAR SOLID

Figure 2. ELEMENTAL MODEL OF VISCOELASTIC SOLID

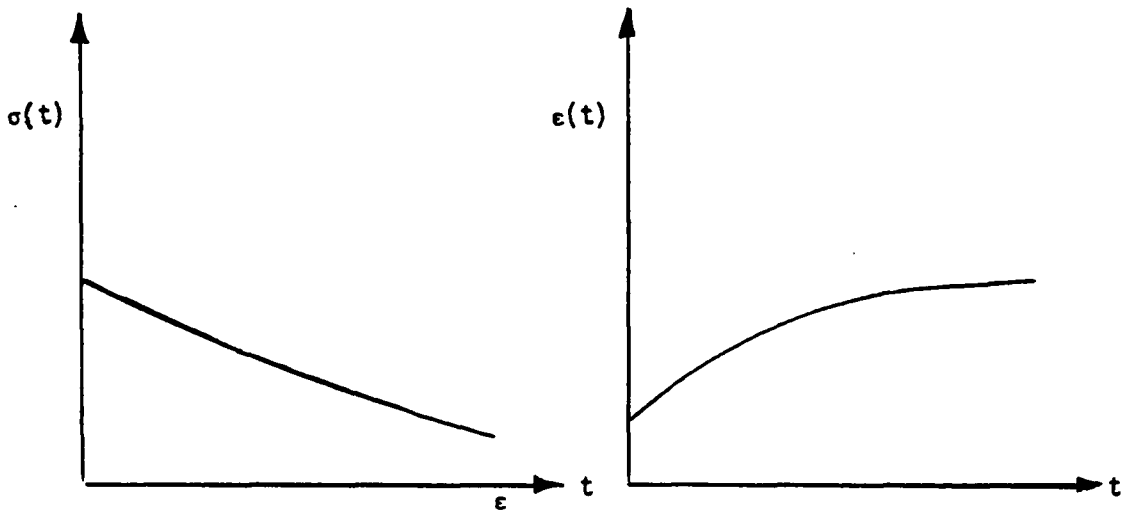

(a) RELAXATION FUNCTION (b) CREEP FUNCTION

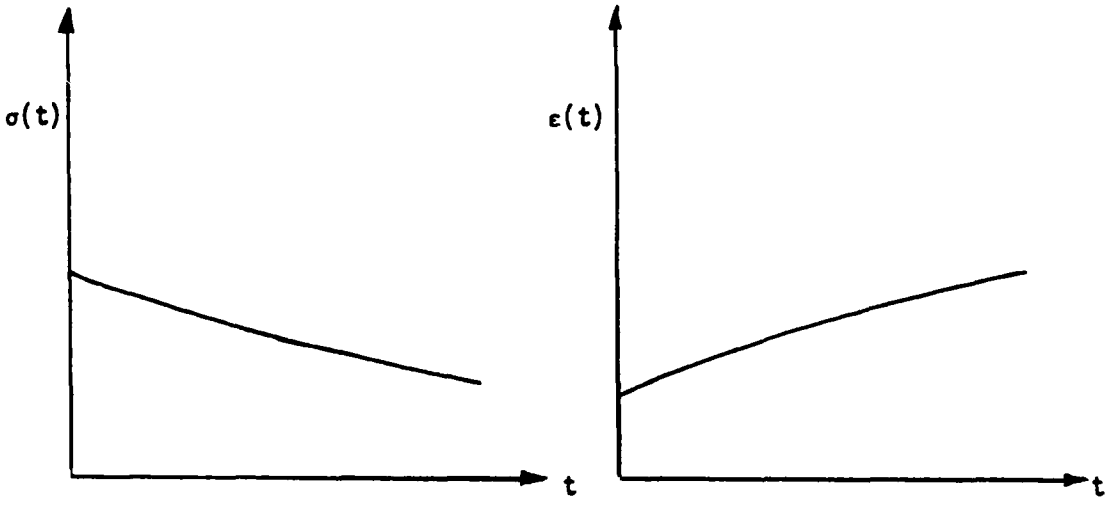

(c) RELAXATION FUNCTION (d) CREEP FUNCTION

FIGURE 3. (a) and (b) SOLUTIONS OF MAXWELL AND VOIGT ELEMENTS,
(c) and (d) SOLUTIONS OF STANDARD LINEAR SOLID

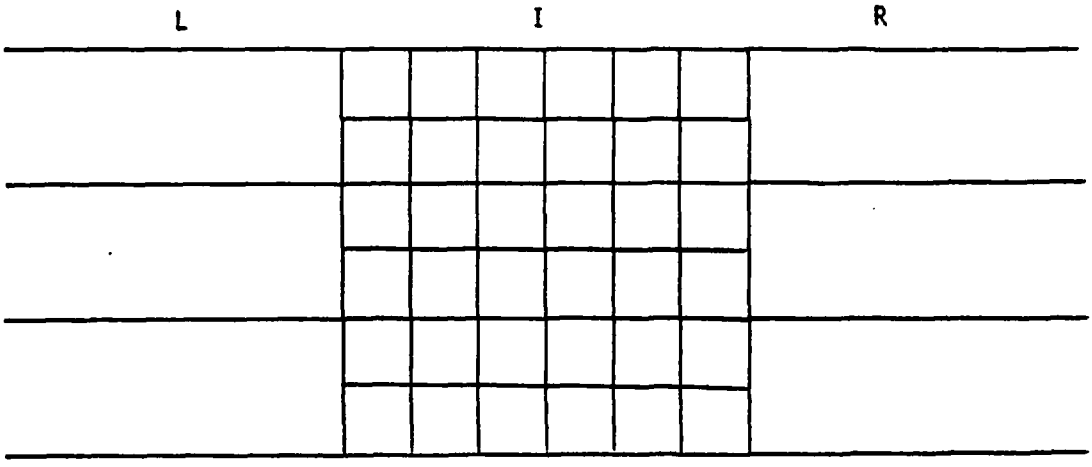

Figure 4. A FINITE ELEMENT NET, BOUNDED BY TWO SEMI-INFINITE HORIZONTALLY LAYERED SYSTEM

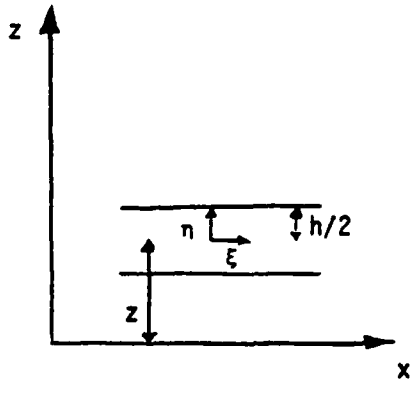

Figure 5. COORDINATES OF AN ELEMENT, η AND ξ ARE THE LOCAL COORDINATES OF THE ELEMENT

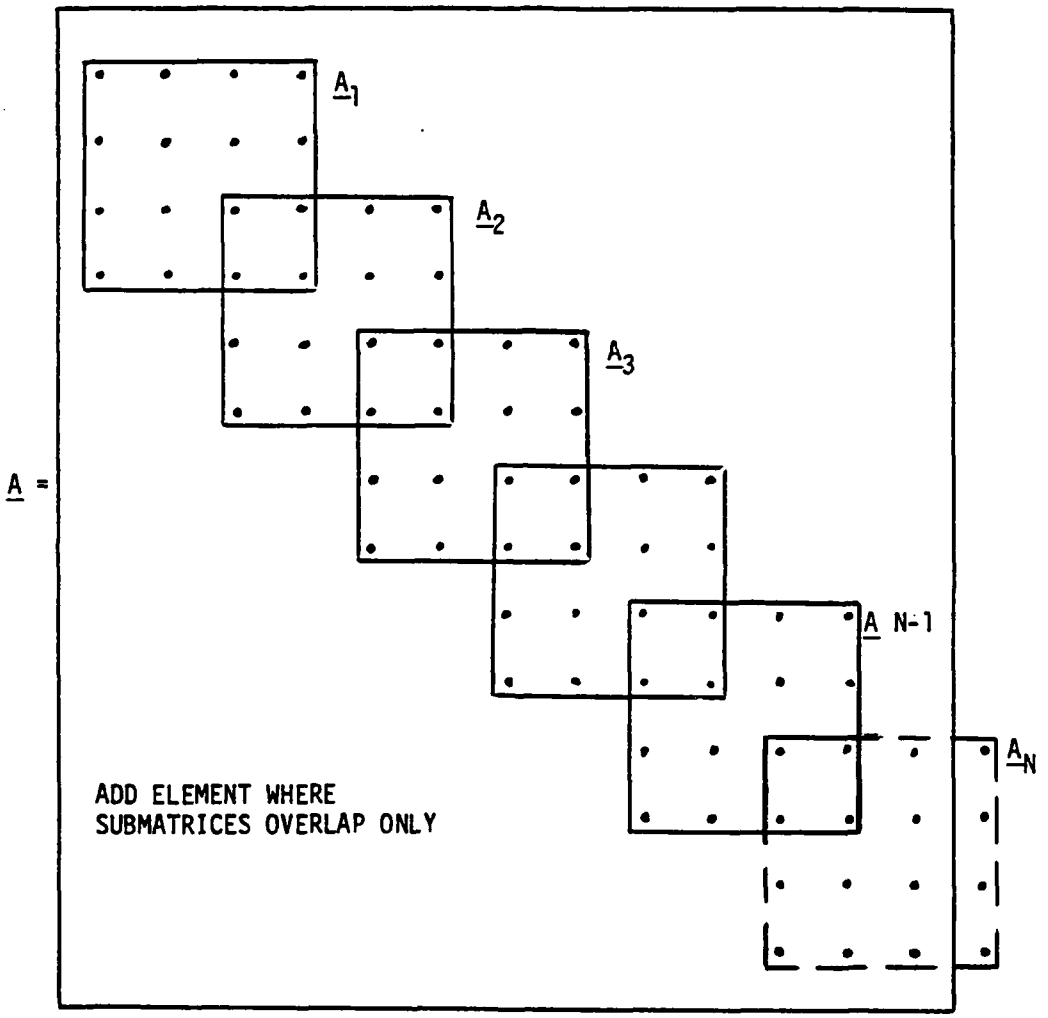

Figure 6. STRUCTURE OF MATRICES A, C, G, AND M

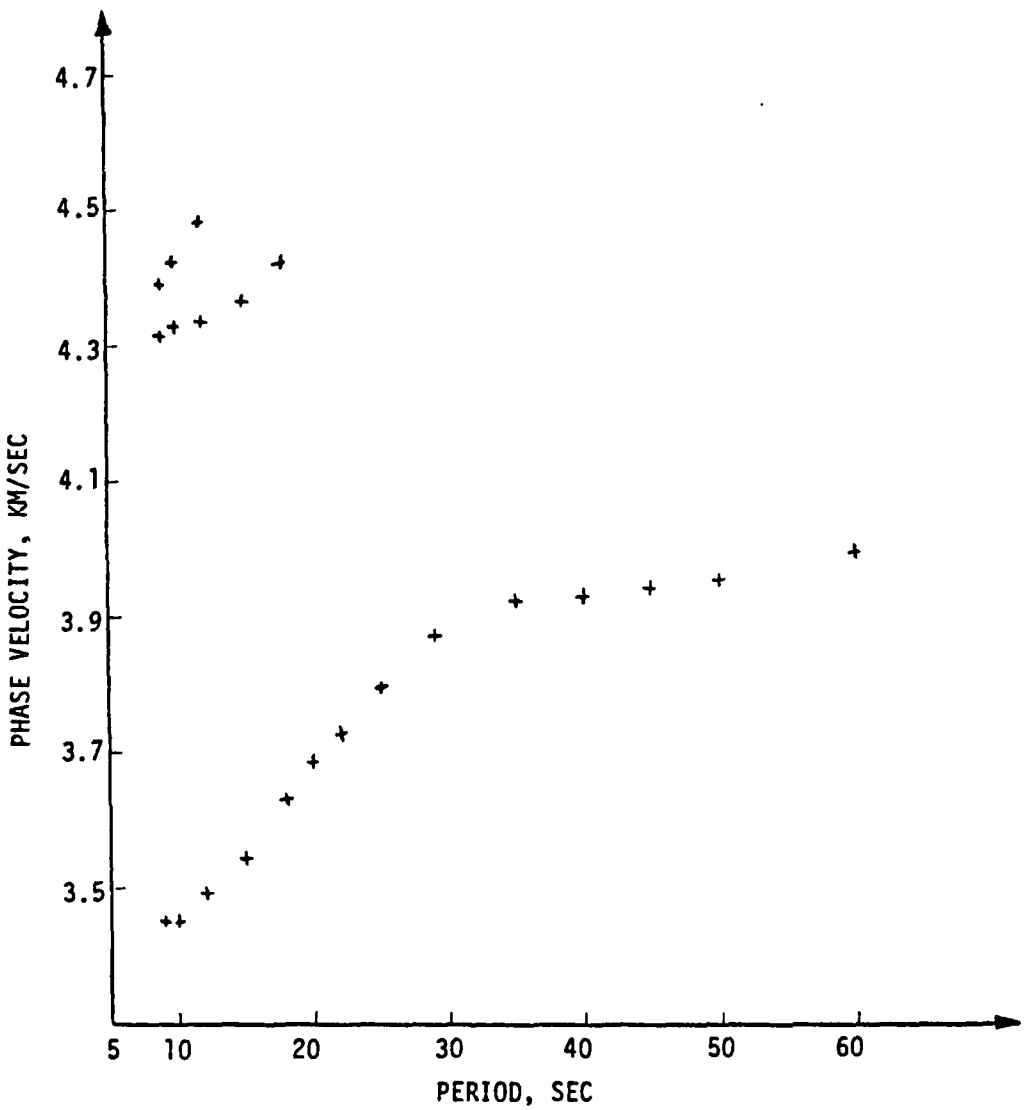

FIGURE 7. FUNDAMENTAL AND FIRST AND SECOND HIGHER MODE RAYLEIGH WAVE PHASE VELOCITIES, BASIN AND RANGE PROVINCES

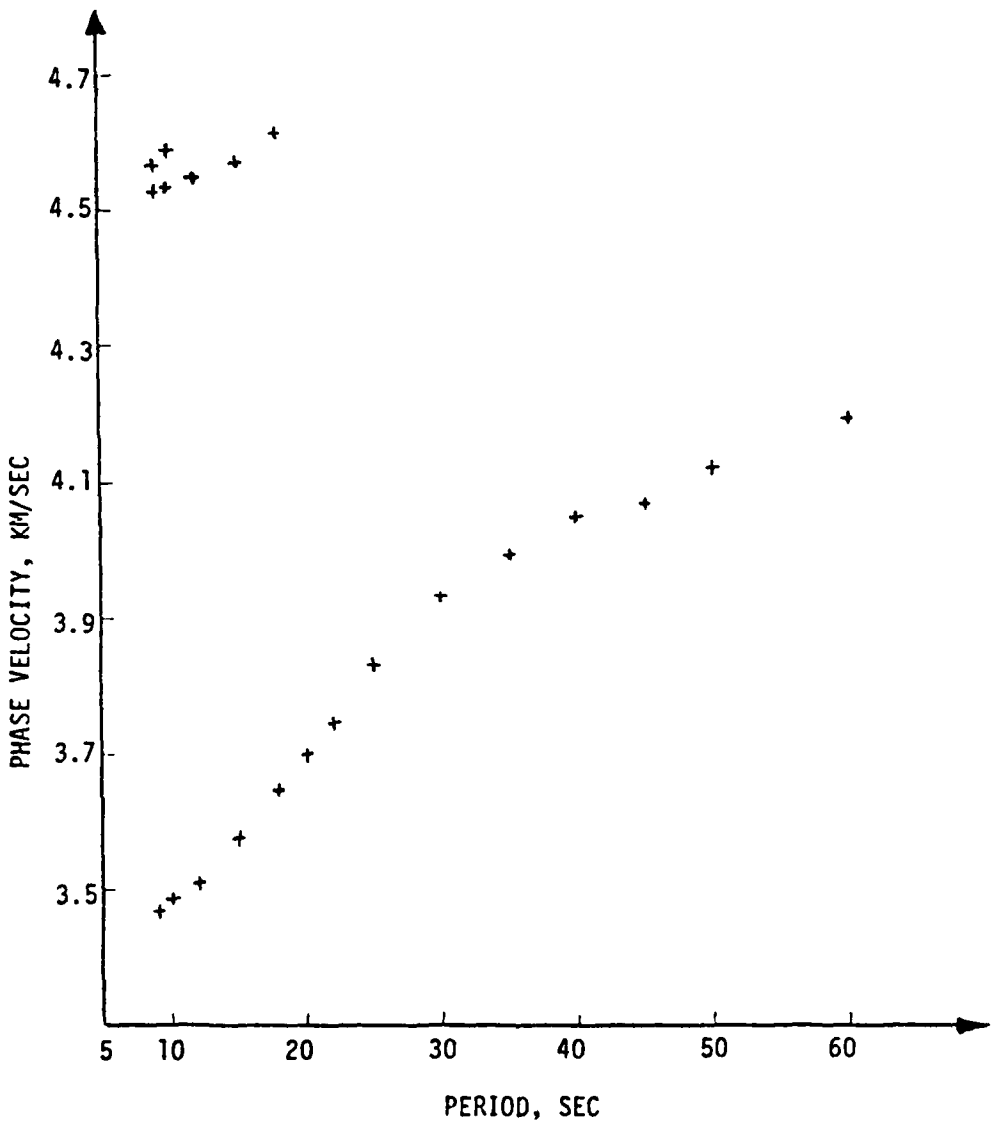

Figure 8. FUNDAMENTAL AND FIRST AND SECOND HIGHER MODE RAYLEIGH WAVE PHASE VELOCITIES, CANADIAN SHIELD

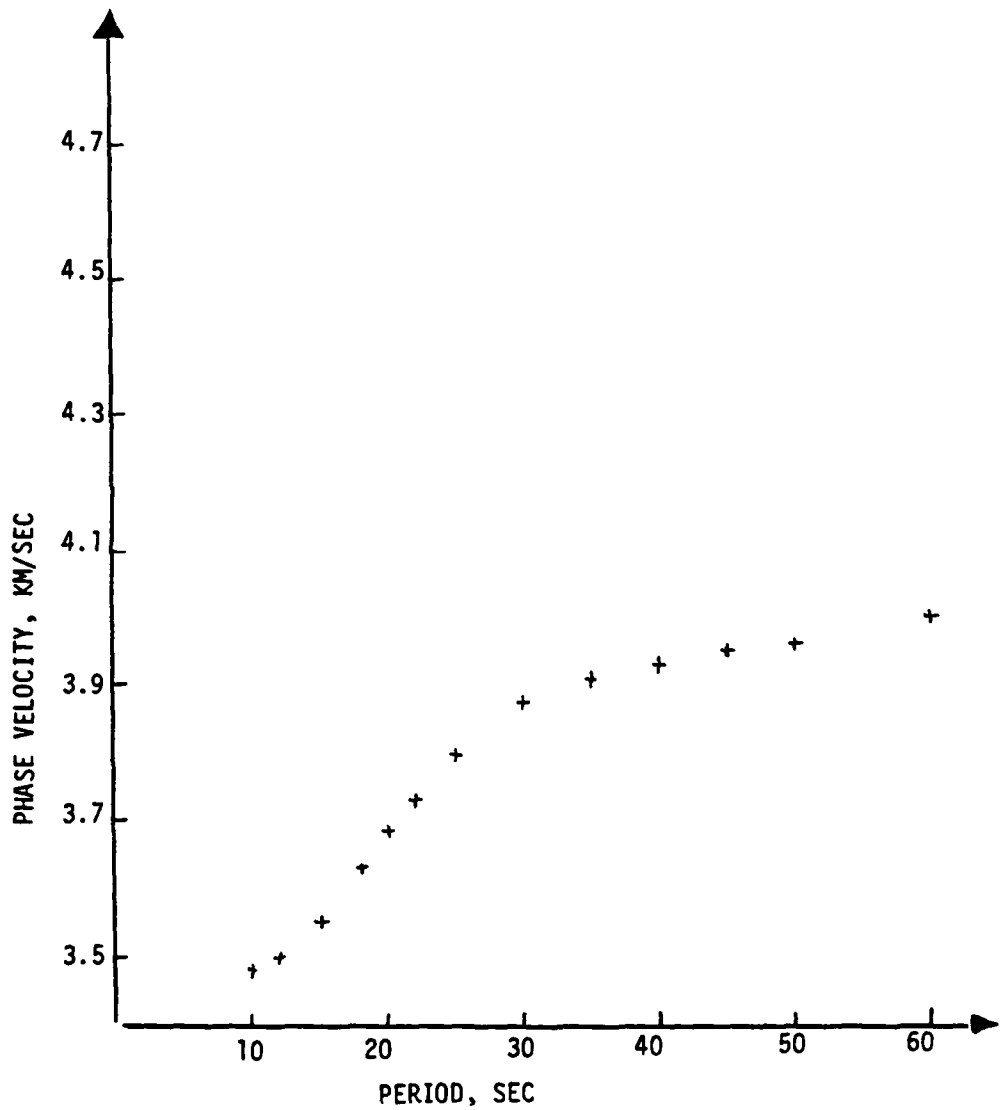

Figure 9. FUNDAMENTAL RAYLEIGH WAVE PHASE VELOCITIES OF ZONE I (THE CASE WHERE ALL THREE ZONES ARE ASSUMED TO BE THE BASIN AND RANGE PROVINCE.)

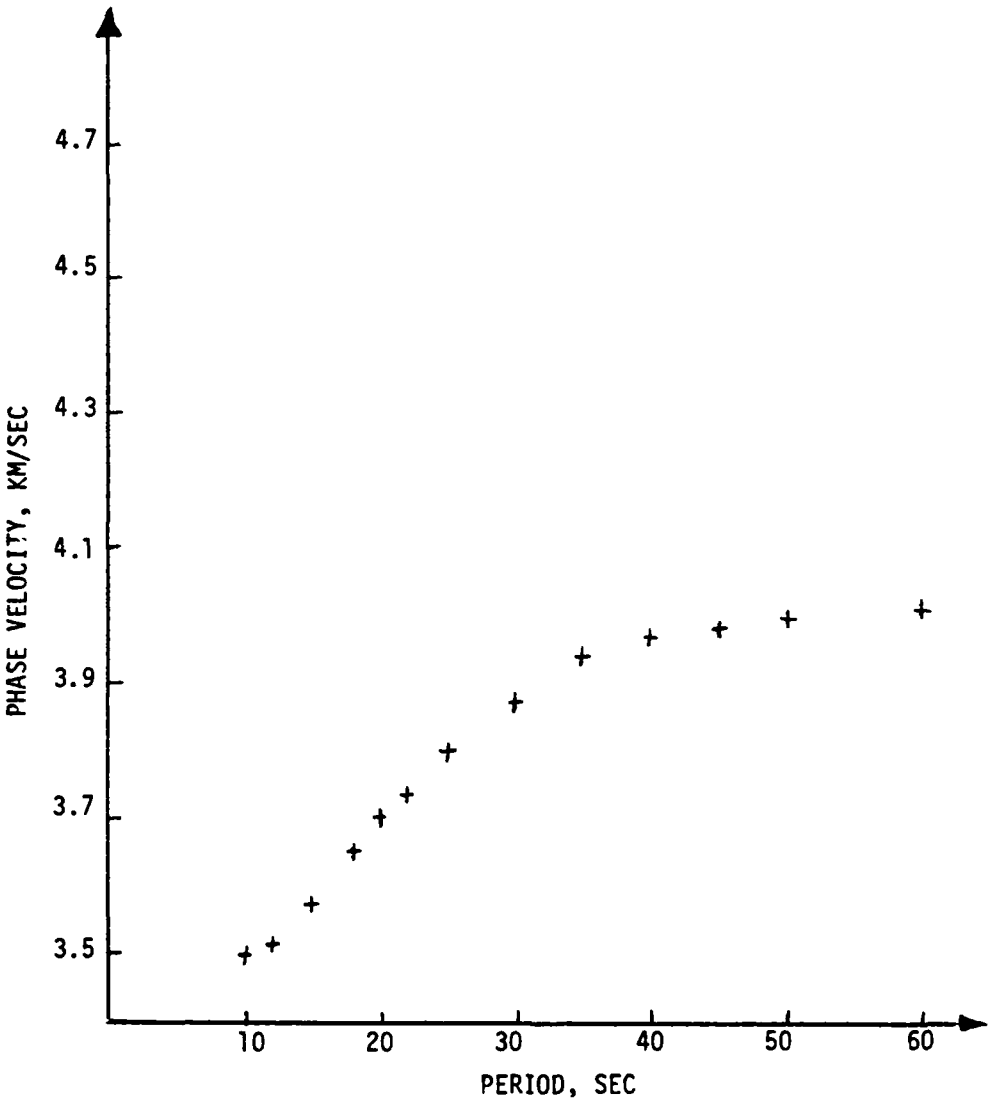

Figure 9A. FUNDAMENTAL RAYLEIGH WAVE PHASE VELOCITIES OF ZONE I (THE CASE WHERE THE VERTICAL BOUNDARY IS AT THE RIGHT HAND SIDE OF THE ZONE L).

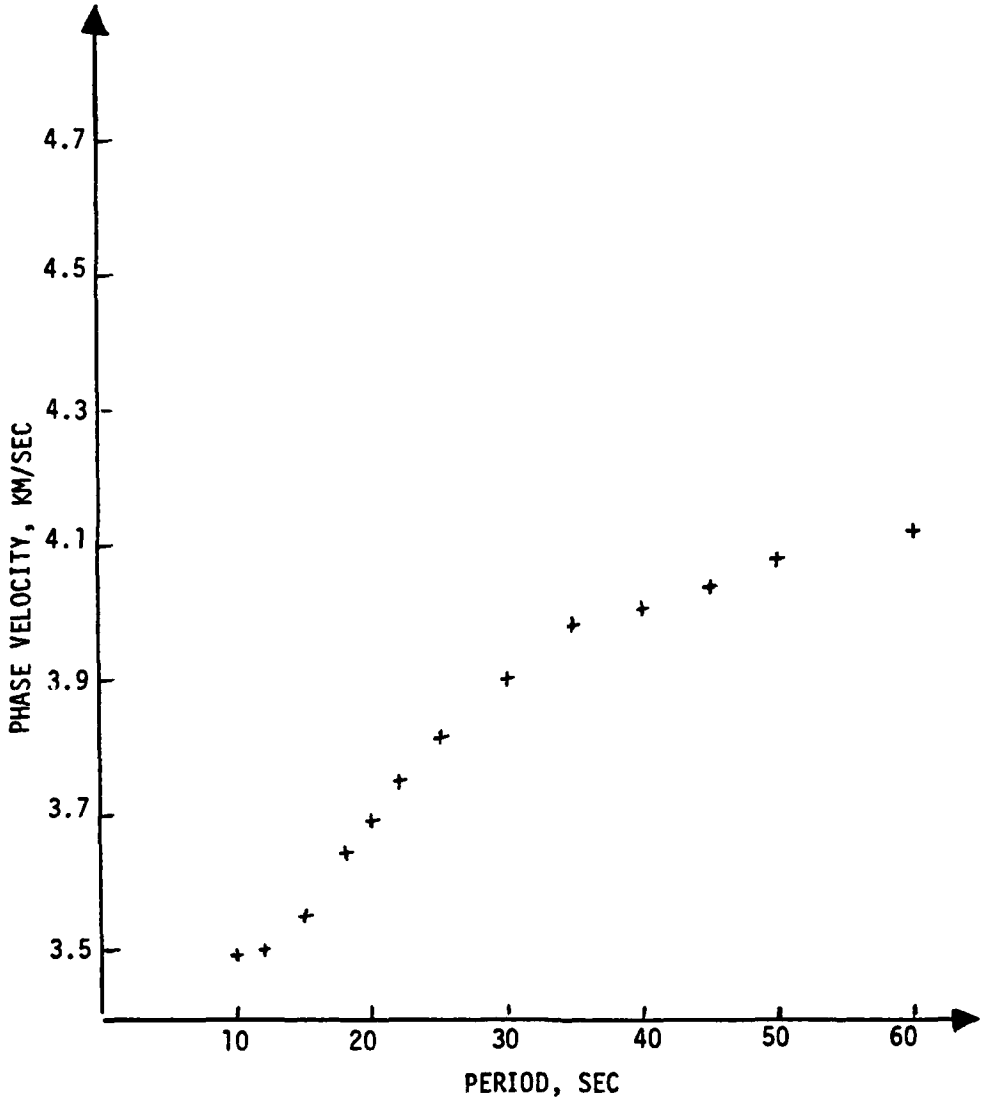

Figure 9B. FUNDAMENTAL RAYLEIGH WAVE PHASE VELOCITIES OF ZONE I (THE CASE WHERE THE VERTICAL BOUNDARY IS AT THE LEFT HAND SIDE OF THE ZONE R).

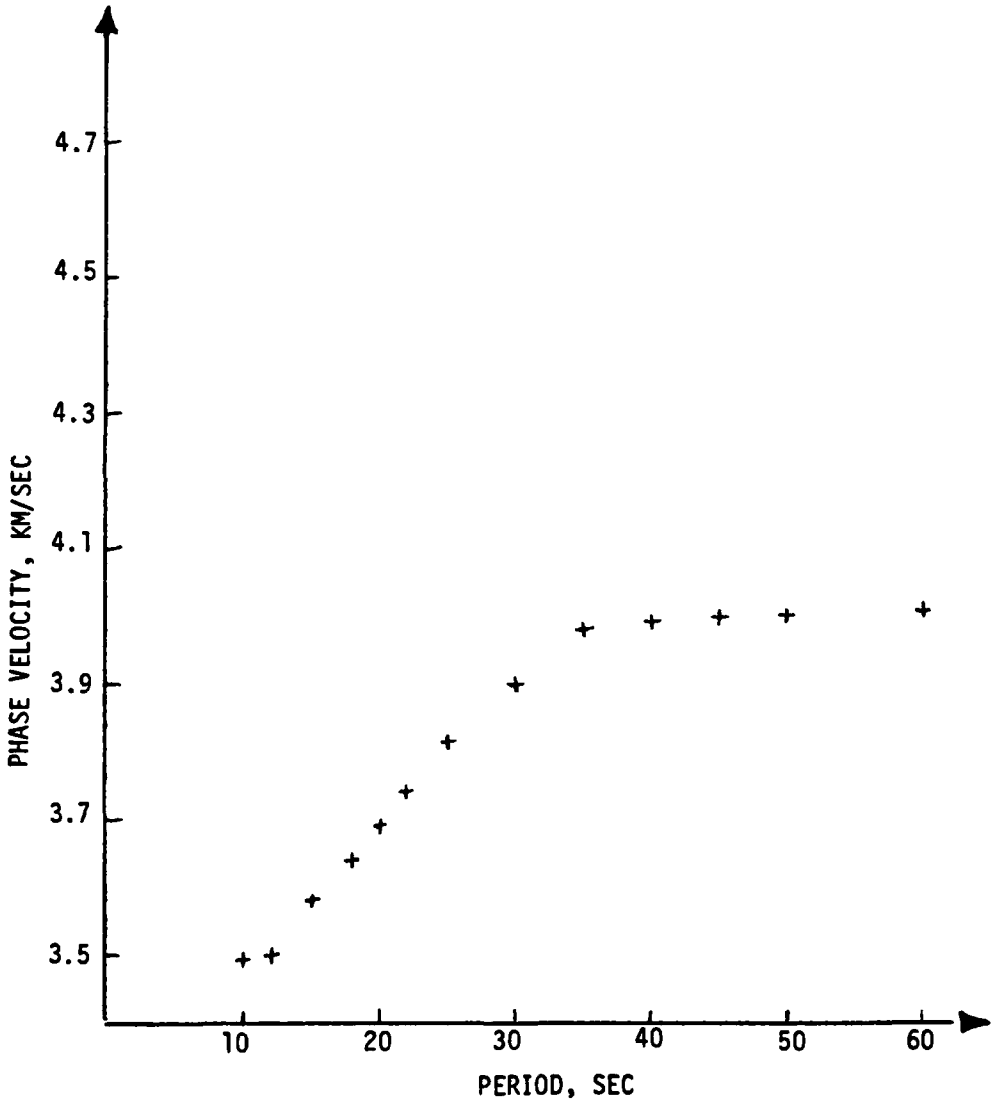

Figure 9C. FUNDAMENTAL RAYLEIGH WAVE PHASE VELOCITIES OF ZONE I (THE CASE WHERE THE VERTICAL BOUNDARY IS AT THE MIDDLE OF ZONE I).

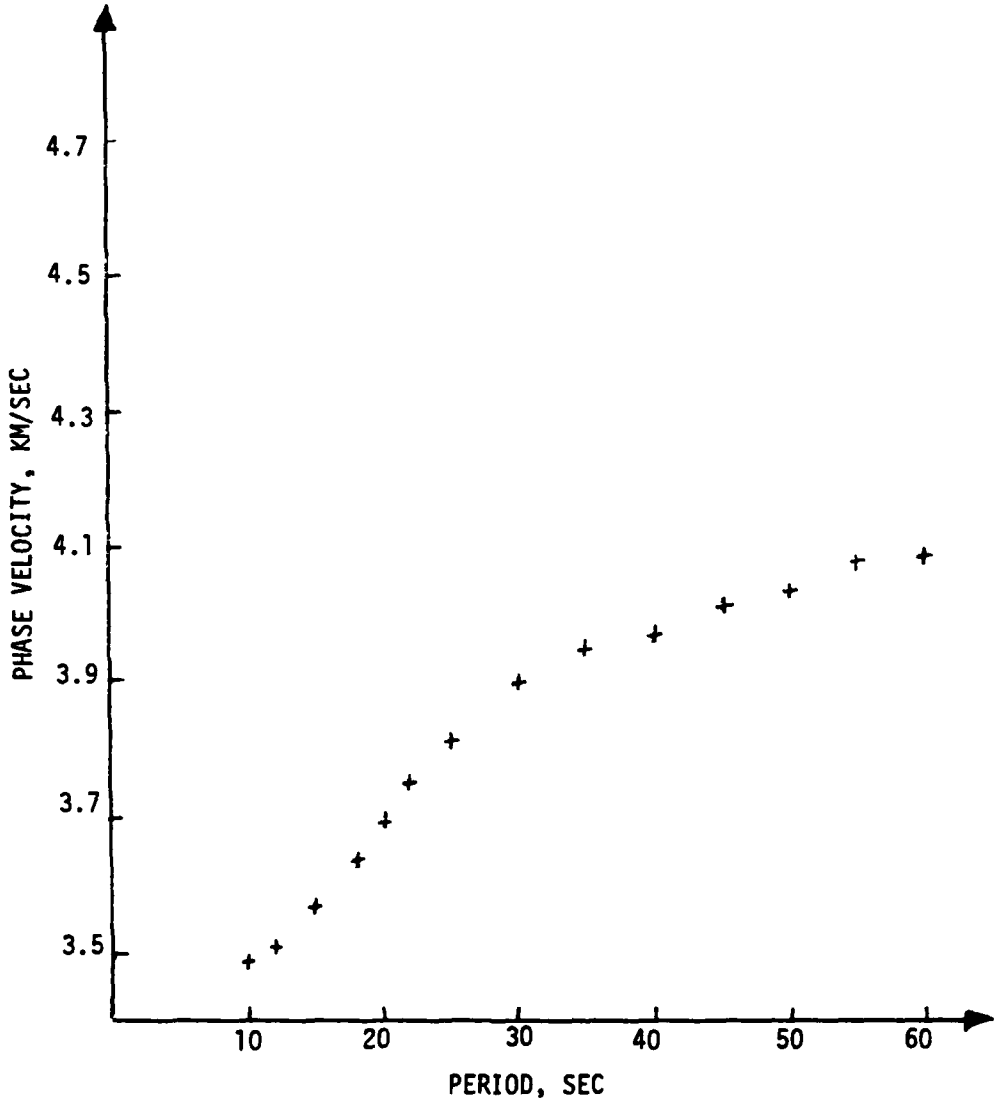

Figure 9D. FUNDAMENTAL RAYLEIGH WAVE PHASE VELOCITIES OF ZONE I (THE CASE WHERE THE POSITION OF VERTICAL BOUNDARY GRADUALLY CHANGES).

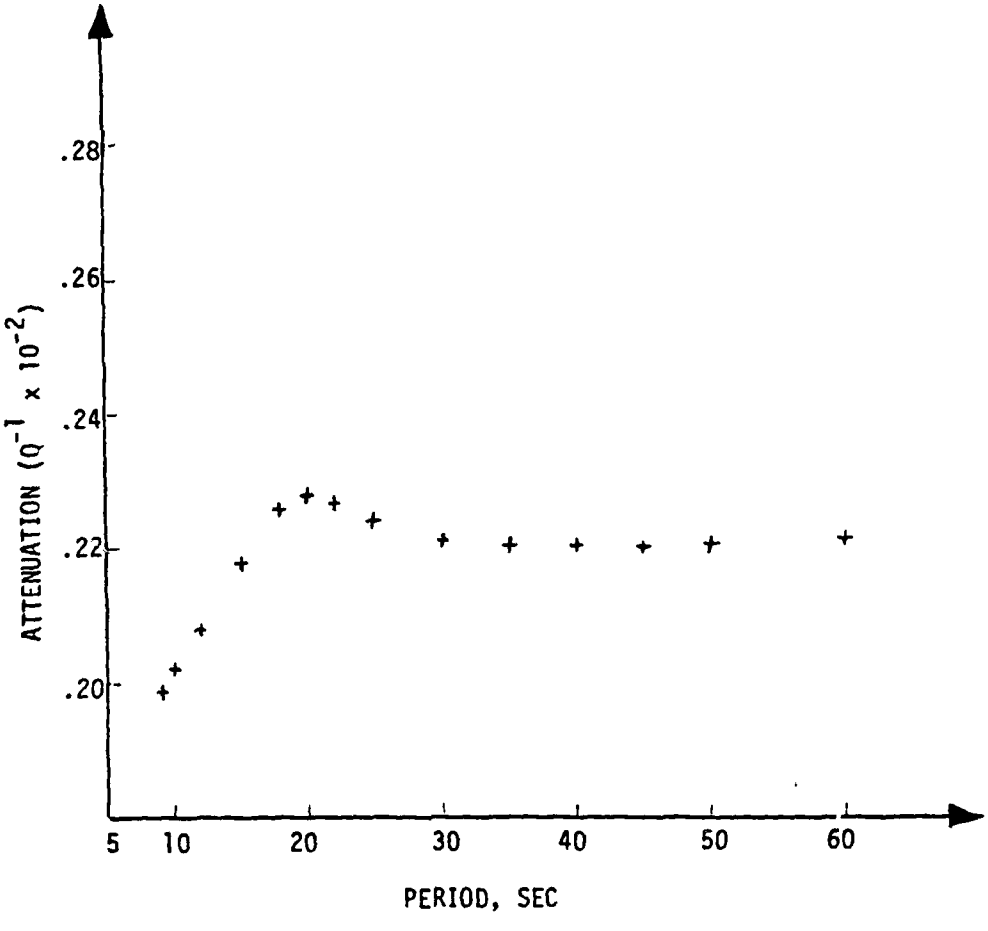

Figure 10. RAYLEIGH WAVE ATTENUATION, BASIN AND RANGE PROVINCES.
(The case where the imaginary part of the input velocity is .1% of its real part)

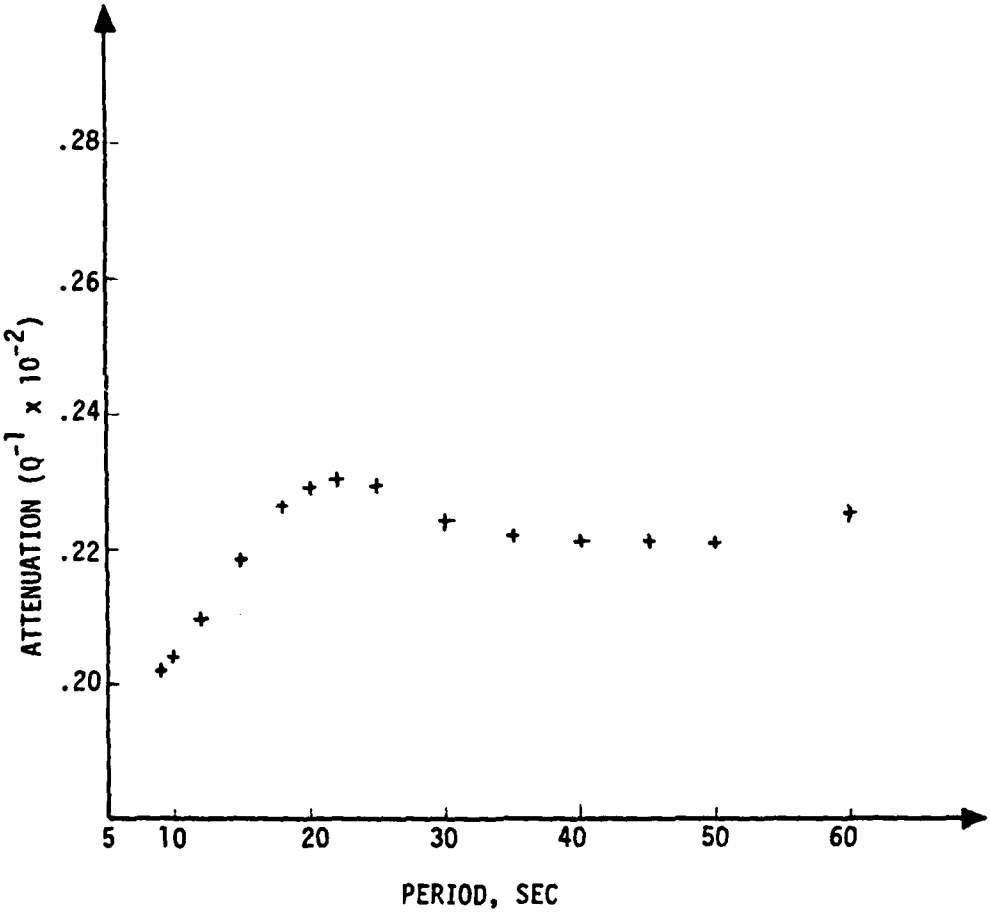

Figure 11. RAYLEIGH WAVE ATTENUATION, CANADIAN SHIELD.
(The case where the real part of the input velocity is .1% of its real part)

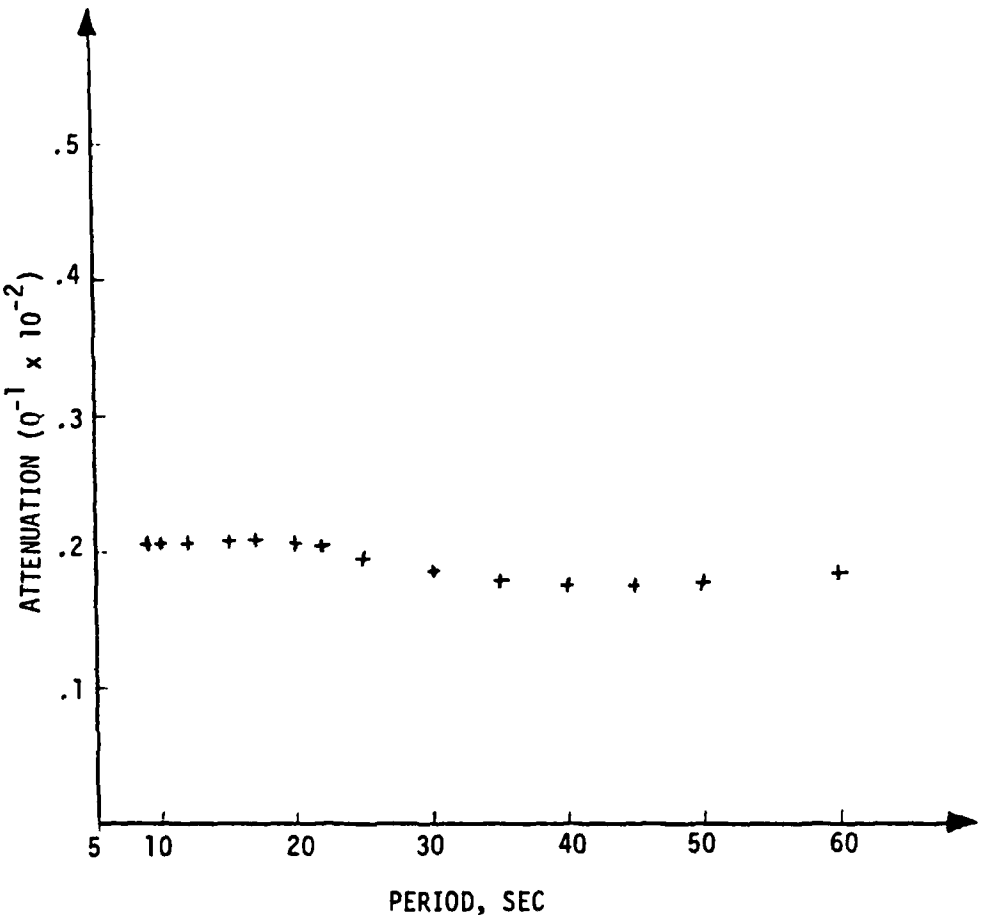

Figure 12. RAYLEIGH WAVE ATTENUATION, BASIN AND RANGE PROVINCES (The case where Q_β is constant)

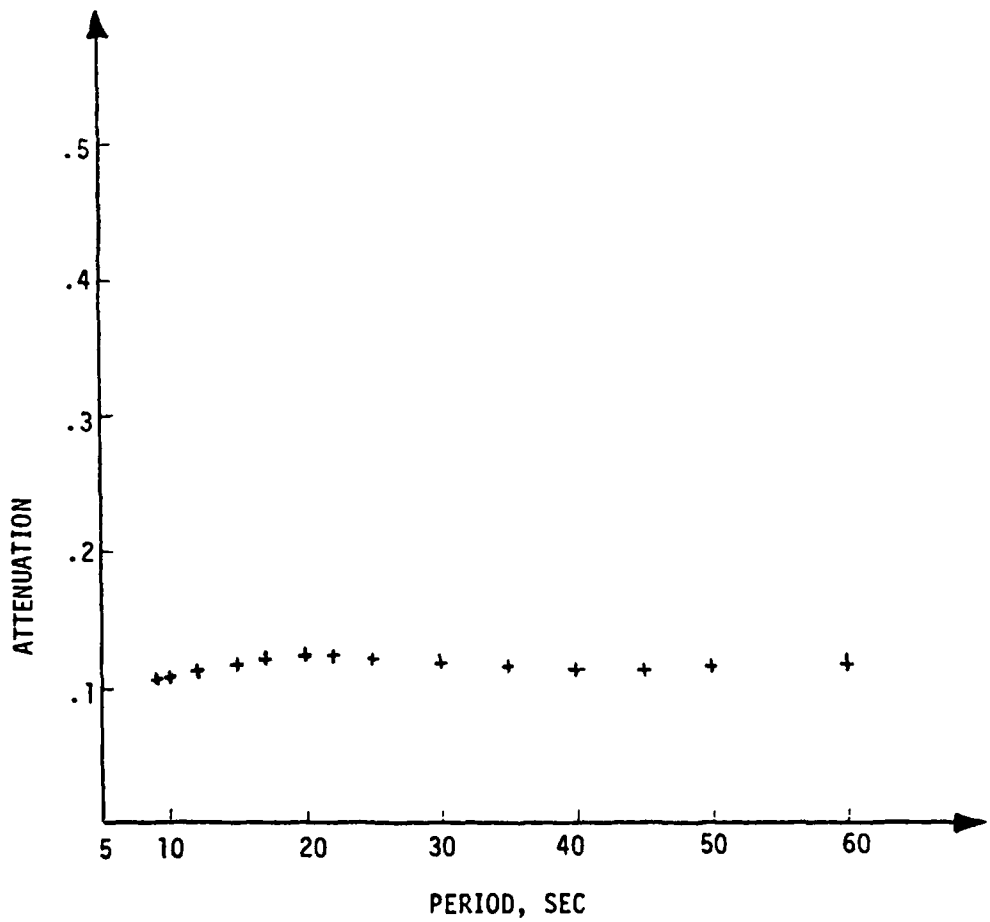

Figure 13. RAYLEIGH WAVE ATTENUATION, CANADIAN SHIELD
(The case where Q_β is constant)

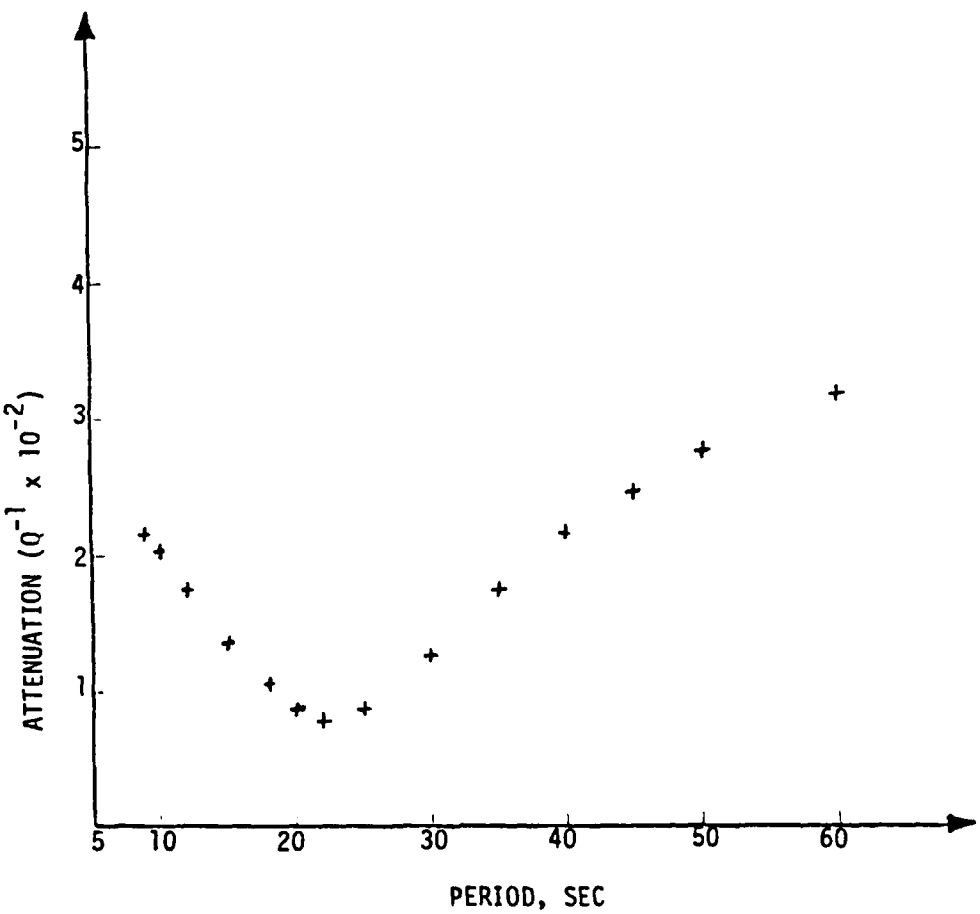

Figure 14. RAYLEIGH WAVE ATTENUATION, BASIN AND RANGE PROVINCES
(The case of Lee and Solomon's data)

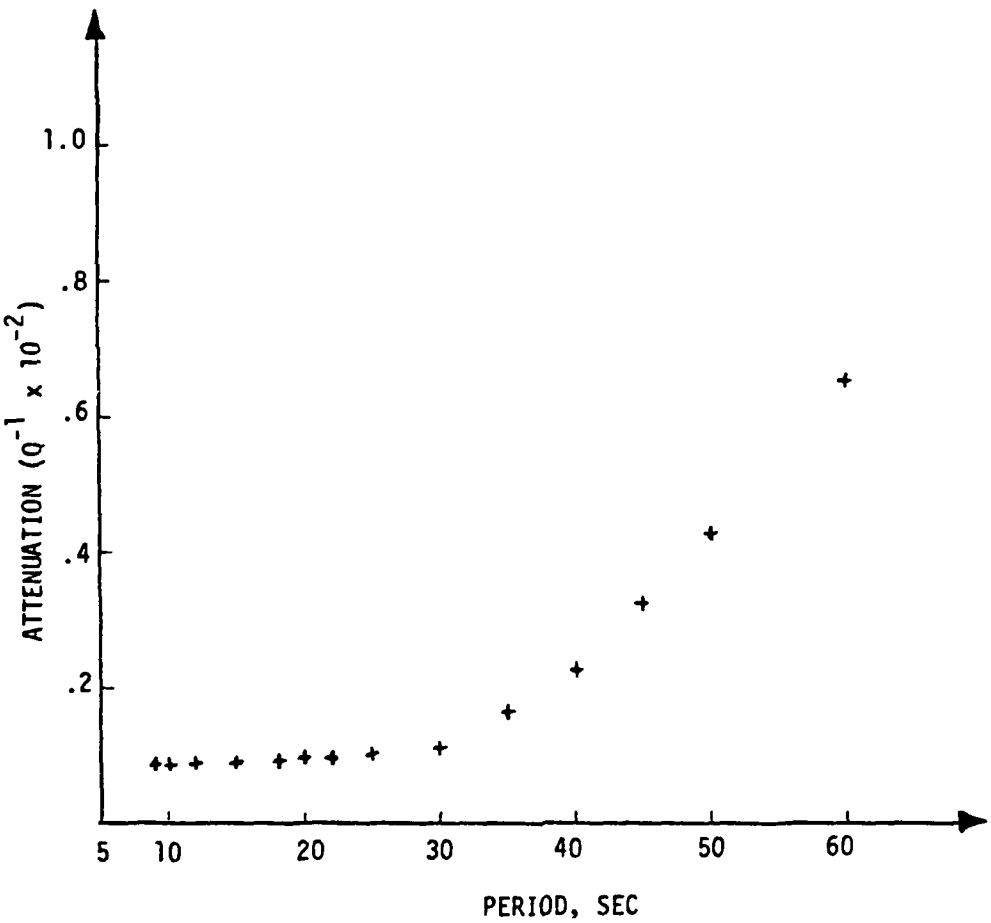

Figure 15. RAYLEIGH WAVE ATTENUATION, CANADIAN SHIELD
(The case of Lee and Solomon's data)

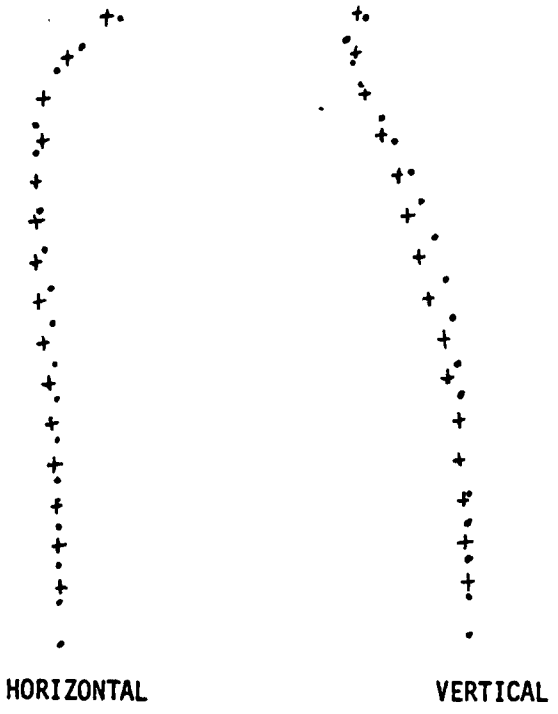

Figure 16. HORIZONTAL AND VERTICAL AMPLITUDES FOR THE FUNDAMENTAL RAYLEIGH MODE OF SIERRA NEVADA FOR A PERIOD OF 6 SECONDS. THE CIRCLES ARE FROM LYSMER AND DRAKE (80).

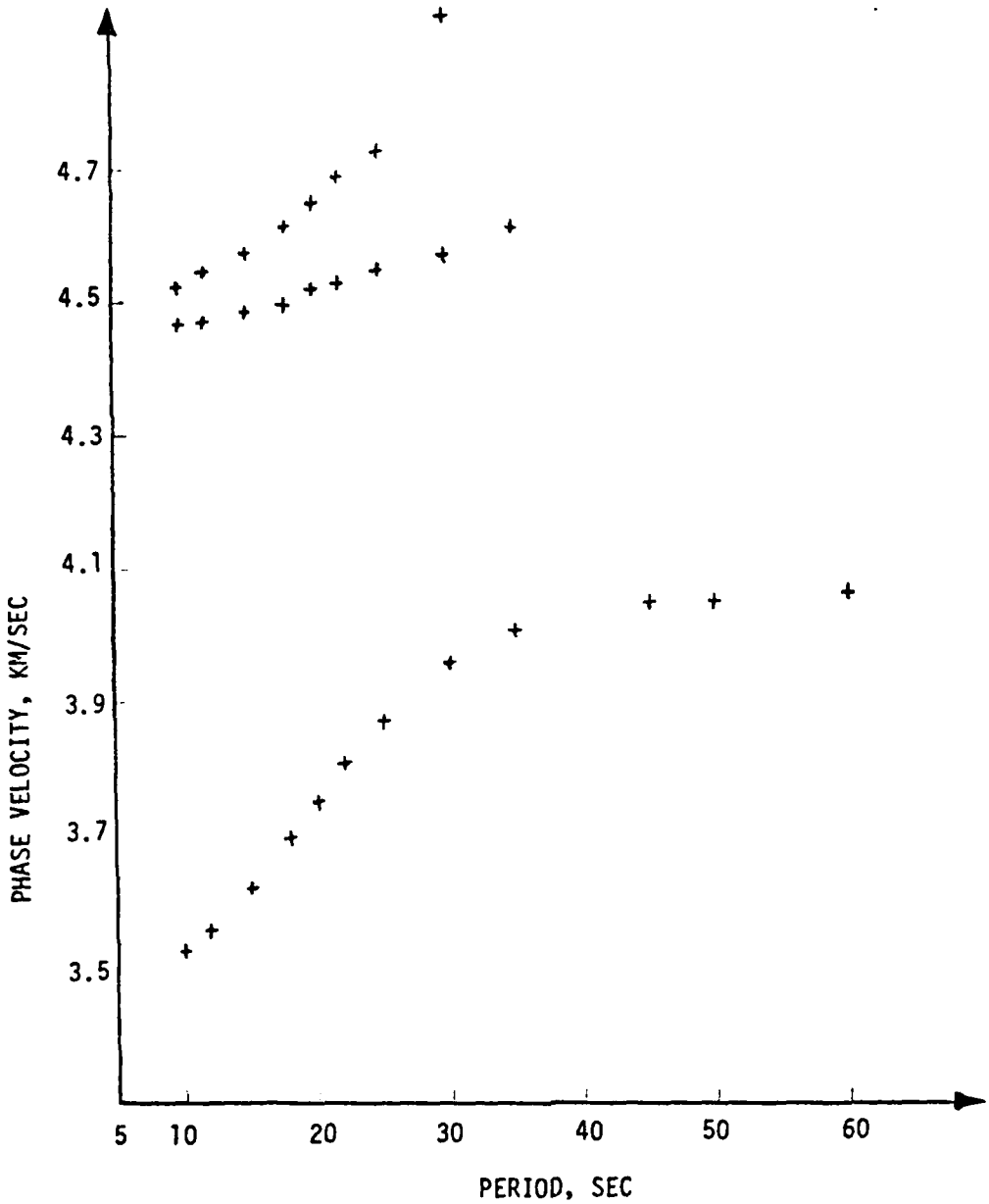

Figure 17. FUNDAMENTAL AND FIRST AND SECOND HIGHER MODE PHASE VELOCITIES, EASTERN UNITED STATES. (Lee and Solomon's model)

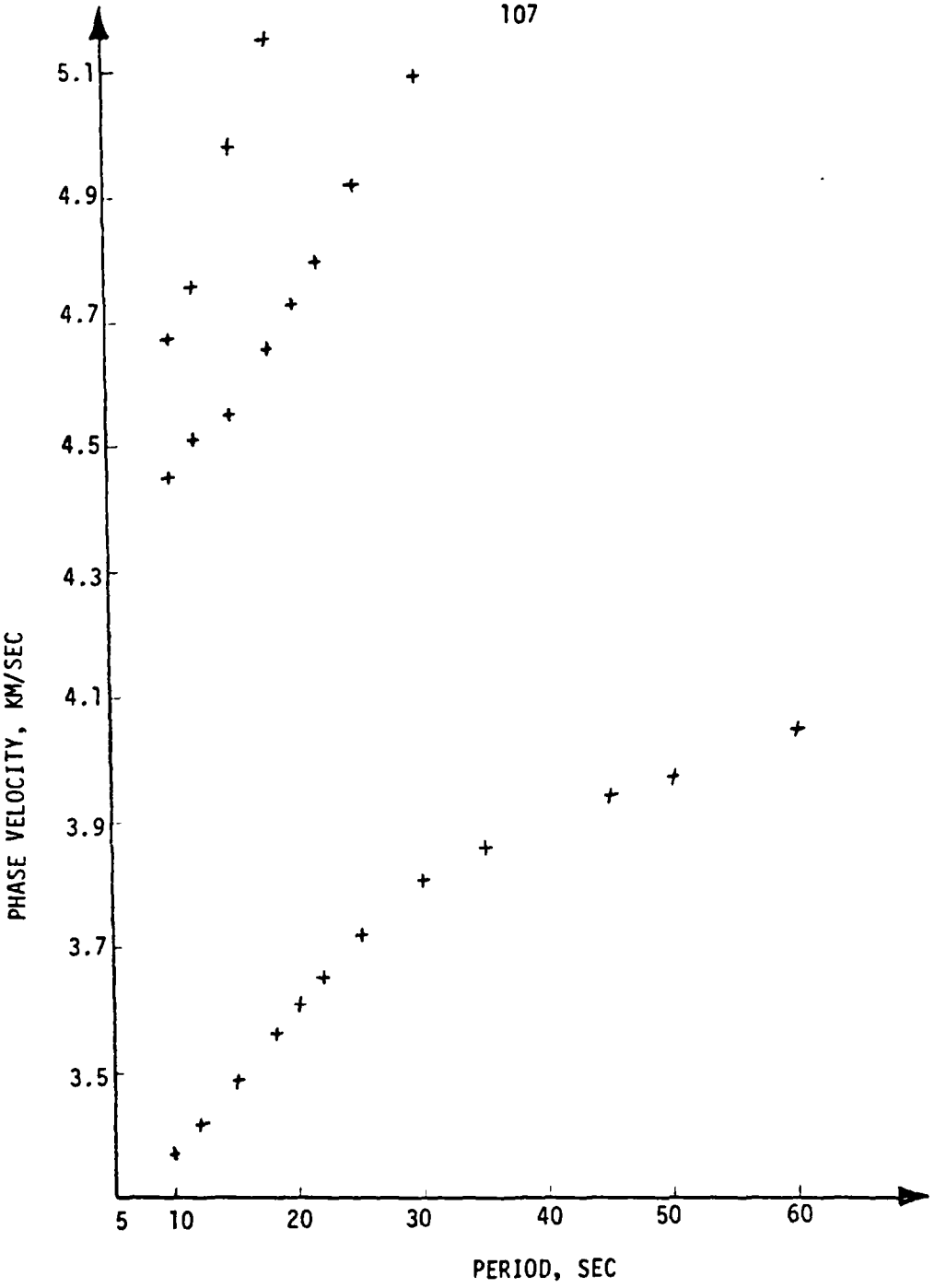

Figure 18. FUNDAMENTAL AND FIRST AND SECOND HIGHER MODE PHASE VELOCITIES, WESTERN UNITED STATES. (Lee and Solomon's model)

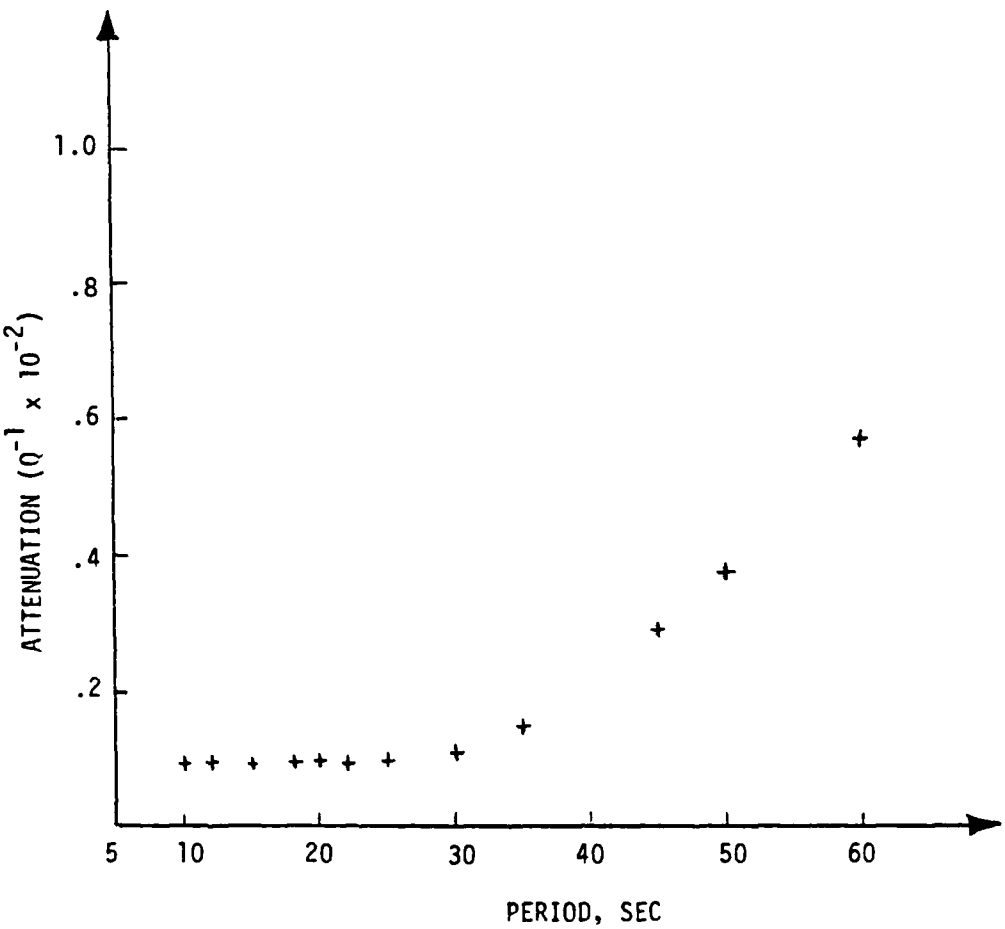

Figure 19. RAYLEIGH WAVE ATTENUATION, EASTERN UNITED STATES (Lee and Solomon's model)

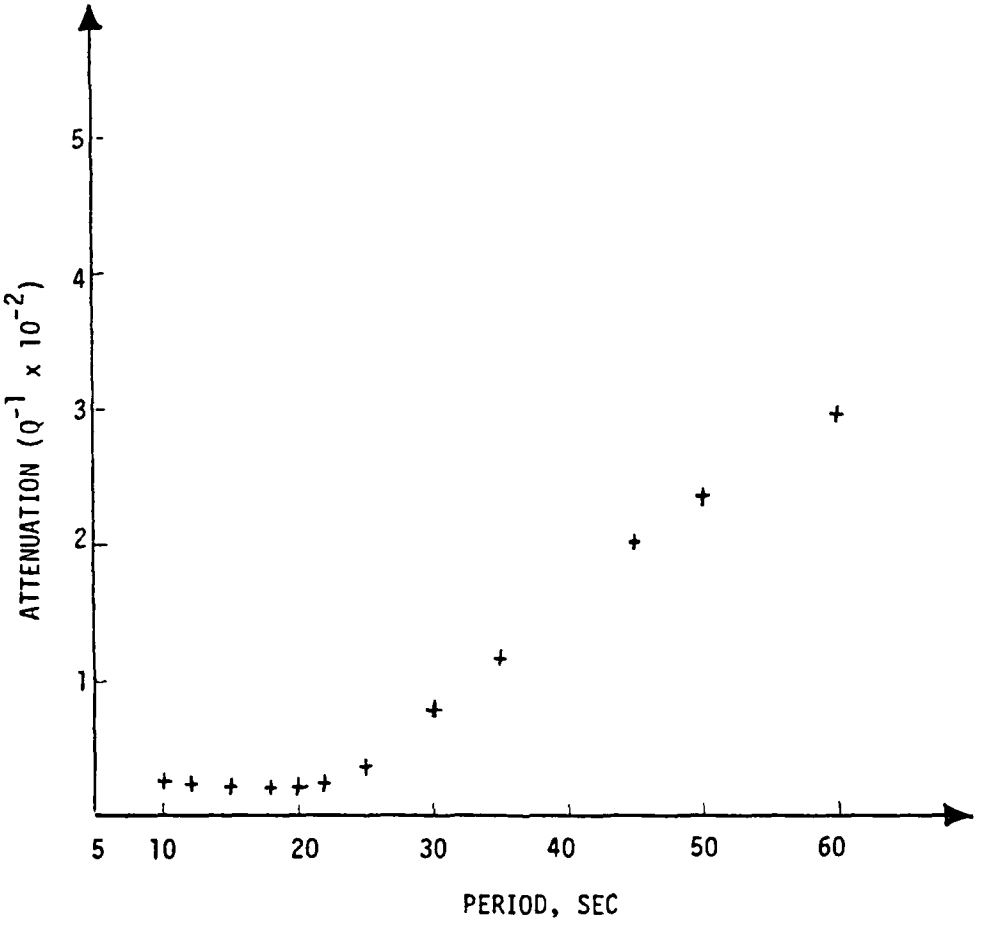

Figure 20. RAYLEIGH WAVE ATTENUATION, WESTERN UNITED STATES
(Lee and Solomon's model)

APPENDIX C

PROGRAM RALEE

This program is a revised form of the Program Raleem, written by L. A. Drake in 1972. The program is designed to analyze the motion of harmonic surface waves in a linearly elastic or viscoelastic layered medium. The layered medium is subdivided into a finite element Region I and one or two semiinfinite regions L and R. The two or three regions are joined together at the finite element boundaries.

The program consists of the main program RALEE, and 11 subroutines: EIGVEC, BOUNDA, SECEVA, SOLVE, ORTHOG, SETUP, INVERTC, MODAL, STIFFER, WRDSC AND BANSOL.

The function of the main and subroutines are as follows.

RALEE: Reads in the input data, assembles the stiffness matrices of the finite element regions and calculates amplitude and energies at the vertical boundaries.

EIGVEC: Computes the entries of the mass and elastic or viscoelastic matrices of the layered systems.

BOUNDA: Computes boundary matrices.

SECEVA: Constructs the eigenvalue problem, and solves it.

SOLVE: Solves an eigenvector corresponding to the eigenvalue, found in SECEVA.

ORTHOG: Finds an eigenvector normal to the one that has already been found.

SETUP: Decomposes the matrix $\underline{V}$, used in the boundary matrix of the subroutine, BOUNDA, into a vector; rewrites this vector into its real and imaginary parts.

INVERTC: Inverts a matrix.

MODAL: This subroutine is used only in the elastic case and selects the compatible eigenvalues.

STIFFER: Computes the stiffness matrix of an element.

WRDSC: Writes vector $\hat{B}$ and the matrix $\underline{A}$ of equation $\underline{A}\hat{X} = \hat{B}$ on Tape 2.

BANSOL: Solves equation $\underline{A}\hat{X} = \hat{B}$.

INPUT DATA

Read In:

I. Layered System

A. Period (F10.5) (one card).

B. Number of column and width of the finite element region (I10, 7F10.5) (one card).

C. Number of elements having the same depth, young modulus, rigidity and width (6 I10) (one card).

D. Number of natural layers and depth of the top of the first layer (I10, 7F10.5) (one card).

E. Number, thickness, compressional and shear velocities and density of the sublayers (I10, 7F10.5) (N cards, $N \leq 15$). Step D and E may be repeated once if there are two layered systems.

II. Finite Element Region

A. Depth to corner of the element and the number of elements having the same depth (4(F10.5, I10)) (Number of cards needed varies in this and the next two cases. For example, there

are four values of depth on each card and each value multiplies by the number of the element having the same depth. Addition of these values plus the values of the following cards must add up to be the number of elements, N^2).

B. Moduli of the elements and the number of elements having the same moduli (2(2 F10.5, I10)).

C. Width of the elements and the number of elements having the same width (4(F10.5, I10)).

A typical Read In data, described above, is given at the end of the program RALEE.

```
      PROGRAM RA_FE (INPUT,TAPE5,OUTPUT,TAPE1,TAPE2)
      DIMENSION H(15,2),HH(16),R(15,15),HV(16,16),AMP(30),PHASE(30)
     1,HA(15),Y(4,2),K1(480),KK(250),S(15,2),SA(15)
     2,HF(250),HS(250)
      COMPLEX E,EOLD,R1,R2,U1,U2,V1,V2,V,A,B,C,FC,DK,FF
     1,A1,A3,B2,B4,C1,C3,S1,S2,AB
      COMPLEX ALP,BET,P1,P2,P3,P4,P5,P6
      COMPLEX HLA(15),GA(15),BR(30),AA(30),ET(30),HE(250),HF(450)
     1,PA(30),PB(30),PC(30),PS(30)
      COMPLEX HL(15,15),G(15,15),AK(8,8),P(15,2),HM(15,2),F(15,2)
     1,VA(30,30),VB(30,30),C (30,30)),FD(30,30),ED(30,30)
     2,ZT(30,30),W(30,30)
      COMMON ND,NF,N1,N2,N3,CMS,IR,IC,II,A1(30),A3(30),B2(30),B4(30),C1
     2(30),C3(30),S1(30),S2(30),LO(30),MVO(30),E(30),R1(30),P2(30),J1(30
     3,J2(30),V1(30),V2(30),EOLD(30),V(30,30),AE(120)
      COMMON/BANARG/NM,MM,NUMBLK,B(6F),A(63,34),C(30,30)
      ND=30
      NN=34
      READ(5,3) T
    3 FORMAT(F10.5)
      READ 1,M,MM
    1 FORMAT(110,7F10.5)
      OMEGA=6.2e3530717954 6/T
      PRINT 111
  111 FORMAT(*NO. COLUMNS WIDTH                    PERIOD*)
      PRINT 1,M,MM,T,OMEGA
      MZ=M+1
      READ 2,IH,IA,IK,IL
    2 FORMAT(4I10)
      PRINT 112
  112 FORMAT(*HORIZONTALLY LAYERED STRUCTURES*)
C     READ NO. OF LAYERS AND DEPTH OF SURFACE
      DO 10 J=1,2
      READ 1,NL,D
      PRINT 12
   12 FORMAT(4X,6HLAYERS,10H THICKNESS,30H COMP. VEL. SHEAR VEL. DENSI
     2)
      K=0
      DO 10 I=1,NL
      READ 1,NS,THI,ALP,BET,RHO
      PRINT 1,NS,THI,ALP,BET,RHO
      Z=THI/NS
      DO 10 L=1,NS
      K=K+1
      HV(K,J)=D
      D=D+Z
      H(K,J)=Z
      HM(K,J)=RHO*(ALP**2-2.*BET**2)
      F(K,J)=RHO*BET**2
   10 S(K,J)=RHO
      N=K
      JR=0
      NZ=N+1
      NP=N+N
      N1=NP-1
      N2=NP-2
      N3=NP-3
```

```
      MM=NP+4
      MP=NP*MZ
      DO 9 I=1,N
    9 HV(I,M+1)=HV(I,2)
C  READ DEPTHS TO CORNER POINTS, COMPRESSIONAL VELOCITIES, SHEAR
C  VELOCITIES AND DENSITIES OF ELEMENTS
      READ 901,(HT(I),KK(I),I=1,IH)
      PRINT 901,(HT(I),KK(I),I=1,IH)
  901 FORMAT(4(F10.5,I10))
      K=0
      DO 702 I=1,IH
      JE=KK(I)
      DO 702 J=1,JE
      K=K+1
  702 HS(K)=HT(I)
      K=0
      DO 703 I=1,N
      DO 703 J=2,M
      K=K+1
  703 HV(I,J)=HS(K)
      READ 701,(HE(I),KK(I),I=1,IA)
      PRINT 701,(HE(I),KK(I),I=1,IA)
  701 FORMAT(2(F10.5,I10))
      K=0
      DO 704 I=1,IA
      JE=KK(I)
      DO 704 J=1,JE
      K=K+1
  704 HF(K)=HE(I)
      K=0
      DO 705 I=1,N
      DO 705 J=1,M
      K=K+1
  705 HE(I,J)=HF(K)
      READ 701,(HF(I),KK(I),I=1,IK)
      PRINT 701,(HE(I),KK(I),I=1,IK)
      K=0
      DO 706 I=1,IK
      JE=KK(I)
      DO 706 J=1,JE
      K=K+1
  706 HF(K)=HE(I)
      K=0
      DO 707 I=1,N
      DO 707 J=1,M
      K=K+1
  707 HS(I,J)=HF(K)
      READ 901,(HT(I),KK(I),I=1,IL)
      PRINT 901,(HT(I),KK(I),I=1,IL)
      K=0
      DO 708 I=1,IL
      JE=KK(I)
      DO 708 J=1,JE
      K=K+1
  708 HS(K)=HT(I)
      K=0
      DO 709 I=1,N
```

```
      DO 709 J=1,M
      K=K+1
709   R(I,J)=RB(K)
      DO 17 I=1,N
      DO 17 J=1,M
      HL(I,J)=R(I,J)*(HL(I,J)**2-2.*G(I,J)**2)
   17 G(I,J)=R(I,J)*G(I,J)**2
      HV(NZ ,1)=HV(N,1)+H(N,1)
      HV(NZ ,MZ )=HV(NZ ,1)
      DO 18 J=2,M
      HV(NZ ,J)=HV(NZ ,1)
   18 HH(J)=(J-1)*WM/M
      HH(1)=0.
      HH(MZ)=WM
      PRINT 20
   20 FORMAT(*0X COORDINATES OF COLUMNS*)
      PRINT 22,(HH(J),J=1,MZ)
   22 FORMAT(1X,21F6.2)
      PRINT 230
  230 FORMAT(*0DEPTH TO CORNERS OF ELEMENTS*)
      DO 24 I=1,NZ
   24 PRINT 22,(HV(I,J),J=1,MZ)
      PRINT 225
  225 FORMAT(*0LAMDA OF ELEMENTS*)
      DO 26 I=1,N
   26 PRINT 22,(HL(I,J),J=1,M)
      PRINT 210
  210 FORMAT(*0SHEAR MODULUS OF ELEMENTS*)
      DO 21 I=1,N
   21 PRINT 22,(G(I,J),J=1,M)
      PRINT 220
  220 FORMAT(*0DENSITY OF ELEMENTS*)
      DO 23 I=1,N
   23 PRINT 22,(R(I,J),J=1,M)
      OMS=OMEGA*OMEGA
C  GENERATE EQUIVALENT BOUNDARY MATRIX
      DO 57 I=1,N
      HA(I)=H(I,2)
      HLA(I)=HM(I,2)
      GA(I)=F(I,2)
   57 FA(I)=S(I,2)
      CA   EIGVEC(HA,HLA,GA,FA,N)
      PRINT 1001
 1001 FORMAT(*0EIGENVALUES OF TRANSMITTED MODES*)
      PRINT 59,E
   59 FORMAT(1X,10E13.6)
      EE=E(IR)*(0.,1.)
      DO 351 I=1,NP
      IF(REAL(E(I)).LE.0.) GO TO 351
      VV=OMEGA/REAL(E(I))
      Q=AIMAG(E(I))/REAL(E(I))
      IF(Q.EQ.0.) GO TO 369
      Q=Q*2.
      PRINT 53,Q
  369 PRINT 59,VV
  351 CONTINUE
      IS=IR
```

```
      DO 61 J=1,NP
      PA(J)=V(J,IR)
   61 PT(J)=E(J)
      PRINT 59,(V(I,IR),I=1,NP)
      LR=1
      CALL BOUNDA(HA,PA,HLA,GA,LR,SD,W,FC,FF)
      P1=0.
      P2=0.
      DO 723 I=1,NP
      PB(I)=0.
      PC(I)=0.
      DO 745 J=1,NP
      PB(I)=PB(I)+W(I,J)*PA(J)
745   PC(I)=PC(I)+AIMAG(W(I,J))*PA(J)
      P1=P1+CONJG(PA(I))*PB(I)
723   P2=P2+CONJG(PA(I))*PC(I)
      P1=OMEGA/2.*AIMAG(P1)
      Q=P2/P1
      PRINT 59,Q
      DO 201 I=1,NP
      DO 201 J=1,NP
      ZT(I,J)=W(I,J)
      CT(I,J)=C(I,J)
201   VB(I,J)=V(I,J)
C  GENERATE EQUIVALENT BOUNDARY MATRIX
      DO 56 I=1,N
      HA(I)=H(I,1)
      HLA(I)=HM(I,1)
      GA(I)=F(I,1)
   56 FA(I)=S(I,1)
      CALL EIGVEC(HA,HLA,GA,FA,N)
      PRINT 1003
 1003 FORMAT(*0EIGENVALUES OF INCIDENT MODES*)
      PRINT 59,E
      FC=E(IR)*(0.,1.)
      DO 352 I=1,NP
      IF(REAL(E(I)).LE.0.) GO TO 352
      VV=OMEGA/REAL(E(I))
      Q=AIMAG(E(I))/REAL(E(I))
      IF(Q.EQ.0.) GO TO 369
      Q=Q*2.
      PRINT 59,Q
369   PRINT 59,VV
352   CONTINUE
      IW=IR
      DO 222 I=1,NP
  222 BR(I)=V(I,IW)
      PRINT 59,(BR(I),I=1,NP)
C  FIND DISPLACEMENT MATRIX FOR REFLECTED MODES
      DO 61 I=2,NP,2
      DO 61 J=1,NP
   61 V(I,J)=-V(I,J)
      LR=0
      CALL BOUNDA(HA,PA,HLA,GA,LR,SD,W,FC,FF)
      P1=0.
      P2=0.
      DO 735 I=1,NP
```

```
      PB(I)=0.
      PC(I)=0.
      DO 755 J=1,NP
      PB(I)=PB(I)+W(I,J)*BR(J)
755   PC(I)=PC(I)+AIMAG(W(I,J))*BR(J)
      P1=P1+CONJG(BR(I))*PB(I)
735   P2=P2+CONJG(BR(I))*PC(I)
      P1=OMEGA/2.*AIMAG(P1)
      Q=P2/P1
      PRINT 59,Q
      DO 51 I=1,NP
      DO 51 J=I,NP
       W(J,I)=W(I,J)
51     C(J,I)=C(I,J)
      DO 202 I=1,NP
      DO 202 J=1,NP
202    VA(I,J)=V(I,J)
      DO 11 I=1,NP
11    BR(I)=BR(I)*100.
      DO 91 I=2,NP,2
      K=I-1
      DO 91 J=2,NP,2
      L=J-1
      V(I,J)= -C(I,J)
      V(K,J)= C(K,J)
      V(K,L)= -C(K,L)
91    V(I,L)= C(I,L)
CALCULATE STIFFNESS AND CONSISTENT MASS MATRICES OF SLOPING STRUCTURE
      NH=NN+NN
      DO 27 I=1,NH
      B(I)=0.
      DO 27 J=1,NH
27    A(I,J)=0.
      REWIND 2
      NUMBLK=0
      LOCJNT=0
      IV=0
      DO 170 J=1,M
      DO 170 I=1,N
      IV=IV+2
      IF(IV-NN) 85,85,190
190   IV=IV-NN
C  WRITE A BLOCK OF EQUATIONS (64) ON TAPE 2
      CALL WRDSC(LOCJNT,NR)
85    IU=IV-1
      LU=IV+1
      LV=LU+1
      JU=IU+NP
      JV=JU+1
      KU=JV+1
      KV=KJ+1
      Y(1,1)=HH(J)
      Y(2,1)=HH(J+1)
      Y(3,1)=HH(J+1)
      Y(4,1)=HH(J)
      Y(1,2)=HV(I,J)
      Y(2,2)=HV(I,J+1)
```

```
      Y(3,2)=HV(I+1,J+1)
      Y(4,2)=HV(I+1,J)
      CALL  STIFFS(Y,HL(I,J),C(I,J),R(I,J),DMS,AK)
      IF(I.EQ.N)GO TO 100
      A(IJ,NP+3)=A(IJ,NP+3)+AK(1,5)
      A(IU,NP+4)=A(IU,NP+4)+AK(1,6)
      A(IJ,3)=A(IU,3)+AK(1,7)
      A(IJ,4)=A(IJ,4)+AK(1,8)
       A(IV,NP+2)=A(IV,NP+2)+AK(2,5)
       A(IV,NP+3)=A(IV,NP+3)+AK(2,6)
      A(IV,2)=A(IV,2)+AK(2,7)
      A(IV,3)=A(IV,3)+AK(2,8)
      A(JJ,3)=A(JU,3)+AK(3,5)
      A(JJ,4)=A(JU,4)+AK(3,6)
      A(JV,2)=A(JV,2)+AK(4,5)
      A(JV,3)=A(JV,3)+AK(4,6)
      A(KU,1)=A(KU,1)+AK(5,5)
      A(KU,2)=A(KU,2)+AK(5,6)
      A(KV,1)=A(KV,1)+AK(6,6)
      A(LU,1)=A(LU,1)+AK(7,7)
      A(LU,2)=A(LU,2)+AK(7,8)
      A(LJ,NP-1)=A(LU,NP-1)+AK(3,7)
      A(LU,NP)=A(LJ,NP)+AK(4,7)
      A(LU,NP+1)=A(LJ,NP+1)+AK(5,7)
      A(LU,NP+2)=A(LU,NP+2)+AK(6,7)
      A(LV,1)=A(LV,1)+AK(8,8)
      A(LV,NP-2)=A(LV,NP-2)+AK(3,8)
      A(LV,NP-1)=A(LV,NP-1)+AK(4,8)
      A(LV,NP)=A(LV,NP)+AK(5,8)
      A(LV,NP+1)=A(LV,NP+1)+AK(6,8)
  100 A(IJ,1)=A(IU,1)+AK(1,1)
      A(IU,2)=A(IU,2)+AK(1,2)
      A(IJ,NP+1)=A(IU,NP+1)+AK(1,3)
      A(IU,NP+2)=A(IU,NP+2)+AK(1,4)
      A(IV,1)=A(IV,1)+AK(2,2)
      A(IV,NP)=A(IV,NP)+AK(2,3)
      A(IV,NP+1)=A(IV,NP+1)+AK(2,4)
      A(JJ,1)=A(JJ,1)+AK(3,3)
      A(JU,2)=A(JU,2)+AK(3,4)
      A(JV,1)=A(JV,1)+AK(4,4)
      I2=I+I
      I1=I2-1
      IF(J.GT.1)GO TO 141
      NF=NP-I1+1
      NI=NP-I2+1
      DO 140  J1=1,NF
      NG=I1+J1-1
  140 A(IU,J1)=A(IJ,J1)+C (I1,NG)
      DO 150  J1=1,NI
      NG=I2+J1-1
  150 A(IV,J1)=A(IV,J1)+C (I2,NG)
      B(IJ)=J.
      B(IV)=0.
      DO 71  K=1,NP
      B(IJ)=B(IU)+(C  (IU,K)-V(IU,K))*BR(K)
   71 B(IV)=B(IV)+(C  (IV,K)-V(IV,K))*BR(K)
  141 IF(J.LT.M)GO TO 170
```

```
      NF=NP-I1+1
      NI=NP-I2+1
      DO 145 J1=1,NF
      NG=I1+J1-1
  145 A(JJ,J1)=A(JJ,J1)-CT(I1,NG)
      DO 155 J1=1,NI
      NG=I2+J1-1
  155 A(JV,J1)=A(JV,J1)-CT(I2,NG)
  170 CONTINUE
  185 CALL WRDSC(LCOUNT,NR)
      IF(LCOUNT-NR)185,315,330
  315 LCOUNT=LCOUNT+1
  330 PRINT 146,NUMB_K
  146 FORMAT(*0NO. OF BLOCKS OF EQUATIONS =*,I4)
      LCO=LCOUNT-1
      PRINT 147,LCO
  147 FORMAT(* NO. OF EQUATIONS =*,I5)
C  SOLVE THE EQUATIONS WRITTEN ON TAPE 2
      CALL BANSOL
      PRINT 601
  601 FORMAT(*0MAXIMUM (COMPLEX) DISPL. OF CORNER POINTS*)
      MN=M*NP
      DO 630 K=1,NR
  630 K1(K)=K
      PRINT 602,(K1(I),B(I),I=1,NR)
  602 FORMAT(4(I2,2F13.6))
COMPUTE AMPLITUDES AND PHASE LEADS OF REFLECTED MODES
      DO 41 I=1,NP
   41 B(I)=B(I)-BR(I)
      PRINT 2016
2016   FORMAT(*0REFLECTED MODE DISPLACEMENT*)
      PRINT 59,(B(I),I=1,NP)
      DO 608 I=1,NP
      AA(I)=0.
      DO 608 K=1,NP
  608 AA(I)=AA(I)+ VA(I,K)*B(K)
      DO 603 I=1,NP
      AMP(I)=CABS(AA(I))
  603 PHASE(I)=ATAN2(AIMAG(AA(I)),(REAL(AA(I))))
      PRINT 604
  604 FORMAT(*0AMPLITUDES OF REFLECTED MODES*)
      PRINT 59,AMP
      PRINT 606
  606 FORMAT(*0PHASE LEADS OF REFLECTED MODES (AT L.H. END OF SLOPING
     2RUCTURE)*)
      PRINT 59,PHASE
      HJ      =10000./REAL(E(JW))
      DO 614 I=1,IR
  614 P(I,1)=AMP(I)**2/REAL(E(I))
      PRINT 620,HJ
  620 FORMAT(*0INCIDENT ENERGY =*,E13.6)
      PRINT 621
  621 FORMAT(* REFLECTED ENERGY*)
      PRINT 59,(P(I,1),I=1,IR)
      MN1=MN+1
      J=1
      DO 618 I=MN1,NR
```

```
      J=J+1
  919 BS(J)=B(I)
      PRINT 2017
 2017  FORMAT(*0 RIGHT BOUNDARY MODE DISPLACEMENT*)
      PRINT 59,(BS(I),I=1,NP)
      DO 612 I=1,NP
      AA(I)=0.
      DO 612 K=1,NP
  612 AA(I)=AA(I)+ VB(I,K)*B(K+MN)
      DO 613 I=1,NP
      AMP(I)=CABS(AA(I))
  613 PHASE(I)=ATAN2(AIMAG(AA(I)),REAL(AA(I)))
      PRINT 605
  605 FORMAT(*0AMPLITUDES OF TRANSMITTED MODES*)
      PRINT 59,AMP
      PRINT 607
  607 FORMAT(*0PHASE LEADS OF TRANSMITTED MODES (AT R.H. END OF SLOPING
     2STRUCTURE)*)
      PRINT 59,PHASE
      DO 511 I=1,NP
      PA(I)=(REAL(ET(I))*WM+PHASE(I))/OMEGA
      VV=WM/PA(I)
  511 PRINT 59,VV
      DO 615 I=1,IS
  615 P(I,2)=AMP(I)**2/REAL(ET(I))
      PRINT 622
  622 FORMAT(*0TRANSMITTED ENERGY*)
      PRINT 59,(P(I,2),I=1,IS)
      P1=0.
      P2=0.
      P3=0.
      P4=0.
      P5=0.
      P6=0.
      DO 47 I=1,NP
      PA(I)=0.
      PB(I)=0.
      PC(I)=0.
      DO 49 J=1,NP
      PA(I)=PA(I)+W(I,J)*BR(J)
      PB(I)=PB(I)+W(I,J)*B(J)
   49 PC(I)=PC(I)+ZT(I,J)*BF(J)
      P1=P1+REAL(BR(I))*AIMAG(PA(I))
      P2=P2+AIMAG(BR(I))*REAL(PA(I))
      P3=P3+REAL(B(I))*AIMAG(PB(I))
      P4=P4+AIMAG(B(I))*REAL(PB(I))
      P5=P5+REAL(BS(I))*AIMAG(PC(I))
   47 P6=P6+AIMAG(BS(I))*REAL(PC(I))
      EI=(P1-P2)*.5*OMEGA
      ER=(P3-P4)*.5*OMEGA
      ETT=(P5-P6)*.5*OMEGA
      EI=ABS(EI)
      ER=ABS(ER)
      ETT=ABS(ETT)
      PRINT 3333
 3333  FORMAT(*0INCIDENT ENERGY*)
      PRINT 59,EI
```

```
      PRINT 4444
4444   FORMAT(*OREFLECTED ENERGY*)
      PRINT 59,ER
      PRINT 5555
5555   FORMAT(*OTRANSMITTED ENERGY*)
      PRINT 59,ETT
      E1=EI+ETT
      P2=0.
      DO 397 I=1,NP
      PC(I)=0.
      DO 405 J=1,NP
405   PC(I)=PC(I)+(SD(I,J)-FD(I,J))*BS(J)
397   P2=P2+CONJG(BR(I))*PC(I)
      PRINT 2050
2050   FORMAT(*OCHANGE IN WAVENUMBER BETWEEN TWO BOUNDARIES*)
      DK=P2*OMEGA/(4*E1)
      PRINT 59,DK
      ET1=ETT+EI
      EI2=ETT-EI
      DK=ET2/ET1*E(IR)
      PRINT 59,DK
      STOP
      END
```

```
      SUBROUTINE EIGVEC(H,HL,G,R,N)
      DIMENSION H(15),R(15)
      COMPLEX E,EO,D,S1,S2,U1,U2,V1,V2,V,AB
      COMPLEX AL,AH,AV,CH,CV,BH,BV,AHO,BHO,CHO,AVO,CVO
      COMPLEX A1,A3,B2,B4,C1,C3,S1,S2
      COMPLEX HL(15),G(15)
      COMMON ND,NP,N1,N2,N3,OMS,IF,IC,II,A1(30),A3(30),B2(30),B4(30),C1
     230),C3(30),S1(30),S2(30),LO(30),MVB(30),E(30),R1(30),R2(30),J1(30
     3,U2(30),V1(30),V2(30),EOLD(30),V(30,30),AB(120)
      DO 9 I=1,NP
    9 EOLD(I)=0.
      AHO=0.
      AVO=0.
      BHO=0.
      CHO=0.
      CVO=0.
      I=0
      DO 22 J=1,N
      H3=H(J)/3.
      AL=HL(J)+G(J)+G(J)
      OM=R(J)*H3*OMS
      AH=AL*H3
      AV=G(J)*H3
      CH=G(J)/H(J)-OM
      CV=AL/H(J)-OM
      BH=(G(J)-HL(J))*.5
      BV=(G(J)+HL(J))*.5
      I=I+1
      A1(I)=AH+AHO
      A3(I)=A1*.5
      B2(I)=BH-BHO
      B4(I)=BV
      C1(I)=CH+CHO
      C3(I)=-CH-1.5*OM
      I=I+1
      A1(I)=AV+AVO
      A3(I)=AV*.5
      B2(I)=-BV
      B4(I)=0.
      C1(I)=CV+CVO
      C3(I)=-CV-1.5*OM
      AHO=AH
      AVO=AV
      BHO=BH
      CHO=CH
   22 CVO=CV
C     SOLVE THE NON-LINEAR EIGENVALUE PROBLEM, (E**2*A + E*B + C)*V = 0
      CALL SECEVA
      X=AIMAG(AL)
      IF(X.EQ.0.0) CALL MODAL
  100 END
```

```
      SUBROUTINE BOUNDM(H,R,HL,G,LR,N1,W,EC,FF)
      DIMENSION H(15),R(15)
      COMPLEX E,EOLD,R1,R2,U1,U2,V1,V2,V,A,B,C,D,AB,EC,FF
      COMPLEX A1,A3,B2,B4,C1,C3,S1,S2
      COMPLEX HL(15),G(15),WA(30,30),WD(30,30),WC(30,30),WB(30,30)
     1,W(30,30)
      COMPLEX AL,AH,AV,BH,BV,CH,CV,AHO,AVO,BHO,CHO,XT,XJ,CVO,
     1BVO,YI,YJ,DK,CK,CL
      COMMON NO,NP,N1,N2,N3,OMS,IP,IC,II,A1(30),A3(30),B2(30),B4(30),C1
     2(30),C3(30),S1(30),S2(30),LO(30),NV3(30),E(30),R1(30),R2(30),U1(3
     3,U2(30),V1(30),V2(30),EOLD(30),V(30,30),AB(120)
      COMMON/BANARG/N4,MM,NUMBLK,B(60),A(60,4),C(30,30)
      DO 10 J=1,NP
      C(1,J)=V(1,J)*A1(1)+V(3,J)*A3(1)
      C(2,J)=V(2,J)*A1(2)+V(4,J)*A3(2)
      C(N1,J)=V(N1,J)*A1(N1)+V(N3,J)*A3(N3)
      C(NP,J)=V(NP,J)*A1(NP)+V(N2,J)*A3(NP)
      DO 10 I=3,N2
   10 C(I,J)=V(I,J)*A1(I)+V(I+2,J)*A3(I)+V(I-2,J)*A3(I-2)
      DO 20 J=1,NP
      IF(LR.EQ.1)GO TO 12
      B=-E(J)*(0.,1.)
      GOTO 13
   12 B=E(J)*(0.,1.)
   13 DO 20 I=1,NP
   20 C(I,J)=C(I,J)*B
      CALL SETUP(V,NP)
      DO 40 I=1,NP
      DO 30 J=I,NP
      V1(J)=0.
      DO 30 K=1,NP
   30 V1(J)=V1(J)+C(I,K)*V(K,J)
      DO 40 J=I,NP
   40 C(I,J)=V1(J)
      XI=0.
      YI=0.
      M=0
      DO 50 I=2,N2,2
      K=I-1
      M=M+1
      XJ=.5*HL(M)
      YJ=.5*G(M)
      C(K,I)=C(K,I)+XI-XJ
      J=K+3
      C(K,J)=C(K,J)+XJ
      J=I+1
      C(I,J)=C(I,J)+YJ
      XI=XJ
   50 YI=YJ
      M=M+1
      C(N1,NP)=C(N1,NP)+YI-.5*HL(M)
      M=
      AHO=0.
      AVO=0.
      BHO=0.
      BVO=0.
      CHO=0.
```

```
      CVO=0.
      XI=0.
      YI=0.
      DO11 I=2,N2,2
      K=I-1
      M=M+1
      H3=H(M)/3
      AL=HL(M)+G(M)+G(M)
      C1=R(M)*H3*OMS
      AH=AL*H3
      AV=G(M)*H3
      B1=.5*HL(M)
      BV=.5*G(M)
      CH=G(M)/H(M)-CM
      CV=AL/H(M)-CM
      XJ=-(HL(M)-G(M))*.5
      YJ=(HL(M)+G(M))*.5
      W(K,K)=AH+AHO
      WA(K,K)=AH+AHO
      WC(K,K)=CH+CHO
      WD(K,I)=(XJ-XI)
      W(K,I)=BHO-BH
      WB(K,I)=BHO-BH
      W(K,I+1)=AH*.5
      WA(K,I+1)=AH*.5
      W(I+1,K)=AH*.5
      WA(I+1,K)=AH*.5
      WC(K,I+1)=-CH-1.5*CM
      WC(I+1,K)=-CH-1.5*CM
      WD(K,K+3)=YJ
      W(K,K+3)=BH
      WB(K,K+3)=BH
      W(I,I)=AV+AVO
      WA(I,I)=AV+AVO
      WC(I,I)=CV+CVO
      WD(I,I+1)=YJ
      W(I,I+1)=BV
      WB(I,I+1)=BV
      W(I,I+2)=AV*.5
      WA(I,I+2)=AV*.5
      W(I+2,I)=AV*.5
      WA(I+2,I)=AV*.5
      WC(I,I+2)=-CV-1.5*CM
      WC(I+2,I)=-CV-1.5*CM
      AHO=AH
      AVO=AV
      BHO=BH
      BVO=BV
      CHO=CH
      CVO=CV
      YI=YJ
11    XI=XJ
      M=M+1
      H3=H(M)/3
      AL=HL(M)+G(M)+G(M)
      C1=R(M)*H3*OMS
      AH=AL*H3
```

```
      AV=G(M)*H3
      BV=.5*G(M)
      B4=.5*HL(M)
      CH=G(M)/H(M)-CM
      CV=AL/H(M)-CM
      XJ=-(HL(M)-G(M))*.5
      YJ=(HL(1)+G(M))*.5
      W(N1,N1)=AH+AHO
      WA(N1,N1)=AH+AHO
      WC(N1,N1)=CH+CHO
      WJ(N1,NP)=(XI-XJ)
      W(N1,NP)=BHO-.5*HL(M)
      WB(N1,NP)=BHO-.5*HL(M)
      W(NP,NP)=AV+AVO
      WA(NP,NP)=AV+AVO
      WC(NP,NP)=CV+CVO
      DO 410 I=1,NP
      DO 410 J=I,NP
      WB(J,I)=WB(I,J)
+10   WD(J,I)=WD(I,J)
      PRINT 59,FC,FF
59    FORMAT(1X,10(13.6)
      IF(LR.EQ.1) GO TO 3032
      DO +11 J=1,NP
      DO +11 I=1,NP
      W(I,J)=W(I,J)*FC
+11   WD(I,J)=WD(I,J)*FC
      CK=FC*FC
      DO +12 J=1,NP
      DO +12  I=1,NP
+12   W1(I,J)=WA(I,J)*CK+WD(I,J)+WC(I,J)
      GO TO 3036
3032   CONTINUE
      CK=FF*FF
      DO +09 J=1,NP
      DO +09 I=1,NP
      W(I,J)=W(I,J)*(-FF)
      WD(I,J)=WD(I,J)*(-FF)
+09   WA(I,J)=WA(I,J)*CK
      DO 3035 I=1,NP
      DO 3035 J=1,NP
3035   WA(I,J)=WA(I,J)+WD(I,J)+WC(I,J)
3036  END
```

```
      SUBROUTINE SECEVA
      COMPLEX E,EO,D,R1,R2,U1,U2,V1,V2,V,AB,EV,EVS,CE,CD,DEV
      COMPLEX A1,A3,S2,B4,C1,C3,S1,B2,C3,D
      COMPLEX W(30,30)
      COMMON ND,NP,N1,N2,N3,CMS,IR,IC,II,A1(30),A3(30),B2(30),B4(30),C1(
     230),C3(30),S1(30),S2(30),LO(30),MVB(30),E(30),R1(30),R2(30),J1(30)
     3,U2(30),V1(30),V2(30),EOLD(3)),V(30,30),AB(120)
      DATA EPS/1.0E-7/,EPS2/1.0E-1)/
      NN1=NP-1
      NN2=NP*2
      DO 700 N=1,NN1
      MVB(N)=N+3*ND
      I=N+1
  700 MVB(I)=I+2*ND
      MVB(NN1)=NN1+ND
      XN=0.
      DO 15 J=1,NP
      X=C1(J)/A1(J)
   15  XN=XN+ABS(X)
      XN=SQRT(XN/NP)
      C=CMPLX(XN,XN+XN)
      DO 102 N=1,NP
      LO(N)=0
      EOLD(N)=0.
      R1(N)=(0.,0.)
      R2(N)=(0.,0.)
      S1(N)=1.
      S2(N)=0
      V1(N)=S1(N)
  102 V2(N)=S2(N)
      EV=XN/NP
      X1=AIMAG(A1)
      IF(X1.NE.0.0) GO TO 800
      DO 106 N=1,NP
      S2(N)=1.
  106 V2(N)=S2(N)
      EV=1.
      DO 900 N=1,NN1,2
      MVB(N)=N+3*ND
      I=N+1
  900 MVB(I)=I+2*ND
      MVB(NN1)=NN1+ND
  800 K=0
      MC=0
      IM=0
      PRINT 2000
      PRINT 2007
  400 K=K+1
      IF(X1.NE.0.0) GO TO 88
      IF(EOLD(K).EQ.0.0) GO TO 110
      EV=EOLD(K)*(1.,0.0001)
      GO TO 87
  110 X=CABS(EV)/2.
      EV=CMPLX(X,X)
   87 CD=1.
   88 DO 112 N=1,NP
      U1(N)=C1(N)*V1(N)
```

```
  112 U2(N)=A1(N)*V2(N)
      DO 113 N=1,N2
      L=N+2
      U1(N)=U1(N)+C3(N)*V1(L)
      U1(L)=U1(L)+C3(N)*V1(N)
      U2(N)=U2(N)+A3(N)*V2(L)
  113 U2(L)=U2(L)+A3(N)*V2(N)
      IF(X1.EQ.0.0) GO TO 89
      IF(IM.EQ.1) GO TO 85
      IM=0
      CD=1.
      X=CABS(EV)/2.
      EV=CMPLX(X,X+X)
      GO TO 89
   85  EV=EV*(1.+.0001)
      IM=2
      CD=1.
   89 IK=0
      DO 200 IT=1,20
      EVS=EV**2
      DO 120 N=1,NP
      V2(N)=(U1(N)-U2(N)*EV)*CD
      NQ=N +ND
      NR=NQ+ND
      NS=NR+ND
      AB(N)    =EVS*A1(N)+C1(N)
      AB(NQ)   =EV*B2(N)
      AB(NR)   =EVS*A3(N)+C3(N)
  120 AB(NS)   =EV*B4(N)
      CE=(0.,0.)
      CALL SOLVE
      DO 130 N=1,NP
      V1(N)=(V2(N)-V1(N)*CD)/EV
  131 CE=CE-U1(N)*V1(N)+U2(N)*V2(N)
      CE=CE*CD
      DO 132 N=1,NP
      U1(N)=C1(N)*V1(N)
  132 U2(N)=A1(N)*V2(N)
      DO 133 N=1,N2
      L=N+2
      U1(N)=U1(N)+C3(N)*V1(L)
      U1(L)=U1(L)+C3(N)*V1(N)
      U2(N)=U2(N)+A3(N)*V2(L)
  133 U2(L)=U2(L)+A3(N)*V2(N)
      CD=(0.,0.)
      DO 140 N=1,NP
  140 CD=CD-U1(N)*V1(N)+U2(N)*V2(N)
      DEV=CE/CD
      EV=EV+DEV
      CD=1./CSQRT(CD)
      C=DEV/EV
      X=ABS(REAL(C))+ABS(AIMAG(C))
      IF(IK.EQ.1) GO TO 300
      IF (X.LT.EPS) IK=1
  200 CONTINUE
      PRINT 2020
      STOP
```

```
      E(K)=EV
      EOLD(K)=EV
      X=ABS(REAL(EV))
      Y=ABS(AIMAG(EV))
      Z=X+Y
      IF(Y/Z.LT.EPS2) LD(K)=1
      IF(X/Z.LT.EPS2) LD(K)=2
      DO 310 N=1,NP
      V1(N)=V1(N)*DD
      V2(N)=V2(N)*DD
      V(N,K)=V1(N)
      U1(N)=  U1(N)*DD
  310 U2(N)=  U2(N)*DD
      IF(LD(K).NE.1) GO TO 316
      X=(V1(1)**2+V1(2)**2)*EV
      IF(X    .GT.0.) GOTO 316
      E(K)=-E(K)
      DO 315 N=2,NP,2
  315 V(N,K)=-V(N,K)
  316 IF (K.EQ.0) GOTO 335
      CE=(0.,0.)
      DO 330 N=1,NP
  330 CE=CE-R1(N)*U1(N)+R2(N)*U2(N)
      X=ABS(REAL(CE))+ABS(AIMAG(CE))
      PRINT 2008,K,IT,E(K),DEV,X
      IF(X.LT.EPS) GO TO 335
      PRINT 2021
      STOP
  335 DO 340 N=1,NP
      R1(N)=R1(N)+V1(N)
  340 R2(N)=R2(N)+V2(N)
      IF(X1.NE.0.0) GO TO 450
      J=LD(K)
      CALL ORTHOG(J)
      DO 445 N=1,NP
      V1(N)=S1(N)
  445 V2(N)=S2(N)
      MC=MC+4
      IF(LD(K).NE.0) MC=MC-2
      IF(MC.EQ.NN2) GO TO 100
      GO TO 400
  450 C=0.
      D=0.
      DO 342 N=2,NP,2
      M=N-1
      C=C-U1(M)*S1(M)+U2(N)*S2(N)
  342 D=D-U1(N)*S1(N)+U2(M)*S2(M)
      C=C*2.
      D=D*2.
   40 DO 392 N=2,NP,2
      M=N-1
      S1(M)=S1(M)-C*V1(M)
      S1(N)=S1(N)-D*V1(N)
      S2(M)=S2(M)-D*V2(M)
      S2(N)=S2(N)-C*V2(N)
      V1(M)=S1(M)
      V1(N)=S1(N)
```

```
      V2(M)=V2(M)
392   V2(N)=S2(N)
      DO 345 N=1,NP
      V1(N)=S1(N)
345   V2(N)=S2(N)
31      IF(LO(K)+IM.EQ.0) IM=1
      MC=MC+1
      IF(MC.EQ.NP) GO TO 350
      GO TO 400
350   X=0.
      C=(0.,-1.)
      DO 610 N=1,NP
      X=AIMAG(E(N))
      IF(X.LE.0.0) GO TO 600
      E(N)=-E(N)
      C=-C
600   DO 610 J=2,NP,2
610   V(J,N)=V(J,N)*C
      I=1
  530   IF(I.GT.NP) GO TO 550
      X=0.
      DO 540 L=I,NP
      AC=REAL(E(L))
      IF(X.EQ.0.) X=AC
      IF(AC.GT.X) GO TO 540
      J=L
      X=AC
540   CONTINUE
      C=E(I)
      E(I)=E(J)
      E(J)=C
      DO 535 L=1,NP
      C=V(L,I)
      V(L,I)=V(L,J)
535   V(L,J)=C
      I=I+1
      GO TO 530
550   CONTINUE
      K=0
      DO 666 I=1,NP
      AD=REAL(E(I))
      IF(AD.LT.0.0) GO TO 666
      K=K+1
666   CONTINUE
      IR=K
      IP=IR
      IN=0
      DO 560 I=1,NP
      AD=REAL(E(I))
      IF(AD.LT.0.0) GO TO 620
      IN=IN+1
      S1(IN)=E(I)
      DO 556 L=1,NP
556   W(L,IN)=V(L,I)
      GO TO 560
620   IP=IP+1
      S1(IP)=E(I)
```

```
      DO 557 L=1,NP
      W(L,IP)=V(L,I)
  557 CONTINUE
      DO 555 I=1,NP
      DO555 J=1,NP
      V(J,I)=W(J,1)
  555 E(I)=S1(I)
 2000 FORMAT(  / 40X,20H OUTPUT FROM SEQEVA  )
 2007 FORMAT(  /12H  NO.  NO.OF,20X,10HEIGENVALUE,27X,15HLAST CORRECTI
     1ON,12X,14HDEVIATION FROM/
     2 7X,5HITER.,5X, 9HREAL PART,14X,13HIMAG. PART,15X, 9HREAL PART
     3, 3X,13HIMAG. PART, 8X,14HORTHOGONALITY /)
 2008 FORMAT( I4,I5,5X,2E23.15,4X,2E12.5,4X,2E12.5)
 2019 FORMAT( /68H NORM OF RESIDUAL VECTOR AFTER THE INITIAL VECTOR H
     1 ONE-ELEMENTS /62H HAS BEEN ORTHOGONALIZED WITH RESPECT TO A
     2F EIGENVECTORS ,E18.5)
 2020 FORMAT(43H1 FAILURE TO CONVERGE IN 20 ITERATION STEPS )
 2021 FORMAT(68H1 FAILURE TO FIND AN EIGENVECTOR ORTHOGONAL TO THE ONE
     1FOUND BEFORE )
  100 END
```

```
      SUBROUTINE SOLVE
      COMPLEX E,ED,D,R1,R2,U1,U2,V1,V2,V,AB,C
      COMPLEX A1,A3,B2,B4,C1,C3,S1,S2
      COMMON ND,NP,N1,N2,N3,OMS,TR,IC,II,A1(30),A3(30),B2(30),B4(30),C
     230),C3(30),S1(30),S2(30),LD(30),MVB(30),E(30),R1(30),R2(30),U1(3
     3,U2(30),V1(30),V2(30),EDLD(30),V(30,30),AB(120)
      DO 100 N=1, N1
      I=N
      J=N+ND
      M=MVB(N)
      DO  50 L=J,M,ND
      C=AB(L)/AB(N)
      I=I+1
      J1=I
      DO  30 K=L,M,ND
      AB(J1)=AB(J1)-C*AB(K)
   30 J1=J1+ND
      AB(L)=C
   50 V2(I)=V2(I)-C*V2(N)
  100 V2(N)=V2(N)/AB(N)
      N=NP
      V2(N)=V2(N)/AB(N)
      DO 250 K=1,N1
      N=N-1
      I=N
      J=N+ND
      M=MVB(N)
      DO 250 L=J,M,ND
      I=I+1
  250 V2(N)=V2(N)-AB(L)*V2(I)
      END
```

```
      SUBROUTINE ORTHOG(J)
      COMPLEX E,ED,D,R1,R2,U1,U2,V1,V2,V,AB,C4,C2
      COMPLEX A1,A3,B2,B4,C1,C3,S1,S2
      COMMON ND,NP,N1,N2,N3,OMS,IR,IC,TI,A1(30),A3(30),B2(30),B4(30),C
     230),C3(30),S1(30),S2(30),LD(30),MVB(30),E(30),R1(30),R2(30),J1(3
     30,U2(30),V1(30),V2(30),FOLD(3)),V(30,30),AB(120)
      C4=0.
      C2=0.
      DO 10 N=2,NP,2
      M=N-1
      C4=C4-U1(M)   *S1(M)+U2(N)   *S2(N)
   10 C2=C2-U1(N)   *S1(N)+U2(M)   *S2(M)
      C4=C4*2.
      C2=C2*2.
      IF(J.NE.0) GO TO 25
      DO 20 N=2,NP,2
      M=N-1
      X=C4*V1(M)
      S1(M)=S1(M)-X-X
      X=C2*V1(N)
      S1(N)=S1(N)-X-X
      X=C2*V2(M)
      S2(M)=S2(M)-X-X
      X=C4*V2(N)
   20 S2(N)=S2(N)-X-X
      GO TO 40
   25 DO 30 N=2,NP,2
      M=N-1
      S1(M)=S1(M)-C4*V1(M)
      S1(N)=S1(N)-C2*V1(M)
      S2(M)=S2(M)-C2*V2(M)
   30 S2(N)=S2(N)-C4*V2(N)
   40 END
```

```
      SUBROUTINE SETUP(V,N)
      COMPLEX F(900),V(30,30)
      REAL RF(900),CF(900),RFI(900),CFI(900)
      NS=N*N
      I=0
      L=0
12    L=L+1
      DO 11 J=1,N
      I=I+1
11    F(I)=V(L,J)
      IF(L.LT.N) GO TO 12
      PRINT 59,I
59    FORMAT(I5)
      DO 10 J=1,NS
      RF(J)=REAL(F(J))
10    CF(J)=AIMAG(F(J))
      CONTINUE
      CALL INVFRTC(RF,CF,N,RFI,CFI)
      DO 20 J=1,NS
20    F(J)=CMPLX(RFI(J),CFI(J))
      I=0
      L=0
25    L=L+1
      DO 26 J=1,N
      I=I+1
26    V(L,J)=F(I)
      IF(L.LT.N) GO TO 25
      RETURN
      END
```

```
      SUBROUTINE INVERTC(AAR,AAI,NP,AR,AI)
      REAL AAR(1,1),AAI(1,1),AR(1,1),AI(1,1)
      REAL AMAXR,AMAXI,KR,KI
      DIMENSION ISPACE(3,32)
      NN=NP*NP
      DO 15 I=1,NP
      ISPACE(3,I)=0
      DO 10 J=1,NN,NP
      AR(I,J)=AAR(I,J)
      AI(I,J)=AAI(I,J)
   10   CONTINUE
   15 CONTINUE
      DO 140 I=1,NP
      AMAXR=0.
      AMAXI=0.
      XR=0.
      DO 60 J=1,NP
      IF(ISPACE(3,J)-1) 20,60,20
   20   KK=1
      DO 50 K=1,NN,NP
      KK=KK+1
      DO 30 K1=KK,KK
      IF(ISPACE(3,K1)-1) 30,50,30
   30   CONTINUE
      IF(AR(J,K)*AR(J,K)+AI(J,K)*AI(J,K)-XR) 50,45,45
   45   IROW=J
      ICOL=KK
      AMAXR=AR(J,K)
      AMAXI=AI(J,K)
      XR=AMAXR*AMAXR+AMAXI*AMAXI
   50   CONTINUE
   60 CONTINUE
      ICOLUM=ICOL
      ISPACE(3,ICOLUM)=ISPACE(3,ICOLUM)+1
      IF(IROW-ICOLUM) 70,90,70
   70 DO 80 L=1,NN,NP
      XR=AR(IROW,L)
      XI=AI(IROW,L)
      AR(IROW,L)=AR(ICOLUM,L)
      AI(IROW,L)=AI(ICOLUM,L)
      AR(ICOLUM,L)=XR
   80 AI(ICOLUM,L)=XI
   90 ISPACE(1,I)=IROW
      ISPACE(2,I)=ICOLUM
      IC=(ICOLUM-1)*NP+1
      AR(ICOLUM,IC)=1.0
      AI(ICOLUM,IC)=0.0
      DO 101 L=1,NN,NP
      XR=AMAXR*AMAXR+AMAXI*AMAXI
      XI=AR(ICOLUM,L)
      AR(ICOLUM,L)=(XI*AMAXR+AI(ICOLUM,L)*AMAXI)/XR
      AI(ICOLUM,L)=(AI(ICOLUM,L)*AMAXR-XI*AMAXI)/XR
  101 CONTINUE
      DO 130 L1=1,NP
      IF(L1-ICOLUM) 110,130,110
  110 XR=AR(L1,IC)
      XI=AI(L1,IC)
```

```
      AI(L1,IC)=0.0
      AR(L1,IC)=1.0
      DO 120 L=1,NN,NP
      AR(L1,L)=AR(L1,L)-AR(ICOLUM,L)*XR+AI(ICOLUM,L)*XI
      AI(L1,L)=AI(L1,L)-AR(ICOLUM,L)*XI+AI(ICOLUM,L)*XR
120   CONTINUE
130   CONTINUE
140   CONTINUE
      DO 170 I=1,NP
      L=NP+1-I
      IF(ISPACE(1,L)-ISPACE(2,L)) 150,170,150
150   JROW=ISPACE(1,L)
      JCOLUM=ISPACE(2,L)
      JR=(JROW-1)*NP+1
      JC=(JCOLUM-1)*NP+1
      DO 160 K=1,NP
      XR=AR(K,JR)
      XI=AI(K,JR)
      AR(K,JR)=AR(K,JC)
      AI(K,JR)=AI(K,JC)
      AR(K,JC)=XR
160   AI(K,JC)=XI
170   CONTINUE
      END
```

```
      SUBROUTINE MODAL
      COMPLEX E,EOLD,P1,P2,U1,U2,V,V2,V,A3,C
      COMPLEX A1,A3,B2,B4,C1,C3,S1,S2
      COMMON ND,NP,N1,N2,N3,OMS,IR,IC,TI,A1(30),A3(30),B2(30),B4(30),C
     2(30),C3(30),S1(30),S2(30),LO(30),MVB(30),E(30),P1(30),P2(30),J1(3
     3,U2(30),V1(30),V2(30),EOLD(3),V(30,30),AB(120)
      K=NP
      N=0
   90 N=N+1
      C=(0.,-1.)
      I=LO(N)+1
      IF(I-2)10,20,40
   10 EV=AIMAG(E(N))
      IF(EV.LT.0.) GOTO 12
      E(N)=CONJG(E(N))
      DO 11 J=1,NP
   11 V(J,N)=CONJG(V(J,N))
   12 E(K)=-CONJG(E(N))
      LO(K)=1
      DO 13 J=1,NP
   13 V(J,K)=CONJG(V(J,N))
      DO 14 J=2,NP,2
   14 V(J,K)=-V(J,K)*C
      K=K-1
      GOTO 50
   20 EV=REAL(E(N))
      E(N)=EV
      X=ABS(REAL(V(1,N)))+ABS(REAL(V(2,N)))
      IF(X.GT.1.E-12) GOTO 34
      DO 33 L=1,NP
   33 V(L,N)=AIMAG(V(L,N))
      GOTO 50
   34 DO 35 L=1,NP
   35 V(L,N)=REAL(V(L,N))
      GOTO 50
   40 EV=AIMAG(E(N))
      IF (EV.LT.0.) GOTO 41
      EV=-EV
      C=-C
   41 E(N)=CMPLX(0.,EV)
   50 DO 51 J=2,NP,2
   51 V(J,N)=V(J,N)*C
      IF(LO(N).NE.2) GOTO 100
      X=ABS(REAL(V(1,N)))+ABS(REAL(V(2,N)))
      IF(X.GT.1.E-12) GOTO 64
      DO 53 L=1,NP
   53 V(L,N)=AIMAG(V(L,N))
      GOTO 100
   64 DO 65 L=1,NF
   65 V(L,N)=REAL(V(L,N))
  100 IF(N-K)90,101,101
  101 II=0
      IC=0
      DO 105 J=1,NP
      IF(LO(J).EQ.1) IC=IC+1
      IF(LO(J).EQ.2) II=II+1
  105 CONTINUE
```

```
      IR=NP-IC-II
      I=1
110   IF(I.GT.IR) GOTO 130
      X=0.
      DO 120 L=I,NP
      IF(LO(L).NE.1) GOTO 120
      AC=ABS(REAL(E(L)))
      IF(X.EQ.0.) X=AC
      IF(AC.GT.X) GOTO 120
      J=L
      X=AC
120   CONTINUE
      L=LO(I)
      LO(I)=LO(J)
      LO(J)=L
      C=E(I)
      E(I)=E(J)
      E(J)=C
      DO 125 L=1,NP
      C=V(L,I)
      V(L,I)=V(L,J)
125   V(L,J)=C
      I=I+1
      GOTO 110
130   IF(I.GT.IR+IC) GOTO 150
      X=0.
      DO 140 L=I,NP
      IF(LO(L).NE.0) GOTO 140
      AC=REAL(E(L))
      IF(X.EQ.0.) X=AC
      IF(AC.GT.X) GOTO 140
      J=L
      X=AC
140   CONTINUE
      L=LO(I)
      LO(I)=LO(J)
      LO(J)=L
      C=E(I)
      E(I)=E(J)
      E(J)=C
      DO 135 L=1,NP
      C=V(L,I)
      V(L,I)=V(L,J)
135   V(L,J)=C
      I=I+1
      GOTO 130
150   IF(I.GE.NP) GOTO 170
      X=0.
      DO 160 L=I,NP
      AC=ABS(AIMAG(E(L)))
      IF(X.EQ.0.) X=AC
      IF(AC.GT.X) GOTO 160
      J=L
      X=AC
160   CONTINUE
      L=LO(I)
      LO(I)=LO(J)
```

```
      LO(J)=L
      C=E(I)
      E(I)=E(J)
      E(J)=C
      DO 155 L=1,NP
      C=V(L,I)
      V(L,I)=V(L,J)
155   V(L,J)=C
      I=I+1
      GOTO 150
170   END
```

```
      SUBROUTINE STIFF(Y,H1,G1,RH,W,AK)
      DIMENSION Y(4,2),E(3),AJ(2,2),Z(2,4),B(4),W(3),A(3,8)
     1,AM(4,4),AN(8,8)
      COMPLEX C(3,3),CA(3,8),AK(8,8),AT(8,8,9),P(3),H1,G1
      E(1)=-.774596692414
      E(2)=0.
      W(1)=.555555555555
      W(2)=.888888888888
      E(3)=-E(1)
      W(3)=W(1)
      L=1
      DO 4 IA=1,3
      DO 4 JA=1,3
      Z(1,1)=-1+E(IA)
      Z(1,2)=1-E(IA)
      Z(1,3)=1+E(IA)
      Z(1,4)=-1-E(IA)
      Z(2,1)=-1+E(JA)
      Z(2,2)=-1-E(JA)
      Z(2,3)=1+E(JA)
      Z(2,4)=1-E(JA)
      B(1)=Z(2,1)*Z(1,1)/4.
      B(2)=-Z(2,2)*Z(1,2)/4.
      B(3)=Z(2,3)*Z(1,3)/4.
      B(4)=-Z(2,4)*Z(1,4)/4.
      DO 1 I=1,2
      DO 1 J=1,2
      AJ(I,J)=0.
      DO 1 K=1,4
    1 AJ(I,J)=AJ(I,J)+Z(I,K)*Y(K,J)/4.
      DET=AJ(1,1)*AJ(2,2)-AJ(1,2)*AJ(2,1)
      AJ1=AJ(1,1)
      AJ(1,1)=AJ(2,2)/DET
      AJ(1,2)=-AJ(1,2)/DET
      AJ(2,1)=-AJ(2,1)/DET
      AJ(2,2)=AJ1/DET
      DO 2 J=1,4
      JJ=J+J
      DO 20 I=1,2
      A(I,JJ-1)=0.
   20 A(I,JJ)=0.
      DO 21 K=1,2
      A(1,JJ-1)=A(1,JJ-1)+AJ(1,K)*Z(K,J)/4.
   21 A(2,JJ)=A(2,JJ)+AJ(2,K)*Z(K,J)/4.
      A(3,JJ-1)=A(2,JJ)
    2 A(3,JJ)=A(1,JJ-1)
      DO 11 I=1,3
      DO 11 J=1,3
   11 C(I,J)=0.
      C(1,1)=H1+G1+G1
      C(2,2)=H1+G1+G1
      C(1,2)=H1
      C(2,1)=H1
      C(3,3)=G1
      DO 3 I=1,3
      DO 3 J=1,8
      CA(I,J)=0.
```

```
      DO 3 K=1,3
    3 CA(I,J)=CA(I,J)+C(I,K)*A(K,J)
      DO 30 I=1,8
      DO 30 J=I,8
      AK(I,J)=0.
      AN(I,J)=0.
      DO 30 K=1,3
   30 AK(I,J)=AK(I,J)+A(K,I)*CA(K,J)
      DO 9 I=1,4
      DO 9 J=I,4
    6 AM(I,J)=W5*B4*B(I)*B(J)
      DO 9 I=1,4
      DO 9 J=I,4
      II=I+I
      JJ=J+J
      AN(II-1,JJ-1)=AM(I,J)
    9 AN(II,JJ)=AM(I,J)
      DO 10 I=1,8
      DO 10 J=I,8
   10 AT(I,J,L)=(AK(I,J)-AN(I,J))*DE
    4 L=L+1
      DO 5 I=1,8
      DO 5 J=I,8
      DO 7 K=1,3
      P(K)=0.
      L=3*(K-1)
      DO 7 M=1,3
      MQ=L+M
    7 P(K)=P(K)+W(M)*AT(I,J,MQ)
      AK(I,J)=0.
      DO 5 M=1,3
    5 AK(I,J)=AK(I,J)+W(M)*P(M)
      END
```

```
      SUBROUTINE WRDSC(LCOUNT,NR)
      COMMON/BANARG/NN,MM,NUMBLK,B(69),A(69,34),C(30,30)
      COMPLEX A,B,C
      NUMBLK=NUMBLK+1
      WRITE(2) (B(I1),(A(I1,J1),J1=1,MM),I1=1,NN)
      DO 310 I1=1,NN
      LCOUNT=LCOUNT+1
      IF(LCOUNT-NR)320,321,330
  320 NZ=NN+I1
      B(I1)=B(NZ)
      B(NZ)=0.
      DO 310 J1=1,MM
      A(I1,J1)=A(NZ,J1)
  310 A(NZ,J1)=0.
  330 END
```

```
      SUBROUTINE BANSOL
      COMMON/BANARG/NN,MM,NUMBLK,B(59),A(59,34),C(30,30)
      COMPLEX A,B,C,D
      NL=NN+1
      MM=NN+NN
      REWIND 1
      REWIND 2
      NB=0
      GO TO 150
  100 NB=NB+1
      DO 125 N=1,NN
      NM=NN+N
      B(N)=B(NM)
      B(NM)=0.0
      DO 125 M=1,MM
      A(N,M)=A(NM,M)
  125 A(NM,M)=0.0
      IF (NUMBLK-NB) 150,200,150
  150 READ (2)(B(NK),(A(NK,M),M=1,11),NK=NL,MM)
      IF (NB) 200,100,200
  200 DO 300 N=1,NN
      IF (A(N,1)) 225,300,225
  225 B(N)=B(N)/A(N,1)
      DO 275 L=2,MM
      IF (A(N,L)) 230,275,230
  230 D=A(N,L)/A(N,1)
      I=N+L-1
      J=0
      DO 250 K=L,MM
      J=J+1
  250 A(I,J)=A(I,J)-D*A(N,K)
      B(I)=B(I)-A(N,L)*B(N)
      A(N,L)=0
  275 CONTINUE
  300 CONTINUE
      IF (NUMBLK-NB) 375,400,375
  375 WRITE (1) (B(N),(A(N,M),M=2,11),N=1,NN)
      GO TO 100
  400 DO 450 M=1,NN
      N=NN+1-M
      DO 425 K=2,MM
      L=N+K-1
  425 B(N)=B(N)-A(N,K)*B(L)
      NM=N+NN
      B(NM)=B(N)
  450 A(NM,NB)=B(N)
      NB=NB-1
      IF (NB) 475,500,475
  475 BACKSPACE 1
      READ (1) (B(N),(A(N,M),M=2,11),N=1,NN)
      BACKSPACE 1
      GO TO 400
  500 K=0
      DO 600 NB=1,NUMBLK
      DO 500 N=1,NN
      NM=N+NN
      K=K+1
```

```
                    FOR F(K)=A(NM,NB)
                        END

NO. COLUMNS WIDTH                          DEPTH
        15  50.000000    0.000000      .608817

VERTICALLY LAYERED STRUCTURES
   LAYERS THICKNESS COMP. VEL.  SHEAR VEL.  DENSITY
        1  14.000000   5.800000   0.000000   2.470000   0.000000   2.610000
        1   5.000000   6.700000   0.000000   2.760000   0.000000   2.630000
        1   1.000000   6.700000   0.000000   2.760000   0.000000   2.630000
        1   8.000000   6.700000   0.000000   2.760000   0.000000   2.630000
        1   2.000000   6.700000   0.000000   2.760000   0.000000   2.630000
        1   4.000000   7.000000   0.000000   2.820000   0.000000   2.630000
        1  16.000000   8.050000   0.000000   4.630000   0.000000   2.870000
        1  10.000000   8.050000   0.000000   4.630000   0.000000   2.870000
        1  20.000000   8.050000   0.000000   4.630000   0.000000   2.870000
        1  10.000000   8.100000   0.000000   4.660000   0.000000   2.920000
        1  10.000000   8.400000   0.000000   4.660000   0.000000   3.440000
        1  20.000000   8.500000   0.000000   4.890000   0.000000   3.500000
        1  20.000000   8.500000   0.000000   4.890000   0.000000   3.590000
        1  10.000000   8.500000   0.000000   4.890000   0.000000   3.590000
        1 100.000000   8.500000   0.000000   4.890000   0.000000   3.590000
   LAYERS THICKNESS COMP. VEL.  SHEAR VEL.  DENSITY
        1  14.000000   5.800000   0.000000   2.540000   0.000000   2.640000
        1   5.000000   6.700000   0.000000   2.760000   0.000000   2.640000
        1   1.000000   6.700000   0.000000   2.760000   0.000000   2.640000
        1   8.000000   6.600000   0.000000   2.580000   0.000000   2.640000
        1   2.000000   6.600000   0.000000   2.550000   0.000000   2.640000
        1   4.000000   7.000000   0.000000   4.470000   0.000000   2.090000
        1  16.000000   7.000000   0.000000   4.420000   0.000000   2.090000
        1  10.000000   7.050000   0.000000   4.420000   0.000000   3.420000
        1  20.000000   7.050000   0.000000   4.700000   0.000000   3.490000
        1  10.000000   7.050000   0.000000   4.750000   0.000000   3.490000
        1  10.000000   7.050000   0.000000   4.720000   0.000000   3.700000
        1  20.000000   7.670000   0.000000   4.180000   0.000000   3.780000
        1  20.000000   7.770000   0.000000   4.330000   0.000000   3.780000
        1  10.000000   7.850000   0.000000   4.270000   0.000000   3.490000
        1 100.000000   7.850000   0.000000   4.470000   0.000000   3.490000
     9.000000          14  14.000000          14  10.000000          14  20.000000          14
    20.000000          14  70.000000          14  70.000000          14  50.000000          14
    50.000000          14  50.000000          14  20.000000          14 100.000000          14
   100.000000          14 140.000000          14 150.000000          14
     5.000000    .011500          15   5.000000    .008500           1
     5.000000    .011500          14   6.700000    .008500           2
     5.700000    .011500          13   6.700000    .008500           4
     5.600000    .011500          11   6.700000    .008500           6
     5.650000    .011500           0   6.700000    .008500           8
     7.000000    .011200           7   7.000000    .008500          10
     7.020000    .011200           5   8.050000    .008500          12
     7.200000    .011200           3   8.050000    .008500          14
     7.220000    .011200           1   8.050000    .008500          11
     7.260000    .011200           4   8.100000    .008500          13
     7.320000    .011200           2   8.400000    .008500          15
     7.670000    .011200           2   8.500000    .008500          17
     7.770000    .011200           2   8.500000    .008500          13
     7.850000    .011200           2   8.500000    .008500          17
     7.650000    .011000          15   3.470000    .008500           1
     7.650000    .011000          14   3.740000    .008500           2
     7.600000    .011000          13   3.740000    .008500           4
     7.650000    .011000          11   3.740000    .008500           6
     7.650000    .011000           0   3.820000    .008500           8
     4.470000    .011600           7   4.630000    .007500          10
     4.420000    .011600           5   4.630000    .007500          12
     4.700000    .011600           3   4.630000    .007500          14
     4.750000    .011600           1   4.630000    .007500          11
     4.720000    .011600           4   4.630000    .007500          13
     4.180000    .011600           2   4.630000    .007500          15
     4.330000    .011600           2   4.540000    .008500          17
     4.270000    .011600           2   4.660000    .007500          13
     4.470000    .011600           2
     2.640000          15   2.640000           1   2.640000          14   2.630000          2
     2.640000          13   2.630000           4   2.640000          11   2.630000          5
     2.640000           0   2.620000           8   2.630000           7   2.630000         11
     2.090000           5   2.090000          12   2.420000           3   2.090000         14
     3.490000           1   2.090000          14   2.490000           4   3.490000         11
     3.700000           3   2.650000          11   2.780000           2   3.650000         13
     3.780000           2   2.650000          13   2.490000           2   3.650000         15
```

REFERENCES CITED

1. Achembach, J. D. Wave Propagation in Elastic Solids. New York: North-Holland, 1973.

2. Alsop, L. E., Goodman, A. S., and Gregerson, S. "Reflection and Transmission of Inhomogeneous Waves with Particular Application to Rayleigh Waves." Bulletin Seismological Society of America 64 (1974), pp. 1635-1652.

3. Anderson, D. L. "The Anelasticity of the Mantle." Geophys. Journal 14 (1969), pp. 135-164.

4. Anderson, D. L. Latest Information from Seismic Observation, The Earth's Mantle. New York: Academic Press, 1967, Chapter 12.

5. Anderson, D. L., Ben Menahem, A., and Archambeau, C. B. "Attenuation of Seismic Energy in the Upper Mantle." Journal Geophys. Research 70 (1965), pp. 1441-1448.

6. Anderson, D. L., and Hart, R. S. "Absorption and the Low-Velocity Zone." Nature 263 (1976), pp. 397-398.

7. Auld, B. A. Acoustic Fields and Waves in Solids. New York: John Wiley and Sons, 1973, Volume I.

8. Auld, B. A. Acoustic Fields and Waves in Solids. New York: John Wiley and Sons, 1973, Volume II.

9. Babich, V. M., Chikhachve, B. A., and Yanovskaya, T. B. "Surface Waves in a Vertically Inhomogeneous Elastic Half-space with a Weak Horizontal Inhomogeneity." IZV. Earth Physics 4 (1976), pp. 24-31.

10. Bäth, M. Mathematical Aspects of Seismology. New York: Elsevier, 1969.

11. Bathe, K. J., and Wilson, E. L. Numerical Method in Finite Element Analysis. New Jersey: Prentice-Hall, 1976.

12. Blake, T. R. "On Viscosity and Inelastic Nature of Waves in Geological Media." Bulletin Seismological Society of America 66 (1976), pp. 453-465.

13. Bland, D. R. The Theory of Linear Viscoelasticity. New York: Pergamon Press, 1960.

14. Borcherdt, R. D. "Energy and Plane Wave in Linear Viscoelastic Media." Journal Geophys. Research 78 (1973), pp. 2442-2453.

15. Borcherdt, R. D. "Rayleigh Type Surface Wave on a Linear Viscoelastic Half-Space." Journal Acoust. Society of America 55 (1974), pp. 13-15.

16. Borcherdt, R. D. "Reflection and Refraction of Type-IIS Wave in Elastic and Anelastic Media." Bulletin Seismological Society of America 67 (1977), pp. 43-67.

17. Buchen, P. W. "Plane Wave in Linear Viscoelastic Media." Geophysics Journal 23 (1971), pp. 531-542.

18. Bullen, K. E. An Introduction to the Theory of Seismology. Cambridge University Press, 1965.

19. Capon, J. "Analysis of Rayleigh Wave Multipath Propagation at LASA." Bulletin Seismological Society of America 60 (1970) pp. 1701-1731.

20. Capon, J. "Comparison of Love and Rayleigh Wave Multipath Propagation at LASA." Bulletin Seismological Society of America 61 (1971), pp. 1327-1344.

21. Cathles, L. M. The Viscosity of the Earth's Mantle. Princeton, New Jersey: Princeton University Press, 1975.

22. Christensen, R. M. Theory of Viscoelasticity: An Introduction. New York: Academic Press, 1971.

23. Crampin, S. "Distinctive Particle Motion of Surface Waves as a Diagnostic of Anisotropic Layering." Geophys. Journal 40 (1975), pp. 177, 186.

24. Crampin, S. "A Review of the Effects of Anisotropic Layering on the Propagation of Seismic Waves." Geophys. Journal 49 (1977), pp. 9-27.

25. Desai, C. S., and Abel, F. Introduction to the Finite Element Method. New York: Van Nostrand, 1972.

26. Drake, L. A. "Rayleigh Wave at a Continental Boundary by the Finite Element Method." Bulletin Seism. Society of America 62 (1972), pp. 1259, 1268.

27. Drake, L. A. "Rayleigh Waves in an Alluvial Valley." Science 240 (1972), pp. 113-114.

28. Drake, L. A. "Love and Rayleigh Waves in a Nonhorizontally Layered Media." Bulletin Seism. Society of America 62 (1972), pp. 1241-1258.

29. Drake, L. A. The Propagation of Love and Rayleigh Waves in Non-horizontally Layered Media. Berkeley, Calif.: University of California, Doctoral Dissertation, 1971.

30. Dziewonski, A. M., and Hales, A. L. Numerical Analysis of Dispersed Seismic Waves, Method in Computational Physics. New York: Academic Press, 1972.

31. Evernden, J. F. "Direction of Approach of Rayleigh Waves and Related Problems, Part I." Bulletin Seism. Society of America 43 (1953), pp. 335-374.

32. Evernden, J. F. "Direction of Approach of Rayleigh Waves and Related Problems, Part II." Bulletin Seism. Society of America 44 (1954), pp. 159-184.

33. Evernden, J. F. "Variation of Rayleigh Wave Amplitude with Distance." Bulletin Seism. Society of America 61 (1971), pp. 231-240.

34. Ewing, W. M., Jardetsky, W. S., and Press, F. Elastic Waves in Layered Media. New York: McGraw-Hill, 1957.

35. Ferry, J. D. Viscoelastic Properties of Polymers. New York: John Wiley and Sons, 1970.

36. Flügge, W. Viscoelasticity. Waltman, Mass.: Blaispell, 1967.

37. Fung, Y. C. Foundation of Solid Mechanics. New Jersey: Prentice-Hall, 1965.

38. Futterman, W. I. "Dispersive Body Waves." Journal Geophysical Reserach 67 (1962), pp. 5279, 5291.

39. Gjevik, B. "Ray Tracing for Seismic Surface Waves." Geophysics 29 (1974), pp. 29-39.

40. Gliko, A. G. "Effective Moduli and the Structure of Two-Phase Media." IZV. Earth Physics 5 (1976), pp. 32-45.

41. Gordon, R. B. "Diffusion Creep in the Earth's Mantle." Journal Geophys. Research 70 (1965), pp. 2413-2418.

42. Gordon, R. B. "Thermally Activated Process in the Earth: Creep and Seismic Attenuation." Geophys. Journal 14 (1967), pp. 33-43.

43. Gordon, R. B. "Anelastic Properties of the Earth." Rev. Geophys. 4 (1966), pp. 457, 474.

44. Gross, B. Mathematical Structure of the Theory of Viscoelasticity. Paris: Hermann, 1953.

45. Hart, R. S., Anderson, D. L., and Kanamori, H. "Shear Velocity and Density of an Attenuating Earth." Earth Planet. Sci. Letters 32 (1976) pp. 25-34.

46. Hashin, Z. "Theory of Mechanical Behavior of Heterogeneous Media." Appl. Mech. Rev. 17 (1964), pp. 1-7.

47. Haskell, N. A. "The Dispersion of Surface Waves on Multilayered Media." Bulletin Seism. Society of America 43 (1953), pp. 17-34.

48. Hayes, M. A. and Revlin, R. S. "Plane Waves in Linear Visco-elastic Materials." Quart. Appl. Math 32 (1974), pp. 113-121.

49. Herrin, E. A Comparative Study of Upper Mantle Models: Canadian Shields and Basin and Range Provinces, The Nature of Solid Earth. New York: McGraw-Hill, 1972, pp. 216-231.

50. Jackson, D. D., and Anderson, D. L. "Physical Mechanisms of Seismic Wave Attenuation." Rev. Geophys. 8 (1970), pp. 1-63.

51. Jefferys, H. "Importance of Damping in Geophysics." Geophys. Jour. 40 (1975), pp. 23-27.

52. Kanamori, H. "Velocity and Q of Mantle Waves." Phys. Earth Planet Int. 2 (1970), pp. 259-295.

53. Kanamori, H., and Anderson, D. L. "Importance of Physical Dispersion in Surface Wave and Free Oscillation Problems." Rev. Geophys. 15 (1977), pp. 105-112.

54. Kausel, E., Roesset, J. M., and Waas, G. "Dynamic Analysis of Footing on Layered Media." J. Eng. Mech. Div. ASCE 101 (1975), pp. 679-693.

55. Kennett, B. L. "The Intersection of Seismic Waves with Horizontal Velocity Contrasts, III: The Effect of Horizontal Transition Zones." Geophys. Jour. 41 (1975), pp. 29-36.

56. King, P. J., and Sheard F. W. "Viscosity Tensor Approach to Damping of Rayleigh Waves." Jour. Appl. Phys. 40 (1969), pp. 5189-5190.

57. Knopoff, L. Q, Review of Geophysics 2 (1964), pp. 625-660.

58. Knopoff, L., and Gangi, A. F. "Transmission and Reflection of Rayleigh Waves by Wedges." Geophys. 25 (1960), pp. 1203-1214.

59. Kogan, S. Ya. "A Brief Review of Seismic Wave Absorption Theories, I, II." Izv. Earth Phys. 11, 12 (1966), pp. 671-683.

60. Kolsky, H. "The Propagation of Stress Pulses in Viscoelastic Solids." Phil. Mag. 1 (1956), pp. 693-710.

61. Kolsky, H. "The Role of Experiment in the Development of Solid Mechanics: Some Examples." Adv. Appl. Mech. 16 (1976), pp. 309-368.

62. Kovach. R. L. Seismic Surface Waves: Some Observations and Recent Developments, Physics and Chemistry of the Earth. New York: Pergamon, 1966, Chapter 6.

63. Kovach. R. L. and Robinson, R. "Upper Mantle Structure in the Basin and Range Province, Western North America, from the Apparent Velocities of S Waves." Bulletin Seism. Society of America 59 (1969), pp. 1653-1665.

64. Kovach, R. L. "Seismic Surface Waves and Crustal and Upper Mantle Structure." Rev. Geophys. 16 (1978), pp. 1-13.

65. Lamb, G. L. "The Attenuation of Waves in a Dispersive Medium." Jour. Geophys. Res. 67 (1972), pp. 5273-5278.

66. Lapwood, E. R. "The Transmission of Rayleigh Pulse Around a Corner." Geophys. 26 (1961), pp. 174-196.

67. Landau, L. D., and Lifshitz, E. M. Theory of Elasticity. London: Pergamon Press, 1959.

68. Langhaar, H. L. Energy Method in Applied Mechanics. New York: John Wiley and Sons, 1962.

69. Lee, W. B., and Solomon, S. C. "Simultaneous Inversion of Surface Wave Phase Velocity and Attenuation: Love Wave in Western North America." Jour. Geophys. Res. 83 (1978), pp. 3389-3400.

69a. Lee, W. B., and Solomon, S. C. "Simultaneous Inversion of Surface Wave Phase Velocity and Attenuation: Rayleigh and Love Wave Over Continental and Oceanic Paths." Bulletin Seism. Society of America 69 (1979), pp. 65-95.

70. Lin, T. H. Theory of Inelastic Structure. New York: John Wiley and Sons, 1968.

71. Lindsay, R. B. Mechanical Radiation. New York: McGraw-Hill, 1960.

72. Litvitz, T. A., and Davis, C. M. Structural and Shear Relaxation in Liquids, Physical Acoustics, 2A. New York: Academic Press, 1965. pp. 281-349.

73. Liu, H. P., and Archambeau, C. B. "The effect of Anelasticity on Period of the Earth's Free Oscillations (Toroidal Mode)." Geophys. Jour. 43 (1975), pp. 795-814.

74. Liu, H. P., Anderson, D. L., and Kanamori, H. "Velocity Dispersion Due to Anelasticity; Implication for Seismology and Mantle Composition." Geophys. Jour. 47 (1976), pp. 41-58.

75. Liu, H. P., and Archambeau, C. B. "Correction to Paper, The Effect of Anelasticity on Period of the Earth's Free Oscillations (Toroidal Modes)." Geophys. Jour. 47 (1976), pp. 1-7.

76. Lockett, F. J. "The Reflection and Refraction of Waves at an Interface between Viscoelastic Materials." Jour. Mech. Phys. Solids 10 (1962), pp. 53-64.

77. Lomintz, C. "Linear Dissipation in Solids." Jour. Appl. Phys. 28 (1957), pp. 201-205.

78. Lysmer, J. "Lumped Mass Method for Rayleigh Waves." Bulletin Seism. Society of America 60 (1970), pp. 89-104.

79. Lysmer, J., and Waas, G. "Shear Waves in Plane Infinite Structure." Jour. Eng. Mech. Div. ASCE 98 (1972), pp. 85-105.

80. Lysmer, J., and Drake, L. A. A Finite Element Method for Seismology, Method in Computational Physics, 11. New York: Academic Press, 1972, pp. 181-216.

80a. Mack, H. Personal Communication.

81. Magnitsky, V. A., and Zharkov, V. N. Low Velocity Layers in the Upper Mantle, Earth Crust and Upper Mantle. P. J. Hart (ed.) 1969, pp. 664-675.

82. Mal, A. K., and Knopoff, L. "Transmission of Rayleigh Waves Past a Step Change in Elevation." Bulletin Seism. Society of America 55 (1965), pp. 319-334.

83. Mason, W. P. "Internal Friction Mechanism that Produces an Attenuation in the Earth's Crust Proportional to the Frequency." Jour. Geophys. Res. 74 (1969), pp. 4963-4966.

84. Mathson, A. J. Molecular Acoustics. New York: John Wiley and Sons, 1971.

85. McGarr, A., and Alsop. L. E. "Transmission of Rayleigh Waves at Vertical Boundaries." Jour. Geophys. Res. 72 (1967), pp. 2169-2180.

86. McGarr, A. "Amplitude Variation of Rayleigh Waves Propagating Across a Continental Margin." Bulletin Seism. Society of America 59 (1969a) pp. 1281-1306.

87. Mitchell, B. J. "Radiation and Attenuation of Rayleigh Wave from the Southeastern Missouri Earthquake of October 21, 1965." Jour. Geophys. Res. 78 (1973), pp. 886-889.

88. Mukitina, I.V., and Molotkov, A. I. The Propagation of Rayleigh Waves in an Elastic Half-Spece which is Inhomogeneous in Two Coordinates." Izv. Earth Phys. 4 (1967), pp. 3-8.

89. Norrie, D. H., and de Vries, G. The Finite Element Method: Fundamental and Applications. New York: Academic Press, 1973.

90. Orowan, E. "Seismic Damping and Creep in the Mantle." Geophys. Jour. 14 (1967), pp. 191-218.

91. Papaconstantinou, C. "Interactive Solution of Generalized Eigenvalue Problem." Jour. Inst. Math. Applic. 17 (1976), pp. 255-260.

92. Parks, J. H., and Rockwell, D. A. "Surface Acoustic Wave Velocity Induced by Radiative Absorptions." Jour. Appl. Phys. 48 (1976), pp. 971-975.

93. Ponter, A. R. S. "An Energy Theorem for Time Dependent Materials." Jour. Mech. Phys. Solids 17 (1969), pp. 63-71.

94. Press, F. and Healy, J. "Absorption of Rayleigh Waves in Low-Loss Media." Jour. Acoust. Soc. Amer. 26 (1957), pp. 1323,1325.

95. Randall, M. J. "Attenuative Dispersion and Frequency Shifts of the Earth's Free Oscillations." Phys. Earth Planet Int. 12 (1976), pp. p1-p4.

96. Rayleigh, J. W. S. B. "On Wave Propagated Along the Plane of an Elastic Solid." London Math. Society Proceedings 17 (1885), pp. 4-11.

97. Richards, T. H. Energy Methods in Stress Analysis. New York: John Wiley and Sons, 1977.

98. Richter, C. F. Elementary Seismology. San Francisco, Calif.: Freeman, 1958.

99. Roy, R. F., Decker, E. R., Blackwell, D. D., and Birch, F. "Heat Flow in the United States." Jour. Geophys. Res. 73 (1968), pp. 5207-5222.

100. Ruhe, A. "Algorithms for the Nonlinear Eigenvalue Problem." SIAM. Jour. Numer. Anal. 10 (1973), pp. 674-689.

101. Schwab, F., and Knopoff, L. "Surface Waves on Multilayered Anelastic Media." Bulletin Seism. Soc. Amer. 61 (1971), pp. 893-912.

102. Schwarzl, F. R., and Struik, L. C. E. "Analysis of Relaxation Measurements." Adv. Mol. Relax. Proc. 1 (1968), pp. 201-255.

103. Segerlind, L. J. Applied Finite Element Analysis. New York: John Wiley and Sons, 1976.

104. Segol, G., Abel, J. F., and Lee, P. C. Y. "Finite Element Mesh Gradation for Surface Waves." Jour. Geo. Eng. Div. ASCE 101 (1975), pp. 1177, 1181.

105. Segol, G., Lee, P. C. Y., and Abel, J. F. "Amplitude Reduction of Surface Waves by Trenches." Jour. Eng. Mech. Div. ASCE 104 (1978), pp. 821-841.

106. Silva, W. "Body Wave in a Layered Anelastic Solids." Bulletin Seism. Society of America 66 (1976), pp. 1539-1554.

107. Smith, W. D. "The Application of Finite Element Analysis to Body Wave Propagation Problems." Geophys. Jour. 42 (1975), pp. 747-768.

108. Solomon, S. C. "Seismic Wave Attenuation and Partial Melting in the Upper Mantle of North America." Jour. Geophys. Res. 77 (1972a), pp. 1483-1502.

109. Strick, E. "The Determination of a Dynamic Viscosity and Transient Creep Curves from Wave Propagation Measurements." Geophys. Jour. 13 (1967), pp. 197-218.

110. Takeuchi, H., Saito, M., and Kobayashi, N. "Study of Shear Velocity Distribution in the Upper Mantle by Mantle Rayleigh and Love Waves." Jour. Geophys. Res. 67 (1962), pp. 2831-2839.

111. Takeuchi, H., and Saito, M. Seismic Surface Wave, Method in Computational Physics, 11 New York: Academic Press, 1972, pp. 217-295.

112. Tasi, Y. M., and Kolsky, H. "Surface Wave Propagation for Linear Viscoelastic Solids." Jour. Mech. Phys. Solids 16 (1968), pp. 99-109.

113. Thompson, G. A., and Burke, P. B. "Regional Geophysics of the Basin and Range Province." Annl. Rev. Earth Planet Sci. 2 (1974), pp. 213-238.

114. Tolstoy, I. Wave Propagation. New York: McGraw-Hill, 1973.

115. Tryggvason, E. E. "Dissipation of Rayleigh Wave Energy." Jour. Geophys. Res. 70 (1965), pp. 1449-1455.

116. Vacher, R., and Boyer, L. "Viscoelastic Model and Acoustic Wave Propagation in Anisotropic Media." Jour. Acoust. Soc. Amer. 58 (1975), pp. 385-390.

117. Waas, G. Linear Turf Dimensional Analysis of Soil Dynamics Problems in Semiinfinite Layer Media. Berkeley, Calif.: University of California, Ph. D. Thesis, 1972.

118. Walsh, J. B. "Attenuation in Partially Melted Material." Jour. Geophys. Res. 73 (1968), pp. 2209-2216.

119. White, J. E. Seismic Wave: Radiation, Transmission and Attenuation. New York: McGraw-Hill, 1965.

120. Wilkinson, J. M. The Algebraic Eigenvalue Problem. Oxford: Oxford University Press, 1965.

121. Wu, T. T. "The Effect of Inclusion Shape on the Elastic Moduli." Int. Jour. Solid Struct. 2 (1966), pp. 1-8.

122. Zener, C. Elasticity and Anelasticity of Metals. Chicago: The University of Chicago Press, 1948.

123. Ziegler, H. An Introduction to Thermomechanics. New York: North-Holland, 1977.

124. Zienkiewicz, O. C. The Finite Element Method in Engineering Science. New York: McGraw-Hill, 1971.